MATRIX ANALYSIS OF LARGE DEFORMATION ELASTIC-PLASTIC PROBLEMS

BY

Jayasiri Sarath Gunasekera
M.Sc., B.Sc.

Thesis submitted for the degree of
Doctor of Philosophy in the
Faculty of Engineering
University of London

Department of Mechanical Engineering
Imperial College of Science and Technology
London, S.W.7.

April 1972

A B S T R A C T

The finite element displacement method is used to solve elastic-plastic problems with small and large deformations. Large deformations are taken into account by a Langrangian derivation based on the Green's strain tensor, and examples are given to illustrate this. An alternative method is also discussed based on the Eulerian derivation. The elastic-plastic material is represented by the Prandtl-Reuss relations together with the yield criterion of von-Mises. A computer program is developed and the analysis is carried out step-by-step using small linearised increments. The method is checked by comparing the finite element results of some problems with known theoretical or experimental solutions. Application of the method to study the transient stages of a metal processing problem is demonstrated.

ACKNOWLEDGEMENTS

The author wishes to express his sincere thanks to Professor J.M. Alexander for the guidance, valuable advice and continual interest which he showed in all aspects of the work.

The financial support offered during the course of this project from the following, are gratefully acknowledged.

(i) The Government of Ceylon

(ii) The University of Ceylon, Peradeniya, Ceylon

(iii) McMaster University, Hamilton, Canada

(iv) Imperial College, London

(v) Metropolitan Vickers Fund.

Thanks are also due to Mr. T.W. Turner, Research Assistant, Department of Mechanical Engineering, Imperial College, who made available the experimental results on dieless drawing.

Finally the author wishes to express his gratitude to his colleagues and other academic, technical, clerical and library staff at Imperial College for their help and encouragement towards the completion of the work.

CONTENTS

		Page
ABSTRACT		1
ACKNOWLEDGEMENTS		2
CONTENTS		3
NOMENCLATURE		7
CHAPTER 1	Introduction	9
1.1	General	9
1.2	Literature survey	12
1.2.1	Material nonlinearity	12
1.2.2	Geometric nonlinearity	14
1.2.3	Combined nonlinearity	17
CHAPTER 2	General Theory	19
2.1	Small displacements	19
2.1.1	**B** and **D** matrices	21
2.2	Plasticity	22
2.2.1	Yield surface	23
2.2.2	Flow rule	23
2.3	Elastic-plastic stress-strain matrix	24
CHAPTER 3	Large Deformation Theory	28
3.1	Green's strain tensor	28
3.2	Geometric nonlinearity	29
CHAPTER 4	An Alternative Derivation of the Stiffness Matrix	32
4.1	The concept of natural modes	32
4.2	The natural mode technique	32
4.3	Theory for the three-dimensional TET4 element	33
4.3.1	Small displacement theory for the elastic case	34

		Page
4.3.2	Large displacements	37
4.3.3	Plasticity	39
CHAPTER 5	Computational Procedures	40
5.1	Outline of the flow sequence	40
5.2	Boundary conditions	41
5.3	Assembly of element stiffnesses to form the overall stiffness matrix	43
5.4	Solution of the simultaneous equations	43
5.4.1	Gaussian elimination	44
5.4.2	Matrix factorisation	44
5.4.3	Direct inversion of **K**	44
5.4.4	Iterative methods (Gauss-Siedell iterative technique)	45
5.5	Evaluation of the correct loading step at every increment	46
5.6	Iterative techniques within a load increment	49
CHAPTER 6	Small Displacement Elastic-Plastic Finite Element Solutions	51
6.1	Analysis of a thick-walled cylinder with internal pressure	51
6.1.1	Theoretical solution	51
6.1.2	Finite element solutions and comparison	52
6.2	Perforated strip under tension	53
6.2.1	Results and comparison	54
CHAPTER 7	Large Deformation Elastic-Plastic Solutions	55
7.1	One variable theory (solution for the conical plate)	55
7.1.1	Experimental work	55

		Page
7.1.2	Finite Element Analysis	55
7.1.3	Results and Discussion	57
7.2	Expansion of a hole in thin (flat) plate	59
7.2.1	Experimental work	60
7.2.2	Finite Element Analysis	60
7.2.3	Results and Discussion	61
CHAPTER 8	Application to other problems	62
8.1	Analysis of the Dieless Drawing Process	62
8.1.1	Consideration of the variation of material properties due to temperature	64
8.1.2	An approximate theoretical solution	65
8.1.3	Finite Element Solution	70
8.1.4	Results and Discussion	72
8.2	The steady state plasticity flow problem	76
CHAPTER 9	Conclusions and Discussion	79
9.1	Suggestions for future work	85
TABLES		87
FIGURES		90
REFERENCES		128
APPENDICES		137
Appendix A	On the geometrically similar expansion of a hole in a thin infinite plate	i
Appendix B	Curve fitting for stress-strain data	ii
Appendix C	General large deformation formulation for the three-dimensional case	iv

		Page
Appendix D	Derivation of the element stiffness matrix for the axisymmetric case	vii
Appendix E	Derivation of the element stiffness matrix for the plane strain case (using natural modes)	x
Appendix F	Description and use of the computer programs	xiii
Appendix G	Listing of the computer programs	xxvii

NOMENCLATURE

A	Area of cross-section
$\mathbf{B}$	Strain displacement matrix
$\mathbf{D}$	Stress strain matrix
E	Young's Modulus
E_p	Plasticity modulus
F	Force on the specimen
G	Modulus of rigidity
$\mathbf{I}$	Unit matrix
$\mathbf{K}$	Overall stiffness matrix
$\mathbf{k}$	Element stiffness matrix
$\mathbf{k}_L$	Initial displacement matrix
$\mathbf{k}_\sigma$	Initial stress matrix (Geometric matrix)
$\mathbf{k}_T$	Total tangential stiffness matrix
$\mathbf{k}_N$	Natural stiffness matrix
$\mathbf{k}_e$	Elastic stiffness matrix
$\boldsymbol{\ell}$	Length matrix
ℓ	Length of a side of an element
m	Number of nodal points
n	Number of elements
$\mathbf{O}$	Null matrix
$\mathbf{R}$	Nodal forces
$\boldsymbol{\tau}$	Nodal displacements
T	Temperature
$u\ v\ w$	Displacements (Velocities)
$x\ y\ z$	Cartesian co-ordinates
$r\ \theta\ z$	Polar co-ordinates
α	Generalised co-ordinates

Nomenclature continued.

ϵ	Strain
$\bar{\epsilon}$	Equivalent strain
σ	Stress
$\bar{\sigma}$	Equivalent stress
ψ	Stream function
ν	Poisson's ratio
ρ	Element nodal displacements
P	Element nodal forces
δ_{ij}	Kronecker delta
ϕ	Flexibility matrix

Subscripts

D	Deviatoric
e	Elastic
ep	Elastic-plastic
H	Hydrostatic
i, j	Tensor notation
l	Large displacement
N	Natural
o	Small displacement
p	Plastic

Superscripts

t	Transpose of a matrix

Note All matrices are denoted by bold letters, e.g. $\underline{A} = \mathbf{A}$

Transpose of a matrix is also denoted by curly brackets

e.g. $a^t = \{a\}$

CHAPTER 1

1 INTRODUCTION

1.1 General

The finite element method of analysis is now well established and widely used for the solution of structural problems. Following the initial paper by Turner et al. (72) various types of elements have been developed and several kinds of non-linearities are dealt with, notably for problems of nonlinear material and nonlinear geometric behaviour. There exist now, general purpose computer programs which can be used with any type of element for the solution of large-scale problems.

Recently much attention has been given to nonlinear type of problems. There are, in general, two basic forms of nonlinearities; one arising from the nonlinear material behaviour and the other due to the nonlinear geometric behaviour; the latter being due to large displacements. The most common type of material nonlinearity occurs in the elastic-plastic material where the stress-strain relations are usually expressed in an incremental form.

It is now well known that all nonlinear problems should be analysed using incremental and/or iterative techniques. There are several methods to solve problems of elastic-plastic material. These methods have been divided into two main categories: the initial strain (or stress) method and tangent modulus method. In the first one, the plasticity effects are treated as initial strains (or stresses) and the problem is solved as an elastic one using only the elastic stiffness. The main advantage of this method is the ease with which it can be implemented in a general finite element

analysis, and that the stiffness matrix once developed for the elastic case remains unaffected by changes in the material properties. In the latter method the incremental linear constitutive relation, based on the plasticity theory used, is introduced directly into the governing equations. This would of course, modify the element stiffness at each incremental load step, thereby changing the overall stiffness matrix. For elastic-plastic problems involving small displacements, the tangent modulus method has some disadvantages, as compared to the alternative method, due to the changes in the overall stiffness matrix which has to be solved at each load increment. However, when the combined (geometric and material) nonlinear problem is considered the incremental approach becomes quite attractive. Here the nonlinearity arising from the changes in geometry could easily be incorporated at each incremental step together with the effects due to plasticity (because the relations derived from the flow theory of plasticity happen to be themselves incremental).

This thesis deals with the application of combined forms of nonlinearity to elastic-plastic materials. Prandtl-Reuss equations are used for the elastic-plastic material together with the yield criterion of von-Mises . Strain hardening is assumed to be of the form $\bar{\sigma} = \sigma_o (1 + \beta \bar{\epsilon}_p)^n$ although any other form could have been incorporated easily. Anisotropy resulting from directional hardening is neglected in the analysis, although this too may have been taken into account with a proper knowledge of such data.

The nonlinearity due to large deformations are taken into account by the use of Green's strain tensor. The so-called 'Initial stress matrix' (also referred to as 'Geometric matrix') and the 'Initial

displacement matrix' are derived from the Green's strain. However, by a proper updating of the coordinates of the continuum, the 'Initial displacement' matrix has been conveniently discarded. The 'Initial stress matrix' has been derived, alternatively, using the concept of natural modes which was initiated by Argyris (4).

Several problems are solved using the proposed method. (The computer programs appear in Appendix F). The models for the finite element analysis are chosen where theoretical solutions and/or experimental results are available. The problem of the thick walled cylinder is compared with theoretical results and the problem of the perforated strip is compared with existing experimental observations and finite element analysis, by other authors.

The model chosen for the combined nonlinear effect is the expansion of a hole in a conical plate made of an elastic-plastic material. This problem is of considerable interest due to the presence of large deformations, together with elasticity and plasticity. The problem has been solved theoretically using a one variable theory (2). Experiments were performed on a finite mild steel plate and the results are compared with those obtained theoretically.
Application of the method for the solution of the transient stages of a metal processing problem is considered. The process consists of drawing metal bars and hollow tubes by local heat and without dies (hence the name 'Dieless drawing'). The plastic deformation is effected by localised heating using an induction coil. The solutions obtained are compared with existing experimental observations.

1.2 LITERATURE SURVEY

1.2.1 Material Non-linearity (Plasticity)

Some of the early attempts to solve elastic-plastic problems include Marcal's work (44) (45) on a stiffness method which enabled the equilibrium equations to be expressed in terms of displacements. He solved the problem of a thick walled cylinder in the open and closed ended conditions using the Prandtl-Reuss laws of plasticity together with the yield criterion of von-Mises. A matrix displacement method for the analysis of elastic-plastic three dimensional continua was proposed by Argyris (7). He suggested a direct incremental approach and an iterative incremental approach for the solution of the problem by treating plastic strains as initial strains. Pope (62) (63) developed a procedure for the analysis of elastic-plastic, plane stress and plane strain problems when the stress-strain relations are of the incremental type. Using triangular elements the deformations are analysed on a step by step basis.

Marcal and King (50) solved several elastic-plastic two-dimensional problems using the finite element method. Here, a partial stiffness concept has been suggested and it has been used to study plane stress, plane strain and axisymmetric cases, made of von-Mises material obeying Prandtl-Reuss relations. Comparisons with known results have been made for the case of a long cylinder with internal pressure, a tensile specimen with a central hole in plane stress, and a notched tensile specimen. Later, Marcal (47) used this method for the elastic-plastic analysis of pressure vessel components.

Akyuz and Merwin (1) developed a method for the solution of nonlinear problems of elastoplasticity by the finite element method.

By using a piecewise linear load deflection relationship and a step-by-step computational algorithm, they developed a general procedure for the solution of elastoplastic problems. Yamada, Yoshimura and Sakurai (78) followed Marcal and King's work on the elastic-plastic finite element method, but used small and varying increments of load, sufficient just to cause yield in the successive elements.

An 'initial' stress method for the solution of elastic-plastic problems (an alternative to the 'initial strain' method of Argyris) was suggested by Zienkiewicz, Valliappan and King (80). This method has shown to yield more rapid convergence than the alternative approach and to permit large load increments without violating the yield criterion.

A paper by Argyris and Scharpf (13) completely describes all the present methods available for elastic-plastic analysis using the finite element method, in a concise matrix notation. Convergence criteria are set up for the initial strain and the initial stress methods. It is proved that the latter method will only diverge if an actual breakdown of the structure occurs.

Papers by Popov et al. (64) and Zudans (81) deal with elastic-plastic analysis of pressure vessels, using the incremental approach. A discrete element method for the plastic analysis of structures subjected to cyclic loading was given by Armen, Isakson and Pifko (14). Here the Bauschinger effect in multiaxial stress systems is taken into account by the use of Ziegler's modification of Prager's kinematic hardening theory. Applications have been made for several structures and comparison with existing test data for both montonic and reversed loading has shown good correlation.

Tresca's yield criterion and its associated flow rules were used for finite element analysis of elastic-plastic plane stress problems by Anand, Lee and Rossow (3). The material is assumed to be elastic-perfectly plastic and loading has been carried out in small incrementsl steps.

1.2.2 Geometric Nonlinearity

Geometric nonlinearities were first introduced by means of an incremental 'geometric stiffness' also known as the 'initial stress' matrix. Turner et al. (73) extended the method of direct formulation of the stiffness matrix to include the effect of non-uniform heating and large deformations. To overcome the inherent difficulty of the nonlinear problem for practical structures, they used an iterative and a step-by-step procedure; and obtained the force deformation relation for an axially loaded member and for a plate element.

Argyris (5) described a broad generalization of the matrix displacement technique for analysing three-dimensional elastic media; both for small and large displacement ranges. Using a natural definition for the component stresses, nodal loads and the elemental stiffness he established a concise expression for the cartesian stiffness of an arbitrary tetrahedron from which the stiffness of the complete system is obtained. The concept of an additional 'geometric stiffness' is introduced for large displacements which represented the effects of change of geometry on the equilibrium conditions. The geometric stiffness of a tetrahedron is shown to be identical to that of a six-bar pin jointed framework and a step-by-step procedure is suggested to solve the large displacement problem.

Wissmann (77) developed a tensor formulation for the analysis of nonlinear structures; including temperature expansion, pre-stresses, pre-strains and general anisotropies. The basis of the derivation is the fundamental strain expression of nonlinear theory of elasticity which allows for rotations of arbitrary magnitude. The derivation of the stiffness matrices necessary for analysing large deflection and stability problems are developed from the basic nonlinear theory derived by Martin (51). The derivation of stiffnesses for stringer, beam-column and thin triangular elements in plane stress are given here in detail.

Kapur and Hartz (39) developed a finite element approach for the plate buckling problem, involving the use of 'stability coefficient matrices' in conjunction with the stiffness matrices. This approach in matrix form is developed and extended to finite elements in two additional stiffness matrices; the 'initial stress matrix' and the 'initial displacement matrix'. Analysis without the use of initial displacement matrix resulted in overestimated results and it is concluded that the initial displacement matrix should be included in the finite element analysis of large deformation and instability problems.

A paper by Mallet and Marcal (43) describes three alternative mathematical models and computational procedures for nonlinear pre- and post buckling analysis. Schmit et al. (66) developed an analysis capable of predicting the nonlinear behaviour of elastic structural systems that can be idealized with rectangular plate and cylindrical shell discrete elements. Geometric non-linearities in the strain displacement relation are accounted for, in this analysis

and numerical solutions are obtained by direct minimization of the total potential energy.

A similar analysis was carried out by Kawai and Yoshimura (40) for the large deflection problem of a rectangular plate, employing an iterative technique. A paper by Brebbia and Connor (16) on 'Geometrically nonlinear finite element analysis' presents a formulation applicable to arbitrary plate and shallow shell elements. Here, the solutions are obtained by use of the Newton-Raphson method.

Argyris and Scharpf (11) (12) formulated the concept of the natural mode technique on a general basis. The first paper deals with small displacements and the second with large displacements including the derivation of the 'geometric stiffness'. A survey paper on 'Geometrically nonlinear problems of elasticity', by Hartz and Nathan (30) presents a general formulation of the problem of nonlinearity. From this formulation, simplification of the stiffnesses for restricted cases are derived and are compared with the existing formulation.

Chan and Firmin (18) analysed cooling towers by the finite element method and included the effect of large displacement. Dupuis (19) obtained an incremental variational principle involving rate of displacement in Lagrangian and Eulerian description, leading to incremental matrix equations in finite elements. Comparison between these two methods are made by solving 'generalized' plane stress problems.

1.2.3 Combined Nonlinearity

The solution of problems with combined material and geometric nonlinearity has been attempted but are relatively few in the literature. Akuz and Merwin (1) gave a solution to the problem of indentation of an elastoplastic half-space by a rigid punch, using the finite element method. They developed a procedure for the solution of elastic-plastic problems using a piecewise linear load-deflection relationship and a step-by-step computational algorithem. The effect of initial stresses was also considered when the rotation at each step was not negligible, although the strains were assumed small compared with unity.

A paper by Marcal (49) deals with the finite element analysis of combined problems of nonlinear material and geometric behaviours. He developed incremental stiffness matrices for the small strain large displacement analysis. A few case studies examining the behaviour of axisymmetric shells, flat plates and structures in plane stress are given here. A general finite element formulation for problems of large strains and large displacements was developed by Hibbit, Marcal and Rice (32). They have used a Lagrangian approach to the problem and developed an incremental and piecewise linear finite element theory with particular reference to the elastic-plastic behaviour of metals.

A series of papers by Nagamatsu, Murota and Jimma (52 - 57) deal with 'Non-uniform deformation of a block in plane-strain and axisymmetric compression caused by friction'. The material is assumed to be elastic, strain-hardening and deformation is pursued from elastic through partially plastic to totally plastic stages. The problem has been analysed using the calculus of variations and finite elements and

solutions are compared with results obtained experimentally.

Lee and Kobayashi (41) (42) analysed axisymmetric upsetting and plane strain side-pressing of solid cylinders by the finite element method. Solutions have been obtained up to a 30% reduction in height in axisymmetric upsetting and up to 19% reduction in side pressing. Computed solutions have been compared with those found experimentally, but no assessment has been made of the convergence or the accuracy of the solution obtained.

CHAPTER 2

2 GENERAL THEORY OF FINITE ELEMENTS

2.1 Small displacements

The direct stiffness method of finite element analysis is by now well established and widely used for the solution of small displacement and elastic problems (10) (79). Therefore only a brief derivation of the basic equations is given in this section, for continuity and clarity of the rest of the material in this thesis.

The displacement method of finite element analysis is used throughout this analysis. The continuum is first idealized into a number of discrete elements, interconnected by suitable nodal points. The displacements and the forces on the continuum are usually represented at these nodal points, the basic unknown for the problem being the nodal displacements. The other parameters are usually obtained from these displacements. A displacement mode with as many undetermined coefficients (generalized displacements) as there are nodal point displacements, is chosen for the type of element being used.

Consider the general three-dimensional case in which the coordinates are given by x, y, z; then

$$\rho\ (x, y, z) = (u\ v\ w)^t \qquad (2.1)$$

where ρ is the displacement at any point,

and u, v, w the respective displacements in the x, y, z directions.

Hence, $$\rho = f\ (x, y, z)\ \alpha \qquad (2.2)$$

where α are the generalised displacements,

and $f\ (x, y, z)$ the chosen displacement function.

Substituting the displacements and the coordinates at the nodal points, we have,

$$\rho = \mathbf{F}\,\alpha \tag{2.3}$$

where $$\rho = \left(u,\ v,\ w,\ \ldots\ u_n\ v_n\ w_n\right)^t \tag{2.4}$$

n being the number of nodal points per element.

Inverting (2.3) we get,

$$\alpha = \mathbf{F}^{-1}\,\rho \tag{2.5}$$

Now, defining a differential operator **A** which transforms the generalised displacements into strains,

$$\epsilon = \mathbf{A}\,\alpha \tag{2.6}$$

Therefore $\epsilon = \mathbf{A}\,\mathbf{F}^{-1}\rho$

i.e. $$\epsilon = \mathbf{B}\,\rho \tag{2.7}$$

giving the usual strain-displacement matrix. The external forces **P** are assumed to be acting at the nodal points and using the Principle of Virtual Work, we have,

$$\delta\rho^t\,\mathbf{P} = \int \delta\epsilon^t\,\sigma\ dv \tag{2.8}$$

where σ are the stresses.

Substituting equation (2.7) into (2.8) and cancelling the non-zero displacement vector, we get,

$$\rho = \int \mathbf{B}^t\,\sigma\ dv \tag{2.9}$$

The stresses and the strains are usually related as

$$\sigma = \mathbf{D}\,\epsilon \tag{2.10}$$

where **D** is known as the stress-strain stiffness matrix.

Now equation (2.9) becomes,

$$\mathbf{P} = \mathbf{k}\,\rho$$

where $$\mathbf{k} = \int \mathbf{B}^t\,\mathbf{D}\,\mathbf{B}\ dv \tag{2.12}$$

is known as the element stiffness matrix.

2.1.1 B and D Matrices

The derivation of the above two matrices for most of the elements for the elastic case can be found in text books on finite elements and therefore is not considered in detail here. For the general three-dimensional case the stresses and strains can be expressed as,

$$\boldsymbol{\sigma} = \left\{ \sigma_x \ \sigma_y \ \sigma_z \ \sqrt{2}\,\sigma_{xy} \ \sqrt{2}\,\sigma_{yz} \ \sqrt{2}\,\sigma_{zx} \right\} \tag{2.13}$$

$$\boldsymbol{\epsilon} = \left\{ \epsilon_x \ \epsilon_y \ \epsilon_z \ \frac{1}{\sqrt{2}}\gamma_{xy} \ \frac{1}{\sqrt{2}}\gamma_{yz} \ \frac{1}{\sqrt{2}}\gamma_{zx} \right\} \tag{2.14}$$

If the displacements are assumed to be small,

$$\epsilon_x = \frac{\partial u}{\partial x}$$

$$\epsilon_{xy} = \tfrac{1}{2}\gamma_{xy} = \tfrac{1}{2}\left(\frac{\partial u}{\partial y} + \frac{\partial v}{\partial x}\right) \text{ etc.} \tag{2.15}$$

The differential operator **A** for this case can be derived from equation (2.15).

Now using (2.7) we obtain

$$\mathbf{B} = \mathbf{A}\,\mathbf{F}^{-1}$$

The stress-strain matrix for an isotropic elastic material can be shown to be,

$$\mathbf{D} = 2G\left[\mathbf{I}_6 + \frac{\nu}{1-2\nu}\,\mathbf{e}_3\,\mathbf{e}_3^t\right] \tag{2.16}$$

where $\mathbf{I}_6$ = (6 x 6) unit matrix,

and $\mathbf{e}_3 = \{1\ 1\ 1\ 0\ 0\ 0\}$

The overall stiffness matrix **K** is obtained by the appropriate assembly of all the element stiffness matrices.

$$\mathbf{K}\boldsymbol{\tau} = \mathbf{R} \tag{2.17}$$

where $\mathbf{R}$ = the nodal forces,

$\boldsymbol{\tau}$ = the nodal displacements.

This matrix relating all the nodal displacements to the nodal loads is generally singular as it includes the rigid body motions and rotations. These rigid body motions should be suppressed by applying suitable boundary conditions before any attempt is made to solve the set of simultaneous equations.

2.2 Plasticity

The mechanical behaviour of a perfectly plastic solid is defined by the yield criterion and the flow rule. The yield condition specifies the state of stress under which plastic flow will occur. For each of these states of stress, the flow rule specifies the components of the plastic strain rate to within an arbitrary common factor. The perfectly plastic solid is therefore inviscid and the state of stress necessary to cause a certain type of plastic flow does not depend on the speed of deformation.

Alternatively, if the perfectly plastic solid is assumed to be incompressible (which is generally found to be true as an experimental fact), a given state of strain rate does not yield a single valued state of stress. This is because the hydrostatic stress is indeterminate from a known state of strain rate.

These difficulties arise only when the material is perfectly plastic and the inclusion of elasticity and strain hardening yields single valued correspondence between the stresses and the strains. In plasticity the total stresses and the total strain cannot be related directly, as it is well established that such a unique relation does not exist. The strains not only depend on the final state of stress but also on the complete loading history. Thus to develop a workable

relation for stress and strain, these quantities have to be replaced by their respective increments. This avenue of the theory of plasticity is known as the 'incremental strain theory' or the 'flow theory of plasticity'.

2.2.1 Yield Surface

It has been generally accepted (as an experimental fact) that yielding can occur only if the stress σ satisfies the general yield criterion,

$$f(\sigma, k) = 0 \tag{2.18}$$

where k is a hardening parameter.

This yield condition can be visualised as a surface in the space of stress (three-dimensional in general) with the position of the surface dependent on the instantaneous value of the parameter k.

2.2.2 Flow Rule

Von-Mises first suggested the basic constitutive relation defining the plastic strain increment in relation to the yield surface. Prager, Drucker and other workers in this field have proposed the following relationship for the increment of plastic strain which has now been accepted generally (8D).

$$\delta \epsilon_p = \lambda \frac{\partial f}{\partial \sigma} \tag{2.19}$$

or, for any component

$$\delta \epsilon_{np} = \lambda \frac{\partial f}{\partial \sigma_n}$$

where $\delta \epsilon_p$ = increment of plastic strain

and λ = proportionality constant to be determined later.

This rule is known as the 'normality' principle which has been interpreted as a normality requirement of the plastic strain increment vector to the yield surface in the space of stress.

Using the yield criterion of von-Mises in equation (2.18) it can be proved that equation (2.19) gives the well known Levy-Mises relations, which together with Hooke's Law in elasticity, gives the Prandtl-Reuss relations for an elastic-plastic material. This has been proved indirectly in the next section by deriving the stress-strain stiffness matrix using equation (2.19) and then the Prandtl-Reuss relations arriving at identical expressions.

2.3 Elastic-Plastic Stress-strain Stiffness Matrix

Considering the general three-dimensional case, the elastic relation between the stresses σ and the elastic strains ϵ_e can be expressed as

$$\sigma = D_e \epsilon_e$$

where $$D_e = 2G \left[I_6 + \frac{\nu}{1-2\nu} e_3 e_3^t \right] \qquad (2.16)$$

Also, it can be shown that the strain-stress flexibility matrix is given by,

$$\phi_e = D_e^{-1} = \frac{1}{2G} \left[I_6 - \frac{\nu}{1+\nu} e_3 e_3^t \right] \qquad (2.20)$$

The total strain increment can be written as the sum of the elastic and plastic parts,

$$\delta\epsilon = \delta\epsilon_e + \delta\epsilon_p \qquad (2.21)$$

Substituting equation (2.19) and (2.20) in equation (2.21), we obtain,

$$\delta\epsilon = \phi_e \delta\sigma + \lambda \frac{\partial f}{\partial \sigma} \qquad (2.22)$$

Separating the stress $\boldsymbol{\sigma}$ into the hydrostatic and deviatoric parts,

$$\boldsymbol{\sigma} = \boldsymbol{\sigma}_H + \boldsymbol{\sigma}_D \tag{2.23}$$

where $$\boldsymbol{\sigma}_H = \frac{1}{3} (I_1 \; I_1 \; I_1 \; 000)^t \tag{2.24}$$

and $$I_1 = \sigma_x + \sigma_y + \sigma_z \tag{2.25}$$

Equation (2.24) could also be written as,

$$\boldsymbol{\sigma}_H = \frac{1}{3} \mathbf{e}_3 \; \mathbf{e}_3^t \; \boldsymbol{\sigma} \tag{2.24a}$$

Therefore $\boldsymbol{\sigma}_D = \boldsymbol{\mu\sigma}$

where $$\boldsymbol{\mu} = \mathbf{I}_6 - \frac{1}{3} \mathbf{e}_3 \; \mathbf{e}_3^t \tag{2.27}$$

and the following derivations become evident.

$$\begin{aligned} \boldsymbol{\mu}^t &= \boldsymbol{\mu} \\ \boldsymbol{\mu\mu} &= \boldsymbol{\mu}^t \boldsymbol{\mu} = \boldsymbol{\mu} \\ \boldsymbol{\mu D}_e &= \mathbf{D}_e \boldsymbol{\mu} = 2G\boldsymbol{\mu} \end{aligned} \tag{2.28}$$

Assuming the yield criterion de to von-Mises, we get,

$$f(\boldsymbol{\sigma}) = \frac{3}{2} \boldsymbol{\sigma}_D^t \boldsymbol{\sigma}_D - \bar{\sigma}^2 = \frac{3}{2} \boldsymbol{\sigma}^t \boldsymbol{\mu\sigma} - \bar{\sigma}^2 = 0 \tag{2.29}$$

where $\bar{\sigma}$ is the equivalent yield stress.

Therefore equation (2.22) becomes,

$$\delta\boldsymbol{\epsilon} = \boldsymbol{\phi}_e \; \delta\boldsymbol{\sigma} + 3\lambda \; \boldsymbol{\sigma}_D \tag{2.30}$$

It can be shown, from a comparison with a uniaxial state of stress that the unknown parameter λ can be expressed as,

$$\lambda = \frac{1}{2} \frac{1}{E_p} \frac{\delta\bar{\sigma}}{\bar{\sigma}} \tag{2.31}$$

where $$E_p = \frac{d\bar{\sigma}}{d\bar{\epsilon}_p} \tag{2.32}$$

is known as the modulus of plasticity.

Differentiating equation (2.29) we get

$$\bar{\sigma}\,\delta\bar{\sigma} = \frac{3}{2}\,\boldsymbol{\sigma}^{t}\,\boldsymbol{\mu}\,\delta\boldsymbol{\sigma}$$

i.e. $$\delta\bar{\sigma} = \frac{3}{2}\,\frac{1}{\bar{\sigma}}\,\boldsymbol{\sigma}_D^{\,t}\,\delta\boldsymbol{\sigma} \qquad (2.33)$$

Using equations (2.33) and (2.31), equation (2.30) becomes,

$$\delta\boldsymbol{\epsilon} = \boldsymbol{\phi}_e\,\delta\boldsymbol{\sigma} + \frac{9}{4}\,\frac{\boldsymbol{\sigma}_D\,\boldsymbol{\sigma}_D^{\,t}}{E_p\,\bar{\sigma}^2}\,\delta\boldsymbol{\sigma} \qquad (2.34)$$

<u>or</u> $$\delta\boldsymbol{\epsilon} = (\boldsymbol{\phi}_e + \boldsymbol{\phi}_p)\,\delta\boldsymbol{\sigma} \qquad (2.34a)$$

i.e. $$\delta\boldsymbol{\epsilon} = \boldsymbol{\phi}_e\left[\mathbf{I}_6 + \frac{9}{4}\,\mathbf{D}_e\,\frac{\boldsymbol{\sigma}_D\,\boldsymbol{\sigma}_D^{\,t}}{E_p\,\bar{\sigma}^2}\right]\delta\boldsymbol{\sigma}$$

i.e. $$\delta\boldsymbol{\epsilon} = \boldsymbol{\phi}_e\left[\mathbf{I}_6 + \frac{9}{4}\,\frac{2G}{E_p\bar{\sigma}^2}\,\boldsymbol{\sigma}_D\,\boldsymbol{\sigma}_D^{\,t}\right]\delta\boldsymbol{\sigma} \qquad (2.35)$$

It can be proved that,

$$(\mathbf{I} + \lambda\,\mathbf{a}\,\mathbf{a}^{t})^{-1} = (\mathbf{I} - \mu\,\mathbf{a}\,\mathbf{a}^{t}) \qquad (2.36)$$

where $\mathbf{a}$ is a column vector

and $$\mu = \frac{\lambda}{1+\lambda\,\mathbf{a}^{t}\mathbf{a}}$$

The inversion of equation (2.35) using (2.36) yields,

$$\delta\boldsymbol{\sigma} = \mathbf{D}_e\left[\mathbf{I}_6 - \frac{3G}{E_p+3G}\,\frac{\boldsymbol{\sigma}_D\boldsymbol{\sigma}_D^{\,t}}{\boldsymbol{\sigma}_D^{t}\boldsymbol{\sigma}_D}\right]\delta\boldsymbol{\epsilon}$$

<u>i.e.</u> $$\delta\boldsymbol{\sigma} = \mathbf{D}_{ep}\,\delta\boldsymbol{\epsilon} \qquad (2.37)$$

and it can be shown that,

$$\mathbf{D}_{ep} = \mathbf{D}_e - \frac{2G}{(1+E_p/3G)}\,\frac{\boldsymbol{\sigma}_D\boldsymbol{\sigma}_D^{\,t}}{\boldsymbol{\sigma}_D^{t}\boldsymbol{\sigma}_D} \qquad (2.38)$$

This result can be obtained directly by using the Prandtl-Reuss equations.

$$\delta\epsilon'_{ij} = \frac{\delta\sigma'_{ij}}{2G} + \frac{3\sigma'_{ij}\,\delta\bar{\sigma}}{2\bar{\sigma}\,E_p} \tag{2.39}$$

$$\delta\epsilon_{ii} = \frac{(1-2\nu)}{E}\,\delta\sigma_{ii}$$

(From Hill's (33) p. 39).

These can be written in the matrix form as,

$$\delta\epsilon = \phi_e\,\delta\sigma + \frac{3}{2}\frac{\sigma_D\,\delta\bar{\sigma}}{\bar{\sigma}\,E_p} \tag{2.39a}$$

Substitution of equation (2.33) leads to the same expression as in (2.34).

ϕ_e and ϕ_p are known as the elastic and the plastic flexibilities respectively. It is interesting to note that ϕ_e can be inverted except for the trivial case, when $\nu = \frac{1}{2}$ (incompressible material) and ϕ_p is singular and cannot be inverted directly. This is mathematically obvious as any general matrix of the form $\mathbf{A} = \mathbf{a}\mathbf{a}^t$ where $\mathbf{a}$ is a column matrix has the lowest possible rank of 1 and is hence singular. Thus, it would seem a direct displacement method formulation of the stiffness matrix for the case of the rigid-plastic material is not possible.

CHAPTER 3

3 LARGE DEFORMATION THEORY

3.1 Green's Strain Tensor

For small deformations, the infinitesimal theory of strain is quite sufficient and since the displacements and their derivations are assumed to be small the quadratic terms arising in the general strain expression can be neglected. In the large deformation theory the displacements and their derivations could be quite appreciable and the nonlinear terms in the general strain are therefore taken into account.

There are two modes of description of the deformation of a continuous medium, the Lagrangian and the Eulerian. The Lagrangian description employs the coordinates (x_i) of a typical particle in the initial state as the independent variables, while in the case of Eulerian coordinates the independent variables are the coordinates (α_i) of a material point in the deformed state. When the deformations are infinitesimal these two definitions coalesce and there is no need to make any distinction between the two. The Lagrangian definition of strain is used here, and attention is drawn to the derivation of this as follows.

Consider a body (Fig. 1) defined by a coordinate system $x_1\ x_2\ x_3$ chosen so that a point P of the body has coordinates a_i. When the body deforms the point P moves to Q with coordinates α_i with respect to a new coordinate system $\alpha_1\ \alpha_2\ \alpha_3$.

Considering an infinitesimal line element connecting two points P (x_1, x_2, x_3) and P'$(x_1 + d\,x_1, x_2 + d\,x_2, x_3 + d\,x_3)$ and the corresponding points Q and Q' in the deformed state it can be

proved that (22),

$$2\epsilon_{ij} = \frac{\partial u_i}{\partial x_j} + \frac{\partial u_j}{\partial x_i} + \frac{\partial u_k}{\partial x_i} + \frac{\partial u_k}{\partial x_j} \tag{3.1}$$

or if $x_1 = x,\ x_2 = y,\ x_3 = z$

and $u_1 = u,\ u_2 = v,\ u_3 = w$

$$\epsilon_{xx} = \frac{\partial u}{\partial x} + \frac{1}{2}\left[\left(\frac{\partial u}{\partial x}\right)^2 + \left(\frac{\partial v}{\partial x}\right)^2 + \left(\frac{\partial w}{\partial x}\right)^2\right] \tag{3.2}$$

$$\epsilon_{xy} = \frac{1}{2}\gamma_{xy} = \frac{1}{2}\left[\frac{\partial u}{\partial y} + \frac{\partial v}{\partial x} + \frac{\partial u}{\partial x}\cdot\frac{\partial u}{\partial y} + \frac{\partial v}{\partial x}\cdot\frac{\partial v}{\partial y} + \frac{\partial w}{\partial x}\cdot\frac{\partial w}{\partial y}\right]$$

and similarly for other components.

The strain tensor ϵ_{rs} was introduced by Green and St. Venant and is known as Green's strain tensor. When the deformations are not large these reduce to the usual definition of infinitesimal strains. It can be shown that for the small strain case ϵ_{ii} can be interpreted as extension of vectors originally parallel to the coordinate axes while ϵ_{ij} represents stress or changes of angle between vectors originally at right angles. When the strain components are large however, it is no longer possible to give simple geometrical interpretations of the strain tensor ϵ_{rs}.

3.2 Geometric nonlinearity (Ref. p.414 Zienkiewicz (79))

When large deformations are encountered in finite element problems, the nonlinearity due to the change of the geometry of the body has to be taken into account to predict the displacements, strains and stresses accurately.

The strain displacement matrix for the large deformation case would change considerably with the change of the geometry of the structure and thus would not remain constant as in the case of

small displacement analysis. However considering the current state and for a small load increment we can have,

$$\delta \underline{\epsilon} = \overline{B}\, d\rho \tag{3.3}$$

where $$\overline{B} = B_o + B_L(\rho) \tag{3.4}$$

B_o is the usual small displacement matrix, and B_L is due to the large deformations and is usually a function of the displacements, ρ. From the Principle of Virtual Work for a small increment of displacements, it can be shown that,

$$P = \int \overline{B}^t \sigma \, dv \tag{3.5}$$

where P are the nodal forces.

Differentiating equation (3.5), we get

$$\delta P = \int \overline{B}^t \delta\sigma \, dv + \int d\overline{B}^t \sigma \, dv$$

Substituting equation (2.37)

$$\delta P = \int \overline{B}^t D_{ep} \overline{B} \, dv \, \delta\rho + \int \delta\overline{B}^t \sigma \, dv \tag{3.6}$$

From equation (3.4)

$$\delta\overline{B}^t = \delta B_L^t \tag{3.7}$$

Now, equation (3.6) becomes,

$$\delta P = (k_o + k_L + k_\sigma)\delta\rho \tag{3.8}$$

where $$k_o = \int B_o D_{ep} B_o \, dv \tag{3.9}$$

$$k_L = \int B_o D_{ep} B_L \, dv + \int B_L D_{ep} B_o \, dv + \int B_L D_{ep} B_L \, dv \tag{3.10}$$

$$k_\sigma \delta\rho = \int \delta B_L^t \sigma \, dv \tag{3.11}$$

k_o is the usual small displacement stiffness matrix.

k_L is known as the initial displacement stiffness matrix.

$\overline{k} = k_o + k_L$ is known as the large displacement matrix, which could alternatively be obtained by using an infinitesimal strain but adjusting the element coordinates in the computation of the stiffness.

$\mathbf{k}_\sigma$ is known as the initial stress matrix or the geometric matrix and is a symmetric matrix dependent on the stress level.

$$\mathbf{k}_T = \mathbf{k}_o + \mathbf{k}_L + \mathbf{k}_\sigma \qquad (3.12)$$

is known as the total tangential stiffness matrix.

The above derivation has been carried out following Zienkiewicz (79). He has shown that eq. (3.5) which indicates the equilibrium conditions between internal and external forces is generally valid whether displacements and strains are large or small. However, eq. (3.6) would be limited for small strains only. This is because the stress given in eq. (3.5) is the Kirchoff-Piola stress while the current true stress (Euler stress) has to be used for the evaluation of $\mathbf{D}_{ep}$. This limitation may be overcome, perhaps by transforming the Kirchoff stress to the corresponding Euler stress by the use of the initial and final configurations.

The solution to eq. (3.8) may be obtained for small, successive increments of the load. Zienkiewicz (79)(p.417) has pointed out that it is important to check periodically the total equilibrium by using eq. (3.5). This has not been included in the present work and some error accumulation when large numbers of increments are involved may be inevitable.

CHAPTER 4

4 AN ALTERNATIVE DERIVATION OF THE STIFFNESS MATRIX

An alternative derivation of the stiffness matrix is discussed in this chapter. The method, although somewhat compact and direct for some elements, does not seem to be of any particular advantage in general. The stiffness matrices obtained in this method would be identical to the ones obtained earlier in Chapter 2 for the elastic, small displacement case. For large deformations the Eulerian description is adopted, as against the Lagrangian description described earlier, thereby changing the additional matrices involved due to large displacements. The theory given here is only applicable for a tetrahedral element with a constant stress and strain and derivations are made following Argyris (5)(6). Although a computer program was developed for this case, no proper 3-dimensional problem was solved using this program.

4.1 The concept of natural modes

The idea of natural modes in the formulation of the matrix displacement method was first initiated by Argyris in 1962. The natural modes can be defined as the pure straining modes which exclude rigid body displacements. The standard specification of kinematic modes due to displacements in the direction of axes may lead to somewhat complex expressions for some elements and may not display symmetry with respect to the coordinated systems. Thus some advantage may be seen for some particular elements in the derivation of the stiffness matrix when large deformations are experienced. On the other hand the large deformation formulation given in Chapter 3 (Zienkiewicz (79) p. 414) is more general as the basic theory is developed for any element at first and is carried on for special cases afterwards.

4.2 The natural mode technique

Consider an element with n nodal points in space. Deformation of the element is limited by the 3n nodal displacements, which may be imposed in turn at n nodal points. This definition of the state of deformation clearly includes rigid body displacements which

do not give rise to straining of the element and hence do not affect the stiffness of the element. Therefore to describe the straining conditions of the element

$$\gamma = (3n - 6) \tag{4.1}$$

kinematic modes would be sufficient.

(For a three-dimensional body the 6 rigid body motions are the 3 translations and the 3 rotations).

For a plane element in 2-dimension

$$\gamma = (2n - 3) \tag{4.1a}$$

These natural modes defining the pure deformation mode of the element are denoted by ρ_N. The associated stiffness matrix k_N of reduced order (3n - 6) or (2n - 3) is designated as a natural one. The complete description of the displacements require the rigid body motion of the element and is denoted by a vector ρ_o (6 x 1) or (3 x 1).

4.3 Theory for Three-Dimensional, TET4 Element (Fig. 3)

This is the simplest element for three dimensional bodies and can be fitted to any shape or contour without much difficulty. A linearly varying displacement function is assumed inside each element giving rise to a constant state of strain and stress. With four nodal points for every element, each having three degrees of freedom, it would require 4 x 3 nodal displacements for the solution resulting in a 12 x 12 element stiffness matrix.

A fundamental feature of the natural mode technique is the specification of an invariant or natural stiffness which ignores the rigid body components inevitably associated with the full cartesian specification of nodal points. The rigid body motion does not strain

or deform the element and is ignored when defining the stiffness of an element. Thus stiffness matrices of the order of 3 x 3 for the case of plane triangular elements and 6 x 6 for the case of tetrahedral elements are obtained.

A further development of this method is that, instead of describing a state of stress by the classical scheme of direct and shear stresses referred to a cartesian system, a simplification is obtained by defining stress and strain vectors in terms of direct components measured parallel to the three sides of the triangle or six sides of the tetrahedron. This stress strain specification originated by Argyris (8) was denoted as a 'natural one'. The stiffness relating the elongation and nodal forces along the sides is called the natural stiffness of the element.

4.3.1 Small displacement theory for the elastic case

Consider the three dimensional medium to be made up of n tetrahedra whose vertices are connected by m nodal points. The position and geometry of each tetrahedron are specified by

$$\psi_i = (x_i \; y_i \; z_i)^t \qquad (4.2)$$

$$i = 1, 2, 3, 4$$

or, for all four vertices,

$$\psi = (\psi_1 \; \psi_2 \; \psi_3 \; \psi_4)^t$$

The adoption of a linear variation of displacements within each element and the exclusion of the three rigid body movements lead to the (6 x 1) natural load displacement vector ρ_N which uniquely defines the state of deformation in terms of the elongation of the

six edges. A (6 x 1) natural load vector $\mathbf{P}_N$ could be introduced in duality to $\boldsymbol{\rho}_N$ and this would automatically ensure the equilibrium of each tetrahedron taken individually.

Thus we have,

$$\boldsymbol{\rho}_N = (\rho_{12}\ \rho_{23}\ \rho_{34}\ \rho_{41}\ \rho_{13}\ \rho_{24})^t \tag{4.4}$$

$$\mathbf{P}_N = (P_{12}\ P_{23}\ P_{34}\ P_{41}\ P_{13}\ P_{24})^t \tag{4.5}$$

where ρ_{ij} = elongation of side ij

and P_{ij} = self equilibrating load acting on nodal points i and j.

To analyse the assembly of the tetrahedra which represents the idealized system, it is necessary to consider also the more conventional cartesian definition of the nodal displacements and load of an element, i.e.

$$\boldsymbol{\rho} = (\boldsymbol{\rho}_1\ \boldsymbol{\rho}_2\ \boldsymbol{\rho}_3\ \boldsymbol{\rho}_4)^t \tag{4.6}$$

$$\mathbf{P} = (\mathbf{P}_1\ \mathbf{P}_2\ \mathbf{P}_3\ \mathbf{P}_4)^t \tag{4.7}$$

where, $\boldsymbol{\rho}_i = (u\ v\ w)_i^t$ (4.8)

$$\mathbf{P}_i = (U\ V\ W)_i^t \tag{4.9}$$

The relationship between the natural and the cartesian forms can be obtained by defining a matrix $\mathbf{T}$ of dimensions (6 x 12) so that,

$$\boldsymbol{\rho}_N = \mathbf{T}\boldsymbol{\rho} \text{ and } \mathbf{P} = \mathbf{T}^t\mathbf{P}_N \tag{4.10}$$

Natural component stresses and nodal points (Fig. 4)

Defining natural component stresses as the component of the actual stresses parallel to the direction of the six edges, we have

$$\boldsymbol{\sigma}_N = (\sigma_{12}\ \sigma_{23}\ \sigma_{34}\ \sigma_{41}\ \sigma_{13}\ \sigma_{24})_c \tag{4.11}$$

σ_{ij} is not the true stress acting along ij as the contribution from

the other five stresses are present.

The true stress vector is given by,

$$\boldsymbol{\sigma}_{NT} = (\sigma_{12}\ \sigma_{23}\ \sigma_{34}\ \sigma_{41}\ \sigma_{13}\ \sigma_{24}) \tag{4.12}$$

Hence, $$\boldsymbol{\sigma}_{NT} = \mathbf{A}\,\boldsymbol{\sigma}_{N} \tag{4.13}$$

where $\mathbf{A}$ is a transformation matrix made up of the direction cosine of the edges.

The relation between the natural stresses $\boldsymbol{\sigma}_N$ and the natural loads $\mathbf{P}_N$ can be established as,

$$\mathbf{P}_N = V\, l^{-1}\, \boldsymbol{\sigma}_N \tag{4.14}$$

where V = volume of the tetrahedron

$$l = \begin{bmatrix} l_{12} & & \cdots & l_{24} \end{bmatrix}$$

is a diagonal matrix consisting of the length of the edges.

Natural strains and stiffnesses

Considering the isotropic elastic tetrahedron, a relation for the natural strain can be obtained as,

$$\boldsymbol{\epsilon}_N = \frac{1}{E}\, \mathbf{A}_T\, \boldsymbol{\sigma}_N \tag{4.15}$$

where $$\boldsymbol{\epsilon}_N = (\epsilon_{12}\ \epsilon_{27}\ \epsilon_{34}\ \epsilon_{41}\ \epsilon_{13}\ \epsilon_{24})^t \tag{4.16}$$

and $$\mathbf{A}_T = (1+\nu)\,\mathbf{A} - \nu\,\mathbf{e}_6\mathbf{e}_6^t \tag{4.17}$$

and $$\mathbf{e}_6 = (1\ 1\ 1\ 1\ 1\ 1)^t$$

The natural stiffness matrix of the tetrahedron can be obtained as follows.

$$\rho_N = l\,\epsilon_N = \frac{1}{E}\, l\, \mathbf{A}_T\, \boldsymbol{\sigma}_N$$

and using equation (4.14)

$$\rho_N = \frac{1}{EV}\, l\, \mathbf{A}_T\, l\ \mathbf{P}_N$$

or $$\mathbf{P}_N = \mathbf{k}_N \boldsymbol{\rho}_N \tag{4.18}$$

where $$\mathbf{k}_N = E\, V\, \boldsymbol{\ell}^{-1}\, \mathbf{A}_T^{-1}\, \boldsymbol{\ell}^{-1} \tag{4.19}$$

Using equation (4.10) we have the cartesian stiffness matrix $\mathbf{k}$

$$\mathbf{P} = \mathbf{k}\, \boldsymbol{\rho} \tag{4.20}$$

and $$\mathbf{k} = \mathbf{T}^t\, \mathbf{k}_N\, \mathbf{T} \tag{4.21}$$

Assembly of all element stiffnesses to obtain the overall stiffness $\mathbf{K}$ is carried out in the standard manner.

4.3.2 Large displacements (Fig. 5)

The technique is based on a step by step process of sequential linearization corresponding to an incremental representation of the load history. For each step the total displacement vector is obtained from a linear matrix equation which is identical to the small matrix displacement formulation, the only difference arising, in the specification of the stiffness matrix which must be considered as the sum of two component matrices. The first matrix is in fact the standard elastic stiffness matrix, based on for each incremental step the instantaneous dimensions. The second one simulates the effect of change of geometry on the equilibrium conditions and is denoted by the geometric stiffness (also known as the initial stress matrix). It is found to be linearly dependent upon the instantaneous natural nodal loads.

The equilibrium conditions between the nodal forces and the stresses are referred to the instantaneous geometry of the tetrahedra and therefore the stresses are the so-called true stresses based on the current dimensions. The total stress, total strain relationship may take any arbitrary non-linear form in general, (including the effect of plasticity); but, of course, assuming that the stress-strain relation for every increment is linear.

For large deformations, the relation between the natural and cartesian displacements eq. (4.10) has to be given in the incremental form as,

$$d\rho_N = T_N d\rho \tag{4.22}$$

where T_N is derived (Ref (5)) using the current geometry.
$d\rho_N$ and $d\rho$ are the increments of natural and cartesian displacements. During this small increment let the cartesian and natural load, P and P_N change to $P + dP$ and $P_N + dP_N$ respectively. Then, by considering the states before and after the increment it can be shown that,

$$P = T_N^t P_N \tag{4.10}$$

and

$$P + dP = (T_N^t + dT_N^t)(P_N + dP_N) \tag{4.23}$$

where dT_N is the change of T_N with the geometry.
Hence,

$$dP = T_N^t dP_N + dT_N^t P_N \tag{4.24}$$

It can be seen that

$$\begin{aligned} T_N^t dP_N &= T_N^t K_N d\rho_N \\ &= T_N^t K_N T_N d\rho \\ &= K_e d\rho \end{aligned} \tag{4.25}$$

which is the usual small displacement matrix, assuming that within an element the strains remain small,

The second term in equation (4.24) can be expanded as,

$$d T_N^t P_N = \left[d T_{N1}^t \cdots d T_{Ni}^t \cdots \right] \begin{bmatrix} P_{N1} \\ \vdots \\ P_{Ni} \\ \vdots \end{bmatrix}$$

$$= \sum P_{Ni} d T_{Ni}^t \qquad (4.26)$$

$$d T_{Ni}^t = \frac{\partial T_{Ni}^t}{\partial \rho_1} d\rho_1 + \cdots + \frac{\partial T_{Ni}^t}{\partial \rho_k} d\rho_k + \cdots$$

$$= \left[\frac{\partial T_{Ni}^t}{\partial \rho_1} \cdots \frac{\partial T_{Ni}^t}{\partial \rho_k} \cdots \right] d\rho \qquad (4.27)$$

Since, $d\rho_N = T_N d\rho$

it can be shown that,

$$d\rho_{Ni} = T_{Ni} d\rho \qquad (i^{th} \text{ row}) \qquad (4.28)$$

But $$d\rho_{Ni} = \frac{\partial \rho_{Ni}}{\partial \rho_1} d\rho_1 + \cdots + \frac{\partial \rho_{Ni}}{\partial \rho_j} d\rho_j + \cdots$$

$$= \left[\frac{\partial \rho_{Ni}}{\partial \rho_1} \cdots \frac{\partial \rho_{Ni}}{\partial \rho_j} \cdots \right] d\rho \qquad (4.29)$$

Comparing eq. (4.28) and eq. (4.29)

$$T_{Ni} = \left[\frac{\partial \rho_{Ni}}{\partial \rho_1} \cdots \frac{\partial \rho_{Ni}}{\partial \rho_j} \cdots \right] \qquad (4.30)$$

Substituting this is eq. (4.27) we have

$$d T_{Ni}^t = \begin{bmatrix} \frac{\partial^2 \rho_{Ni}}{\partial \rho_1^2} \cdots \frac{\partial^2 \rho_{Ni}}{\partial \rho_1 \partial \rho_k} \cdots \\ \vdots \\ \frac{\partial^2 \rho_{Ni}}{\partial \rho_j \partial \rho_1} \cdots \frac{\partial^2 \rho_{Ni}}{\partial \rho_j \partial \rho_k} \cdots \\ \vdots \end{bmatrix} d\rho$$

$$= \lambda_i \, d\rho \qquad (4.31)$$

Now, eq. (4.26) becomes

$$dT_N^t P_N = \sum P_{Ni} \lambda_i d\rho = K_\sigma d\rho \qquad (4.32)$$

Hence, $$dP = K \, d\rho \qquad (4.33)$$

where $$K = K_e + K_\sigma \qquad (4.34)$$

K_σ is the so-called geometric matrix, which corrects the equilibrium condition for the change of geometry generated by large displacements.

The geometric matrix of the tetrahedron is obtained by combining the geometric matrices of the equivalent pin-jointed six bar framework whose members run along the edges of the tetrahedron.

For a single pin-jointed bar K_σ can be written as (83):

$$K_{\sigma ij} = \frac{P_{ij}}{l_{ij}} \left[\begin{bmatrix} I_3 & -I_3 \\ -I_3 & I_3 \end{bmatrix} - C_{eij}^t C_{eij} \right] \qquad (4.35)$$

where $$C_{eij} = \begin{bmatrix} -C_{ij} & C_{ij} \end{bmatrix} \qquad (4.36)$$

and C_{ij} are the direction cosines of the bar

P_{ij}, l_{ij} are the load and length of the bar respectively.

The geometric stiffness of the tetrahedron is now obtained by the proper assembly of the six geometric stiffnesses. It can be

shown that (5):

$$k_\sigma = \sum_{ij=1,2}^{2,4} M_{ij}^t \, k_{\sigma_{ij}} \, M_{ij} \qquad (4.37)$$

where M_{ij} are (2 x 4) location or identification super matrices consisting of unit or zero sub-matrices of order 3.

For example,

$$M_{12} = \begin{bmatrix} I_3 & O_3 & O_3 & O_3 \\ O_3 & I_3 & O_3 & O_3 \end{bmatrix} \qquad (4.38)$$

The values of P_{ij} are accumulated from the previous loading steps as,

$$P_{ij} = \sum dP_{ij} \qquad (4.39)$$

4.3.3 Plasticity

The following derivation of the elastic-plastic stress-strain matrix assumes a material obeying the Prandtl-Reuss relations and the von Mises yield criterion.

The increment of the cartesian plastic strain $d\epsilon_p$ can be expressed in terms of the cartesian stress and the plastic modulus as,

$$d\epsilon_p = \frac{3}{2} \frac{d\bar{\sigma}}{E_p \bar{\sigma}} \sigma_D \qquad (4.40)$$

Also, we have ,

$$\sigma_D = \left[I - \frac{1}{3} e_3 e_3^t \right] \sigma$$

where σ_D is the cartesian deviatoric stress

and $e_3^t = [\,1\ 1\ 1\ 0\ 0\ 0\,]$

Now, defining a matrix β which relates the natrual stresses to the cartesian stresses, Argyris (6) has shown that,

$$\sigma = \beta \sigma_N \tag{4.41}$$

Hence,

$$d\epsilon_N^P = \beta^t d\epsilon_p \tag{4.42}$$

using eq. (4.40) we get

$$d\epsilon_N^P = \frac{3}{2} \frac{d\bar{\sigma}}{E_p \bar{\sigma}} \beta^t \left[I - \frac{1}{3} e_3 e_3^t \right] \beta \sigma_N$$

It has been shown that, (6)

$$\beta^t \beta = A$$

$$e_3^t \beta = e_6^t = [\,1\ 1\ 1\ 1\ 1\ 1\,] \tag{4.43}$$

Therefore,

$$d\epsilon_N^P = \frac{3}{2} \frac{d\bar{\sigma}}{E_p \bar{\sigma}} \left[A - \frac{1}{3} e_6 e_6^t \right] \sigma_N$$

$$= \frac{3}{2} \frac{d\bar{\sigma}}{E_p \bar{\sigma}} \sigma_{ND} \tag{4.44}$$

where $$\sigma_{ND} = \left[A - \frac{1}{3} e_6 e_6^t \right] \sigma_N \tag{4.45}$$

is called the natrual deviatoric stress.

The von Mises criterion is given in terms of the cartesian stresses as

$$\bar{\sigma}^2 = \frac{3}{2} \sigma_D^t \sigma_D$$

The plastic work done for an increment of plastic strain can be expressed as

$$dW_p = \sigma_N^t d\epsilon_N^p = \sigma^t d\epsilon_p$$

$$= \bar{\sigma}\, d\bar{\epsilon}_p = \bar{\sigma} \frac{d\bar{\sigma}}{E_p} \tag{4.46}$$

Substituting eq. (4.40)

$$dW_p = \frac{3}{2} \frac{d\bar{\sigma}}{E_p \bar{\sigma}} \sigma_N^t \sigma_{ND} \tag{4.47}$$

comparing (4.46) and (4.47),

$$\bar{\sigma}^2 = \frac{3}{2} \sigma_N^t \sigma_{ND} \tag{4.48}$$

The cartesian elastic flexibility is given by,

$$\phi_e = \frac{1}{2G} \left[I_6 - \frac{\nu}{1+\nu} e_3 e_3^t \right]$$

The natural elastic flexibility is obtained by the transformation

$$\phi_{Ne} = \beta^t \phi_e \beta \tag{4.49}$$

$$= \frac{1}{2G}\left[A - \frac{\nu}{1+\nu} e_6 e_6^t \right] \qquad (4.50)$$

The natural plasticity flexibility is obtained by a similar transformation,

$$\phi_P = \frac{9}{4} \frac{1}{E_p \bar{\sigma}^2} \sigma_D \sigma_D^t$$

Hence, $$\phi_{NP} = \beta^t \phi_P \beta \qquad (4.51)$$

$$= \frac{9}{4} \frac{1}{E_p \bar{\sigma}^2} \beta^t \sigma_D \sigma_D^t \beta$$

Now, $$\beta^t \sigma_D = \beta^t \left[I - \frac{1}{3} e_3 e_3^t \right] \sigma$$

$$= \beta^t \left[I - \frac{1}{3} e_3 e_3^t \right] \beta \sigma_N$$

$$= \left[A - \frac{1}{3} e_6 e_6 \right] \sigma_N$$

$$= \sigma_{ND} \qquad (4.52)$$

Hence $$\phi_{NP} = \frac{9}{4} \frac{1}{E_p \bar{\sigma}^2} \sigma_{ND} \sigma_{ND}^t \qquad (4.53)$$

Conclusions

An attempt has been made to present the derivation of the stiffness matrices in a general form illustrating the application by a tetrahedral element with constant strain, using an alternative m thod. Each tetrahedron is treated as an assembly of six pin-jointed bars and natural displacements and forces are defined along the length of these bars. It has been stated (5)(6), that the theory is valid for large strains and deformations, and that the inclusion of plasticity will not limit this validity. The plastic flexibility matrix is clearly only defined for non-ideal plasticity. Further the assumption of small strains within an element is implicit and thus only small elements should be used.

CHAPTER 5

5 COMPUTATIONAL PROCEDURE

The element stiffness of the structure is first evaluated using the elastic or the elastic-plastic matrices and the initial stress matrix. These stiffness matrices are assembled to form the overall stiffness matrix which represents the current relation between the incremental nodal forces and the displacements

$$\mathbf{dR} = \mathbf{K}\mathbf{dr} \tag{2.17}$$

of the body. A complete elastic-plastic solution to a problem is obtained by the successive application of equation (2.17) using a number of linearised incremental steps. The sequence of operations carried out during a typical analysis is best shown by a flow chart as follows.

5.1 Outline of the flow sequence

(1) Perform an elastic analysis of the body in the standard manner. Determine the equivalent stress of all the elements using the relation,

$$\bar{\sigma}^2 = \frac{3}{2}\sigma_D^t \sigma_D \tag{2.29}$$

(2) Find the 1^{th} maximum equivalent stress $\bar{\sigma}_i$ and scale up all quantities to make this element just yield. (This would make 1 elements plastic during the increment). The scale factor for this case would be simply,

$$f = \frac{\bar{\sigma}_o}{\bar{\sigma}_i} \tag{5.1}$$

where σ_o is the initial yield stress of the material at that point.

(3) Evaluate the elastic-plastic stiffness matrix $\mathbf{D}_{ep}$ of all post yield elements and the elastic stiffness $\mathbf{D}_e$ of all elastic and unloading elements. ($\mathbf{D}_{ep}$'s are evaluated using the current state of

stress). Hence evaluate the element stiffness matrix $\mathbf{k}$.

(4) Evaluate the Initial Stress matrix $\mathbf{k}_\sigma$ for all elements and hence the overall stiffness matrix of the body, $\mathbf{K}$.

(5) Choose a suitable test increment (say p x $\mathbf{R}$) and obtain a solution using the current stiffness matrix $\mathbf{K}$. Hence evaluate the increment of strain $d\boldsymbol{\epsilon}$ and the stresses $d\boldsymbol{\sigma}$

(6) Choose $p = p_o$ to cause 1 elastic elements to become plastic. The technique for evaluating p_o is described in section (5.5).

(7) Scale all incremental nodal displacements, forces, element stresses and strains using p_o as the scale factor. Evaluate the total displacements, forces, stresses, strains and the new co-ordinates of the nodal points.

(8) Check the new equivalent stress of all the elements for yielding and unloading. A value of (LY = 0, 1, 2) is assigned for elements which are elastic, plastic and unloading respectively.

(9) Go back to (3) and follow up to (8) to check whether the newly obtained stresses are within a prescribed tolerance to the previous stresses. If so, proceed to (10) and if not, repeat (3) to (8) until the required tolerance is obtained.

(10) Print all results. This completes the procedure for one load increment. For subsequent load increments go back to (3).

5.2 Boundary conditions (Fig. 6)

In finite element analysis the boundary conditions are assumed to be acting at the boundary nodal points only, and any other form of distributed boundary conditions are weighted properly and

assumed to be acting at the adjacent boundary points. In general there could be six possible cases of boundary conditions for the three-dimensional case (and four for the two-dimensional case).

Considering the two-dimensional case here, the restriction at the i^{th} nodal point could be due to the displacement r_x r_y and the forces R_x R_y (x, y would be replaced by r, z). The force boundary condition is easily handled as they are the known variables of the equation $\mathbf{Kr} = \mathbf{R}$.

The displacement boundary condition is more difficult to cope with but two methods have been suggested to overcome this problem. The first method modifies the diagonal flexibility matrix of the boundary nodal points and is only suitable for iterative types of solution. This method handles fixed boundary conditions in x, y or any other inclined direction but does not handle prescribed boundary displacements. The second method modifies the overall stiffness matrix by multiplying the diagonal coefficient corresponding to the boundary nodal point by a large number and replacing the corresponding nodal load by a suitable factor. The method handles prescribed displacements and fixed x and y boundary conditions, but does not take into account the slope boundary condition.

Both these methods have been used in the outline given here, but in problems where no slope boundary conditions are specified the second method is adequate and hence is used alone.

5.3 The Assembly of element stiffnesses to form the overall stiffness

The assembly is performed in the standard manner by selecting the proper coefficients of the element stiffness matrices to form the overall stiffness matrix. However, the storage of this matrix in the computer is done in such a way that only a storage of $2m \times 18$ is required as compared to a storage of $2m \times 2m$ for the usual procedure. m is the number of nodal points (for the two-dimensional case) and $18 = 2(8+1)$ where 8 is the maximum number of adjacent nodal points to any nodal point in the idealization. This number which is arbitrarily chosen is found to be quite sufficient for most finite element idealizations and can be varied by simply changing the dimensions of the stiffness array.

5.4 Solution of the simultaneous equations

All finite element analyses finally reduce to the solution of a large number of simultaneous equations. These may be in general nonlinear. In the present analysis stepwise linearity is assumed for every load increment giving rise to a set of linear equations. There are numerous methods for the solution of linear simultaneous equations. The important criterion for selecting a method is the computing time and the storage requirements. Some of the common techniques used in matrix analysis are given here briefly.

5.4.1 Gaussian elimination

The set of equations can be represented by,

$$K r = R \qquad (2.17)$$

The method consists of eliminating term by term the r's (starting with r_1) to reduce K to its upper diagonal matrix. Thus, equation (2.17) reduces to the form,

$$U r = R' \qquad (5.2)$$

where U is the upper triangular matrix.

Now, back substitution, starting with r_n yields the nodal displacements r. There are several variations to this method, but all have the disadvantage of utilising large amounts of computing time.

5.4.2 Matrix factorisation

In this method the overall stiffness matrix K is factorised to its upper and lower triangular forms.

Thus, $$K = LU \qquad (5.3)$$

where L and U are lower and upper triangular matrices respectively.

If K is symmetric,

$$L = U^t \qquad (5.4)$$

Equation (2.17) becomes

$$LUr = R \qquad (5.5)$$

Let $$b = Ur \qquad (5.6)$$

then, $$Lb = R \qquad (5.7)$$

Now equation (5.7) can be solved by back substitution to obtain b, which is used in equation (5.6) to evaluate the nodal displacements r. The method is computationally superior to the Gaussian elimination.

5.4.3 Direct inversion of K

The solution to r can be obtained directly as,

$$\mathbf{r} = \mathbf{K}^{-1}\,\mathbf{R} \qquad (5.8)$$

The method if used directly by obtaining the inversion of the whole matrix **K** is very inefficient. However several methods have been suggested to reduce the excessive computing time (for example by partitioning and tridiagonalising, and using Frontal solution techniques).

5.4.4 Iterative methods (Gauss-Siedel iterative technique)

The solution to the set of equations could be obtained iteratively by assuming an initial guess of the nodal displacements. The criterion for unconditional convergence is that the diagonal term should be greater than the absolute sum of all the other terms in a row. In practice however, the method seems to converge for most finite element problems. The computing time for the solution is several times less compared to the other methods described earlier, in addition to the smaller storage requirements (5.3). This method is adopted for the solution of all the problems solved in this thesis. The process can be best illustrated in a number of steps as follows.

(1) Assume a set of values for **r** (preferably all zero to start with).

(2) Using $r_2 \ldots r_n$ and the 1st equation, solve for r_1.

(3) Similarly using the most recent value of $\mathbf{r}_\lambda$ to evaluate r_j from the jth equation. Repeat for j = 2, n.

(4) This completes one cycle of iteration. Check for convergence by finding the total sum of the errors defined as the difference between the present and previous **r**'s.

(5) If the required degree of tolerance is reached stop

further iteration. If not, go back to (2) and repeat the procedure.

The iterative procedure can usually be accelerated for rapid convergence by the use of an over-relaxation factor. If $\mathbf{e}$ is defined as the error,

$$\mathbf{e} = \mathbf{r}_p - \mathbf{r}_o \tag{5.9}$$

where $\mathbf{r}_p$ and $\mathbf{r}_o$ are the present and old $\mathbf{r}$'s respectively. The new value after over-relaxation is given by,

$$\mathbf{r}_n = \mathbf{r}_o + F\,\mathbf{e} \tag{5.10}$$

An over-relaxation factor of about 1.8 - 2.0 has been found very suitable for most finite element problems and a factor of 1.9 is used for most problems in this analysis.

5.5 Evaluation of the correct loading step at every increment

The stress-strain relationship for any elastic-plastic material is generally nonlinear and to obtain a realistic solution, loading has to be carried out in small incremental steps. During such an incremental loading the material will, at first behave elastically and then at a certain load the element (or elements) with the highest equivalent stress will yield and become plastic. When the loading is continued more elements will yield and enter the plastic domain. All post-yield elements should thereafter be treated as plastic (until any such element starts unloading) and the correct element stiffness evaluated using the current state of stress.

The size of the loading step for every increment could

be evaluated by several means. The simplest, of course, is to give arbitrarily chosen increments to satisfy the problem's requirements, in a given number of steps. This has been followed by several authors and could lead to serious errors in the solution obtained. The method becomes inefficient (time-wise) if the increments are too small, and if they are too large, which is more often the case, the results could go wrong by several hundred percent (especially at the beginning of the loading). This has been illustrated in Fig. 7.

Ideally, the load increment should be stopped as soon as one element enters the plastic domain as this has to be treated as a post-yield element for subsequent loading (thereby changing the stiffness matrix of that element and of the whole body). This means that only one element yields during an increment and for a body with a large number of elements the analysis would take a considerable length of time. The process has been accelerated in two alternative ways without losing much of the accuracy.

(1) When an element yields during a load increment, all elements having an equivalent stress of greater than $k\sigma_o$ where σ_o is the initial yield stress and k is a scale factor (usually ranging from 0.95 - 1.00) are assumed to be plastic for the next load increment. This will make a few elements (having yield stresses close to σ_o) yield during one load increment. The method is however not very satisfactory for problems with very uneven stress distributions.

(2) An alternative and a somewhat better method is to continue

the loading to make a number of elements yield at one time. This method is particularly suitable for problems with uneven stress distributions. (The number of elements that yield during one increment is intuitively chosen for the problem concerned, taking into account the total number of elements and the computer time available to solve the problem).

These two methods reduce the computation time for the solution considerably. Both are however approximate methods, in that the first one assumes a few elements to be plastic when they are still elastic and the second assumes some elements to be elastic when they should be plastic or in the transition period.

The correct load increment for every step is evaluated as follows. Let the stresses before and after a test increment of load be given by σ and $\sigma + \delta\sigma$. Now, the increment $\delta\sigma$ should be chosen in such a way that ℓ elements yield during this step. Let the correct increment be denoted by $p.\ \delta\sigma$ (where p is to be found).

Denoting the present equivalent stress of the element that is going to just yield, at the end of the step, as $\bar{\sigma}$,

$$\bar{\sigma}^2 = \frac{3}{2}\ \sigma_D^t\ \sigma_D \tag{2.29}$$

And after the load increment we have,

$$\bar{\sigma}_o^2 = \frac{3}{2}\ (\sigma_D + p.\delta\sigma_D)^t\ (\sigma_D + p.\delta\sigma_D) \tag{5.11}$$

i.e.

$$\bar{\sigma}_o^2 = \frac{3}{2}\ [\ \sigma_D^t\sigma_D + p\sigma_D^t\ \delta\sigma_D + p\delta\sigma_D^t\sigma_D + p^2\delta\sigma_D^t\ \delta\sigma_D\ ]$$

i.e.

$$\bar{\sigma}_o^2 = \bar{\sigma}^2 + 2Bp + A\ p^2 \tag{5.12}$$

where $$A = \frac{3}{2} \delta\sigma_D^t \, \delta\sigma_D \tag{5.13}$$

and $$B = \frac{3}{4} \left[\sigma_D^t \, \delta\sigma_D + \delta\sigma_D^t \sigma_D \right] \tag{5.14}$$

From equation (5.2) we have,

$$p = \left(-B \pm \sqrt{B^2 + A \, (\bar{\sigma}_o^2 - \bar{\sigma}^2)} \right)/A \tag{5.15}$$

p is evaluated for all elements and the ℓ th minimum value is used.

In most of the examples given in this thesis the above two methods are combined together to yield the best results. For problems where the whole body becomes plastic after several load increments the subsequent loadings have been carried out using relatively larger increments, chosen so as to give the required degree of deformation with the minimum of computing time.

5.6 Iterative technique within load increment

During a load increment the elastic-plastic stiffness matrix for all post-yield elements should be evaluated using the current state of stress (which is unknown). For this, the usual procedure is to use the state of stress before the load increment, which may not produce errors of any large magnitude. However, when the process is repeated for a large number of load increments the accumulative error becomes quite substantial (Fig. 8). The accuracy can be improved by using an iterative technique where the average value of stress is used to evaluate the stiffness matrix. At first the elastic-plastic stiffnesses are evaluated using the previous stress state and the resulting state of stress is used to evaluate a better solution, and so on until a desired degree of convergence is obtained. In practice the method converges quite

rapidly for small steps, the rate of convergence diminishing as the step size is increased.

CHAPTER 6

6 SMALL DISPLACEMENT ELASTIC-PLASTIC FINITE ELEMENT SOLUTIONS

The majority of stress analysis problems fall into this category, where the nonlinearity is only due to the material properties. The solution to this type of problem is obtained using a similar flow chart to that shown in section (5.1). The only changes for the present case are the absence of an initial stress matrix and the updating of nodal-point coordinates at every load increment. Two problems are analysed in this section; one where a theoretical solution is available and the other where experimental and finite element results are available.

6.1 Analysis of a thick walled cylinder with internal pressure

A cylinder of internal and external radii 1" and 2" respectively was used for this analysis (Fig. 9). Plane strain conditions were assumed and the material was assumed to be elastic-plastic and non work-hardening. The following material properties were used in the analysis.

$E = 30 \times 10^6$ lbf/in^2

$\nu = 0.3$

$\sigma_o = 30{,}000$ lbf/in^2

$E_p = 0.0$ for all strains.

6.1.1 Theoretical solution

An analytical solution has been obtained for the expansion of a cylindrical tube for the elastic case and the elastic-plastic case using the yield criterion of Tresca. The values of the radial

and tangential stresses for the plane strain case are given as (from Hill's 'plasticity' (33)),

$$\left.\begin{aligned} \sigma_r &= -\,p\left(\frac{b^2}{r^2}-1\right) \Big/ \left(\frac{b^2}{a^2}-1\right) \\ \sigma_\theta &= p\left(\frac{b^2}{r^2}+1\right) \Big/ \left(\frac{b^2}{a^2}-1\right) \end{aligned}\right\} \qquad (6.1)$$

when the tube is partially plastic the stresses are given as,

$$\left.\begin{aligned} \frac{\sigma_r}{\sigma_\theta} &= -\frac{c^2}{2b^2}\left(\frac{b^2}{r^2}-1\right) \\ \frac{\sigma_\theta}{\sigma_o} &= \frac{c^2}{2b^2}\left(\frac{b^2}{r^2}+1\right) \end{aligned}\right\} \qquad (6.2)$$

for the elastic region $(c \leqslant r \leqslant b)$

and for the plastic region $(a \leqslant r \leqslant c)$ as,

$$\left.\begin{aligned} \frac{\sigma_r}{\sigma_o} &= -\frac{1}{2} - \ln\left(\frac{c}{r}\right) + \frac{c^2}{2b^2} \\ \frac{\sigma_\theta}{\sigma_o} &= \frac{1}{2} - \ln\left(\frac{c}{r}\right) + \frac{c^2}{2b^2} \end{aligned}\right\} \qquad (6.3)$$

where p is the internal pressure,

a, b, c are the inside, outside and elastic/plastic radii respectively.

6.1.2 Finite element solutions

The finite element method was used to solve the problem of the thick walled cylinder under plane strain conditions. The analysis was carried out in small incremental steps using the tangential stiffness method. Triangular ring type elements with three nodal points were used and two alternative finite element mesh

idealizations were used to represent a section of the cylinder. In the first analysis twenty elements and twenty-two nodal points were adopted while twenty elements and seventeen nodal points were adopted in the second analysis (Fig. 10). The stresses at each section were obtained by averaging the stresses of the triangular elements inside each rectangle. The two mesh idealizations gave almost identical results to the theoretically obtained ones, the first mesh idealization being closer to the theoretical one than the second. The stresses are plotted together with the theoretical results (Figs. 11 and 12) for five different positions of the elastic plastic interface and show very good agreement.

The finite element solution assumes the yield criterion due to von-Mises whereas the theoretical solution used the yield criterion due to Tresca. The results in Figs. 11, and 12 are modified to take this into account by multiplying the value of yield stress by the factor $\frac{2}{\sqrt{3}}$.

6.2 Perforated strip under tension

This plane stress problem has been studied both by the finite element method and by experiments and is used to check the general shape of plastic enclaves obtained using the finite element method. The dimensions of the strip used for this analysis (the same as was used by Marcal and King (50) and Zienkiwicz et al (80)) are shown in Fig. 13. The strip was idealized into 136 plane triangular elements and 87 nodal points as shown in Fig. 14. The analysis was carried out using the tangential stiffness method allowing only a few elements to yield at one time. The loading was carried out in small incremental

steps until a sufficiently large plastic zone was obtained for comparison. The following material properties were used in the analysis. (The material is Aluminium alloy 57S which was used by Theokaris and Marketos (71) in their experiments).

$$E = 7000 \text{ Kg/mm}^2$$

$$\nu = 0.2$$

$$\bar{\sigma}_o = 24.3 \text{ Kg/mm}^2$$

$$E_p = 220 \text{ Kg/mm}^2 \quad \text{(constant)}$$

6.2.1 Results and comparison

The results of the analysis are shown in Fig. 15 for six different loadings. The analysis was repeated for the non-work-hardening case ($E_p = 0$) and the results are shown in Fig. 16. The results compare favourably with those obtained by Theokaris and Marketos (71), Marcal and King (50) and by Zienkiewicz et al. (80). For the six loadings, in each case (E_p = constant) the mean stresses at the edge of the strip are given in Table 1. The five loadings in the experimental analysis were not specified in (71) and hence it was not possible to make a direct comparison. The previous finite element results agreed with the present solution.

CHAPTER 7

7 LARGE DEFORMATION ELASTIC-PLASTIC SOLUTIONS

7.1 Expansion of a hole in a thin plate (conical)

The model chosen for the finite element analysis is the problem of expanding a hole in a thin plate having its initial thickness proportional to the radial distance from the centre of the hole. Alexander and Gunasekera (2) have solved this problem for an infinite plate using a one variable theory (Appendix A), and assuming geometrical similarity to be maintained during deformation.

7.1.1 Experimental work

Experiments were performed on a finite mild steel plate with a central hole of finite radius. A detailed description of the experimental procedure appears in Appendix A.

7.1.2 Finite element analysis

The geometry of the axisymmetric plate used for the finite element analysis is shown in Fig. 1, Appendix A. The plate was idealised into 286 triangular ring elements (TRIAX3) and 189 nodal points, as shown in Fig. 18, where one quarter of a cross section of the plate is shown. The hole at the centre of the finite plate was of course expanded from a small finite radius. The plate was fixed at the edge and loading was carried out so that the radial displacements of the nodal points at the edge of the hole remained constant.

Three major finite element analyses were made of this problem, (although some 10 complete runs were made using a coarser mesh idealisation, different boundary conditions and alternative

iterative techniques). In the first analysis loading during each load increment was carried out in small incremental steps until one element reached the initial yield stress of the material and all elements with equivalent stresses greater than 0.95 times the initial yield stress were assumed plastic for the next load increment. The loading was carried out in small incremental steps until the hole expanded from a radius of 0.25 inches to 0.294 inches, in 44 steps.

Iteration within the incremental step was carried out until convergence of the stresses was obtained. The number of iterations required for convergence varied from about 3 at the beginning to about 30 during the last stages. This naturally involved considerable computing time in that about 3000 seconds was needed on the C.D.C. 6600 computer. Without the iteration at every increment the computing time could have been reduced to about 500 seconds but this procedure would lead to errors at every step which becomes cumulative and hence was not adopted here. The computing time obviously depends on the level of accuracy required and a reasonable compromise was usually made during trial runs.

In the second approach 8 elements were made to yield during every incremental step. Towards the last stages of loading fewer elements were made to yield at every step to obtain faster convergence. The results obtained were very similar to the first analysis. The computing time, however, was reduced considerably (to about half the first) for the same deformation. The factors 0.95 and 8 in these two methods were arbitrarily chosen for the present problem to compromise between the accuracy of the solution

obtained and the computing time consumed. In general, for other similar problems these may be assumed 0.9 - 1.0 for the first and from unity to any number (for example about $\frac{1}{20}$th of the total number of elements), for the second factor depending on the number of elements used in the mesh idealisation and the degree of accuracy required in the results.

The above two analyses revealed a considerable compressive stress along the z-direction near the edge of the hole which may have underestimated the displacements along the z-direction. The third analysis was performed using a modified boundary condition to take this into account (by superimposing an equal and opposite tensile stress near the edge of the hole) and also taking advantage of the first two methods. Thus, 8 elements plus the other elements falling in between 0.95 and 1.00 times the initial yield stress were assumed plastic. The computing time was reduced to about one third of the first, to obtain the same deformation. The loading was however carried further to a radius of 0.417 inches in 56 increments.

7.1.3 Results and Discussion

The finite element solutions obtained for this problem are compared with those obtained theoretically (2). The elastic solution shown in Fig. 19 is identical for the two cases. The results towards the edge of the plate (not shown in Fig. 19) revealed some discrepancy due to the fixed boundary condition at the edge of the finite plate. (The theoretical solution of course assumes an infinite plate). This discrepancy (of very small order) was only localised at the edge of the plate and did not affect conditions towards the centre of the plate. A fixed boundary condition at

the edge of the plate would give a higher value of σ_r and a lower value of σ_θ as compared with the infinite plate. (The alternative of course is to use a free boundary condition at the edge of the plate, which in turn would give a lower or zero value for σ_r and a higher one for σ_θ than for the infinite plate).

The theoretical solution obtained when the plate is partially plastic assumes plane stress conditions near the edge of the hole and the principal stresses to be in the r, θ and z directions. This condition is obviously violated due to local large deformations and may have resulted in gross errors near the edge of the hole. In fact axial and shear stresses of considerable magnitude were obtained with the finite element solution. (The axial and shear stresses were of course assumed to be zero in the theoretical analysis). The stresses obtained from the finite element analysis were averaged over each section by considering all elements to be at the same radial distance.

For the elastic-plastic case two sets of results are shown. Figs. 20 and 21 show the solution obtained from the first and second methods (Section 7.1.2) and are compared with the theoretical solution. The results obtained from the third method are shown in Figs. 22 and 23 and are compared both with theoretical and experimental results. For the latter case, loading was carried on in the usual way until no convergence or very slow convergence was obtained. Thereafter fixed small displacement increments were used to obtain a reasonable deformation to be compared with the experiments.

The stresses seem to agree fairly well, close to the

elastic-plastic interface but showed some deviation near the edge of the hole (Figs. 20, 22). The elastic part of the plate is not shown here but the results of course agreed very well with the theoretical ones as before. The deformation in the z-direction near the edge of the hole is smaller than that predicted by the theoretical analysis (Fig. 21) for the first and second methods but this discrepancy is very small for the third method (Fig. 23) where a better boundary condition is used near the edge of the hole.

7.2 Expansion of a hole in a thin plate (flat)

The problem of expanding a hole in a (flat) plate of constant thickness is of more practical interest than that of the tapered axisymmetric plate considered earlier. Many investigators (Appendix A References) have attempted to solve this problem using a one variable theory. However as pointed out by Alexander and Gunasekera (2), the solution obtained from such an analysis would not be correct for this case, as the plate during deformation does not maintain the geometric similarity required by the one variable theory. A theoretical solution for the elastic small displacement case has been obtained by Alexander and Ford (Appendix A, Ref. 1) and the stresses and the strains are given by the Lamé equations,

$$\sigma_r = -\frac{\sigma_o}{\sqrt{3}\,\phi^2} \tag{7.1}$$

$$\sigma_\theta = +\frac{\sigma_o}{\sqrt{3}\,\phi^2} \tag{7.2}$$

$$\sigma_z = 0 \tag{7.3}$$

$$\epsilon_r = -\frac{\sigma_o (1+\nu)}{\sqrt{3}\, \phi^2\, E} \tag{7.4}$$

$$\epsilon_\theta = +\frac{\sigma_o (1+\nu)}{\sqrt{3}\, \phi^2\, E} \tag{7.5}$$

$$\epsilon_z = 0 \tag{7.6}$$

The velocity in the elastic region is given by,

$$v = \frac{2\, \sigma_o (1+\nu)}{\sqrt{3}\, E\, \phi} \tag{7.7}$$

7.2.1 Experimental work

Experiments on a flat plate made of mild steel were performed in a similar way to that of the conical plate (Appendix A). A circular flat plate of diameter 12 inches and thickness 0.5 inch was manufactured with an inside hole of diameter 0.5 inch. The plate was then mounted on a lathe and the expansion of the hole was achieved by forcing a hardened tapered mandrel into the hole whilst slowly rotating the plate. Graphite grease lubricant was used to reduce friction and a continual supply of cold water was poured to prevent overheating. The hole was expanded from a radius of 0.25 inch to a radius of 0.32 inch.

7.2.2 Finite element analysis

The plate was idealised as before, into 133 triangular ring elements and 115 nodal points, as shown in Fig. 24. The analysis was carried out using the third method described in sec-

tion 7.1.2 and on very similar lines. This time 4 elements and the elements having equivalent stresses greater than 0.95 times the initial yield stress were assumed plastic. Similar boundary conditions were used. The hole was expanded from a radius of 0.25 inches to 0.32 inches in 17 incremental steps. The computing time taken for this problem on the University of London C.D.C. 6600 computer was about 600 seconds. Without any iteration during every increment this could be reduced to about 100 seconds.

7.2.3 Results and Discussion

The finite element solution obtained (Fig. 25) for the elastic case was compared with the theoretical solution. The agreement is excellent as before. For the elastic-plastic case however, there is no correct theoretical solution and hence a comparison cannot be made. The stresses obtained using the finite element method are shown in Fig. 26 and follow a close resemblance to the ones obtained with the conical plate. Fig. 27 shows the profile of the flat plate after deformation. The finite element solution agreed quite well with the experimental results.

CHAPTER 8

8 APPLICATION TO OTHER PROBLEMS

8.1 Analysis of the Dieless Drawing Process

Dieless drawing is a new metal forming process, still in its development stages. The process consists of drawing bars (solid and hollow) of constant cross section without the use of dies. The bar which is fixed at one end is locally heated to a high temperature by an induction coil and is pulled at the free end while moving the induction coil in the opposite direction. The process is somewhat similar to wire drawing or extrusion except that the heating coil acts as the die. There are some advantages of the process from a manufacturing point of view. The use of no dies and no container (or pressure vessels) would make the process less expensive than the other conventional methods. The forces necessary to pull the bars are very nominal and fairly large reductions have been obtained in a single pass.

However, the process has several disadvantages; for example it is slow because of the time required to heat the bar. Also, the deformation is predominantly tensile so that any incipient flaws or fissures are accentuated leading to cracking both on the surface and in the interior of the bar. For some materials it is difficult to control the process so as to achieve a uniform cross-section of the drawn bar.

Fig. 28 shows a typical layout of the process. The velocities of the free end of the bar and the induction coil are coupled and their ratio in theory determines the amount of reduc-

tion obtained during the deformation. The temperature required to pull the specimen successfully, is quite critical in certain cases and is determined experimentally.

When the steady state is reached the velocities of the free end of the bar, v_1 and the induction coil, v_c can be related in terms of the areas as,

$$A_1 v_c = A_2 (v_1 + v_c) \tag{8.1}$$

Thus,

$$\frac{v_c}{v_1} = \frac{A_1}{A_2 - A_1} \tag{8.2}$$

and

$$\frac{A_1}{A_2} = \frac{v_1 + v_c}{v_c} \tag{8.3}$$

Three methods have been suggested for the solution of this problem. The first is an approximate theoretical solution for the steady state which assumes plane sections remain plane and may not be suitable for very large reductions. The second is by using the finite element displacement method which could only give a solution to the transient stage of the process. The solution may however be carried out to approach the steady state solution.

Although approximate, the most economical method is the first, while the finite element displacement method would use a large amount of computer time, and yet may give only an approximate result due to the accumulation of errors during the large number of load increments.

An alternative method is to combine the first two methods to get a solution without using an enormous amount of computing time.

The third method is to use a different formulation of the finite element method as indicated in section 8.2. This involves using a stream function ψ, and its derivatives (the velocity components) as the basic unknowns instead of the usual displacements. This method is not used to solve the problem of dieless drawing, but the formulation (section 8.2) would give rise to a kinematically admissible velocity field.

The success of the process to obtain a smooth uniform product depends on a number of factors, the more important being the temperature distribution, the reduction, the speed of the draw and the change of the material properties with temperature. It has been found experimentally that it is very difficult to obtain a uniform draw for certain materials (e.g. mild steel), while some other materials (e.g. titanium) behave very well, giving a product of uniform cross section.

8.1.1 Consideration of the variation of material properties due to temperature

The dimensions of a typical specimen (a solid cylindrical bar of strainless steel) used in dieless drawing experiments are shown in Fig. 29*. The approximate variation of the temperature along the length of the bar obtained during an experiment using an optical pyrometer is shown in fig. 30. For the present case the variation of the temperature along the radial direction of the bar is neglected.

It has been found experimentally that the material properties of the stainless steel at higher temperatures varied con-

---

* All experimental data used in this Chapter were made available by the kind permission of Mr. T.W. Turner, Research Assistant, Department of Mechanical Engineering, Imperial College.

siderably from those at lower temperatures. Fig. 31 shows several plots of stress-strain data for the EN 58J steel used for this analysis at four different temperatures. A stress-strain relation of the form $\bar{\sigma} = \sigma_o (1 + B \bar{\epsilon}p)^n$ was assumed and the values of σ_o, B and n were evaluated using the method described in Appendix B. These values for the four temperatures 800^o, 900^o, 1000^o and 1100^oC are shown in Table 2.

The values of plastic modulus E_p, necessary for the finite element analysis is evaluated by interpolating the values of E_p at the two adjoining temperatures, for the same value of the equivalent plastic strain ϵ_p. When the material moves during the deformation the corresponding new temperatures at every element are evaluated using the given temperature profile.

The variation of the temperature along the specimen gave rise to a somewhat different form of unloading when elements after entering the heating coil, moved away from it. Such elements changed from the plastic state to the elastic state due to the hardening of the material from cooling. The equivalent strain and the stress of these elements did not drop during unloading as in the usual case, but the material properties changed on cooling giving a higher value of yield stress which made the element elastic. This is illustrated in fig. 32.

8.1.2 An approximate theoretical solution for dieless drawing

It is possible to obtain an approximate solution to the problem of (steady state) dieless drawing of circular bars by assuming plane sections remain plane. For convenience, the coil is assumed to be stationary and the two ends to be moving with

velocities v_1 and v_2 (fig. 33).

Assuming the material to be rigid-plastic (and hence incompressible) we have,

$$\dot{\epsilon}_r + \dot{\epsilon}_\theta + \dot{\epsilon}_z = 0 \qquad (8.4)$$

where $\dot{\epsilon}_r$, $\dot{\epsilon}_\theta$ and $\dot{\epsilon}_z$ are the strain rates in the r, θ and z directions.

i.e. $$\frac{\partial u}{\partial r} + \frac{u}{r} + \frac{\partial v}{\partial z} = 0 \qquad (8.5)$$

or $$\frac{1}{r}\frac{\partial}{\partial r}(ur) + \frac{\partial v}{\partial z} = 0$$

where u and v are the velocities along the r and z directions.

Velocities

Assuming the velocity v over any cross section to be constant, we have

$$A\,v = A_1\,v_1 \qquad (8.6)$$

Hence $$v = \frac{A_1 v_1}{A}$$

where A = area of cross section and

suffix 1 denotes the entry section.

Using equation (8.5) and (8.6) we have,

$$\frac{1}{r}\frac{\partial}{\partial r}(u\,r) = \frac{A_1 v_1}{A^2}\frac{\partial A}{\partial z} \qquad (8.7)$$

Solving for u in (8.7) and noting that u is finite at r = 0,

$$u = \frac{r}{2}\,\frac{A_1 v_1}{A^2}\,\frac{dA}{dz} \qquad (8.8)$$

Strain rates

$$\dot{\epsilon}_r = \frac{\partial u}{\partial r} = \frac{A_1 v_1}{2A^2}\,\frac{dA}{dz} \qquad (8.9)$$

$$= \frac{u}{r} = \dot{\epsilon}_\theta$$

Hence $$\dot{\epsilon}_z = -2\dot{\epsilon}_r = -2\dot{\epsilon}_\theta \qquad (8.10)$$

$$\dot{\bar{\epsilon}}^2 = \frac{2}{3}\,\dot{\boldsymbol{\epsilon}}^t\dot{\boldsymbol{\epsilon}} = \dot{\epsilon}_z^2 \qquad (8.11)$$

Strains

Strains are obtained by integrating the strain rates with respect to time. Therefore we have,

$$\bar{\epsilon} = \int \dot{\bar{\epsilon}}\, dt = \int \frac{\dot{\epsilon}}{d\delta/dt}\, d\delta \qquad (8.12)$$

where δ = displacement along z direction,

i.e.

$$\bar{\epsilon} = \int_o^z \frac{\dot{\bar{\epsilon}}}{\dot{v}}\, d\delta = \int_o^z \frac{\dot{\bar{\epsilon}}}{\dot{v}}\, dz \qquad (8.13)$$

Substituting (8.9) and (8.11) we get,

$$\bar{\epsilon} = -\int_{A_1}^{A} \frac{dA}{A}$$

$$= \log \frac{A_1}{A} \qquad (8.14)$$

Equation (8.14) can also be obtained directly.

Hence, $\epsilon_z = \bar{\epsilon} = -2\epsilon_r = -2\epsilon_\theta \qquad (8.15)$

Stresses

Using the Levy-Mises relations for a rigid-plastic material we have,

$$\sigma_r' = \frac{2}{3}\frac{\bar{\sigma}}{\dot{\bar{\epsilon}}}\dot{\epsilon}_r$$

$$= -\frac{\bar{\sigma}}{3}$$

Hence $\sigma_r' = \sigma_\theta' = -\frac{\bar{\sigma}}{3}$

and $\sigma_z' = \frac{2\bar{\sigma}}{3} \qquad (8.16)$

where σ_r', σ_θ' and σ_z' are the deviatoric stresses in r, θ and z directions.

Using the condition that $\sigma_r = 0$ when $r = r_{\text{outside}}$, we get,

$$\sigma_m = \frac{\bar{\sigma}}{3}$$

where σ_m is the mean stress.

Hence $\sigma_z = \bar{\sigma}$ (8.17)

Forces

Equilibrium along z-direction gives

$A \sigma_z = F$ at all sections,

Hence $A \bar{\sigma} = F$ (8.18)

Stress-strain relationship

At a given temperature and neglecting the strain rate effect, the following stress-strain relation has been found to fit most of the materials.

$$\bar{\sigma} = \sigma_o (1 + B\bar{\epsilon})^n \quad (8.19)^*$$

where σ_o, B and n are constants at a given temperature.

Using equations (8.18) and (8.19) we get,

$$F = A \sigma_o (1 + B\bar{\epsilon})^n \quad (8.20)$$

i.e. $$F = A \sigma_o (T) (1 + B(T) \log \frac{A_1}{A})^{n(T)} \quad (8.20a)$$

In equation (8.20a) the unknowns are the temperature T and the area, A. If one is known the other can be obtained by solving equation (8.20a).

To find the temperature distribution knowing the profile

Considering any section of area A, we have,

$$\bar{\sigma} = \frac{F}{A}$$

and $$\bar{\sigma} = \log \frac{A_1}{A}$$

---

* Note In general however,

$$\bar{\sigma} = f(\bar{\epsilon}, \dot{\bar{\epsilon}}, T) \quad (8.19a)$$

and if it is possible to obtain such a function for the material considered, equation (8.19) should be replaced by (8.19a)

Now, Fig. 34 illustrates the method to obtain the corresponding temperature T.

Let the two closest upper and lower stresses to at $\bar{\epsilon}$, be σ_1 and σ_2 at temperatures T_1 and T_2.

T can now be obtained by interpolating between temperatures T_1 and T_2.

To find the profile given the temperature distribution

Evaluate the coefficients σ_o, B and n for the given temperature T. The area of cross-section corresponding to this temperature is obtained by the solution of equation (8.20),

i.e. $F = A\ \sigma_o\ (1 + B \log \frac{A_1}{A})^n$.

An alternative method is to tabulate the temperatures and the areas from the previous method and interpolate to obtain the profile for a given temperature distribution.

Solution

A computer program was developed to predict the temperature distribution knowing the profile of the deformed zone. Experimental data were available for a 1.5" diameter circular bar of EN 58J steel. The experimentally obtained profile is shown in fig. 35. The reduction obtained was 2.58 with the coil moving at 0.85 in/min and the free end moving at 1.347 in/min. The load on the specimen during the steady-state was 4.8 tons. The material properties of the EN 58J steel are shown in fig. 31, and table 2. The theoretically predicted temperature distribution is shown in fig. 36. The variation of stresses, strains and the velocity are shown in figs. 37 and 38 (Table 3).

8.1.3 Finite element solutions

Three major approaches were made to obtain a solution for the problem of dieless drawing using the finite element method. The first was the usual method which allows a fixed number of elements to yield at a time and/or the elements having a yield stress greater than 0.95 of the initial yield stress at that temperature. The primary disadvantage of this method was the large amount of computing time used, due to the large number of iterations required for the convergence of the stresses, within any load increment.

The second method was used without any iteration within a load increment, but using the fourth order Runge-Kutta method to obtain the solution to the next step. This method is computationally superior to the first method, provided the number of iterations required for convergence in the first is greater than 4. The method was used with prescribed displacements throughout, instead of automatically determining the incremental step to make a fixed number of elements yield.

The third method combines the approximate theoretical method with the finite element method. In this method, a finite element analysis is performed on the final deformed shape, of the specimen in the steady state. Approximate stresses and strains are first evaluated using the approximate theory and are used for the finite element analysis.

The mesh idealisation used in the first two methods for the cylindrical specimen of EN 58J steel is shown in Fig. 29. One half of the bar was considered due to symmetry and was idealised into 96 triangular ring elements and 68 nodal points. For simplicity the heating coil (i.e. the temperature profile) was assumed to be fixed

and the two ends of the specimen were assumed to be moving, with different velocities. A reduction of approximately 50% was required for this case and one end was therefore moved at approximately twice the speed of the other end, producing the effect of the moving coil.

The finite element analyses on the bar were carried out using small incremental steps. In the first method the steps were automatically controlled by the number of elements going plastic up to a certain load and then fixed displacements were used. In the second method all the increments were manually controlled to give the desired deformation in a reasonable number of load increments. It has been observed during trial runs that it is more accurate to use automatically controlled incremental steps during the initial stages of the plastic deformation. However when the plastic zone became sufficiently large very slow or no convergence was experienced using this type of control, and manually controlled prescribed displacements were given to obtain rapid convergence.

For the third method, the finite element analysis was performed on the deformed shape of the specimen in the steady state. The mesh idealisation used for one half of the specimen is shown in Fig. 42. The deforming zone was idealised into 120 triangular ring elements and 84 nodal points. Again the heating coil was assumed to be stationery and both ends moving. The reduction obtained for this case was 2.58 and therefore the velocity ratio of the two ends was used as 2.58.

The material properties for the EN 58J steel used are shown in Fig. 31. The predicted temperature distribution, stress

and strain distributions using the approximate theory are shown in Figs. 36, 37, 38. This temperature distribution was assumed for the finite element analysis. The elements of the specimen were assumed to be work hardened (to an extent depending on the reduction, therefore the position of the element) and an initial strain equal to that given by the approximate theory was assumed for all the elements*. The loading was applied in small incremental steps until the whole specimen became plastic.

The last method indicated does not provide a solution on its own. The method was used mainly to check the accuracy of the approximate theoretical method and to provide a better stress distribution for the specimen. The stresses obtained using the first two methods were not found to be accurate. (For example when compared with the results from the approximate theory they were found to be too high.

8.1.4 Results and Discussion

The finite element analysis was applied to the undeformed specimen using small incremental displacement steps. The displacements up to about five load increments were controlled automatically to make approximately six elements yield during each increment. The temperature distribution assumed for this analysis is shown in Fig. 30. The spread of the plastic enclaves during the early stages of loading is shown in Fig. 39. The plastic zone first occurred at the section of highest temperature and then spread towards either end during the early stages of deformation.

---

* S. Kamyab, Private Communication, 1971.

The subsequent load increments were applied in steps varying from .002 to .02 inches controlled manually. During these increments the plastic zone did not extend appreciably any more and was positioned around the high temperature zone. Elements entering the heated zone became plastic and elements leaving the heated zone became elastic once again.

The deformed shape after ninety load increments when the specimen was extended 1.8 inches is shown in fig. 40. The specimen started necking at the point of the highest temperature and as can be seen from fig. 41 the necking seems to be extended over a large region due to the relative motion of the heating coil. The necking is not localised as for example in a cold or hot tensile test but spreads over a long region fairly smoothly. The deformed shape after one hundred and eighty load increments is shown in fig. 41. The comparison with the experimentally obtained profile is shown in fig. 43, and seems to be in good agreement. The time taken for the complete run was about 1800 seconds in the C.D.C. 6600 computer. As is shown by the dots in fig. 41 (which were equally placed along the specimen before deformation) the extension is greater in the middle of the section compared to the ends, as is to be expected.

The results obtained using the first and second methods are very similar although the first method showed no covergence for larger load increments. Thus a great number of load increments (about three hundred) were required for the first method involving about twice the computer time required for the second method. The superiority of the fourth order Runge-Kutta technique is very well

demonstrated here. Due to the close similarity of the two sets of results obtained only one set is presented here. The strain and stress variation along the length of the bar is shown in fig. 44. It can be seen in comparison with the approximate theoretical solution that the strains seem to agree fairly well although the comparison for stresses does not seem very good. The theoretical solution given here is very approximate as it assumes plane sections to remain plane during deformation and hence there are no radial or tangential stresses. These assumptions are obviously violated particularly for larger reductions, the deviation from the true state becoming less for smaller reductions.

Towards the last few load increments the solution of the simultaneous equations (using the Gauss-Siedel iterative technique) took an increasingly longer time to converge. This indicates that the overall stiffness matrix is not well conditioned for these increments and hence the results obtained may not be very accurate. During further increments of load the specimen necked very slowly; the rate being very small compared to the initial stages. The loading process was however stopped, approximately when the necked diameter reached the desired reduction. One of the reasons for this localised slow necking may be the inaccuracy of the solution obtained during the last stages. Another reason of course may be the dieless drawing process itself; which seems to work well for certain materials but not for others.

The third method used, assumes the deformed shape of the specimen and an approximate state of strain in order to obtain the varying degree of hardening along the specimen. This determines

the corresponding plastic modulus for the material along the length of the bar. The temperature profile obtained from the approximate theoretical solution is assumed. The reduction obtained for this case is 2.58 and therefore the two ends of the specimen were moved in that ratio. The loading was applied incrementally as before.

The stress distribution along the length of the specimen when almost the whole specimen was plastic is shown in fig. 45. This state was achieved after twenty load increments. The stresses, along the radius at any section, did not vary appreciably. This is shown in fig. 46, where the stresses are plotted at various sections along the length of the specimen. The stress distribution along the length agrees fairly well with the theoretically obtained stress distribution.

It can be concluded that the finite element method is capable of giving an approximate solution to some large deformation elastic-plastic problems. The displacements and the strains obtained using this method seem to be fairly accurate but not the stresses. An alternative method is suggested to obtain the stresses. This assumes the final deformed shape, and the loading is applied from this position and assuming a stress free but work hardened body. The stress distribution when the whole body becomes plastic may give an approximate solution, to the state of stress within the body during the actual steady state deformation.

8.2 The Steady state plastic flow problem

This type of problem is found mainly in the processing of materials and a few examples would be extrusion, rolling and wire drawing. Although a point in the material will have varying velocities at different times the velocity field with respect to a co-ordinate system fixed in space will remain the same during the steady state. It is not possible to obtain a complete solution to this problem using the displacement method of finite elements. However the displacement method can be used to solve the transient stages of such a process and to approach steady state solution. As the steady state is approached the stiffness matrix will become very ill-conditioned giving finite displacements for infinitesimal increments of loads and a realistic solution to the problem may not be possible.

The problem may be solved in an alternative way using the stream function ψ and its derivatives as the basic unknowns instead of the usual displacements. It would be possible to obtain a kinematically admissible velocity field using this method, but it is difficult to predict whether this method will provide a statically admissible stress field owing to the unknown hydrostatic stress.

Theory

Considering the general axisymmetric case of steady state plastic flow, we have,

$$u = \frac{1}{r}\frac{\partial \psi}{\partial z}$$

$$v = -\frac{1}{r}\frac{\partial \psi}{\partial r} \qquad (8.21)$$

where ψ is the stream function

and u, v the velocities along the r, z directions.

The strain rates can be expressed as,

$$\epsilon_r = \frac{\partial u}{\partial r}$$

$$\dot{\epsilon}_\theta = \frac{u}{r}$$

$$\dot{\epsilon}_z = \frac{\partial v}{\partial z} \tag{8.22}$$

$$\dot{\epsilon}_{rz} = \frac{\partial u}{\partial z} + \frac{\partial v}{\partial r}$$

Now assuming a polynomial approximation for ψ for the type of element considered, we can obtain as in the displacement method

$$\dot{\boldsymbol{\epsilon}} = \mathbf{B}\,\boldsymbol{\delta} \tag{8.23}$$

where $\boldsymbol{\delta} = f(\psi, u, V)$ at the nodal points. Using the Levy-Mises relations for the rigid-plastic material (neglecting the effect of elasticity) we have,

$$\boldsymbol{\sigma}' = \lambda\,\dot{\boldsymbol{\epsilon}} = \frac{2}{3}\frac{\bar{\sigma}}{\dot{\bar{\epsilon}}}\,\dot{\boldsymbol{\epsilon}} \tag{8.24}$$

where $\boldsymbol{\sigma}'$ are the deviatoric stresses and $\dot{\boldsymbol{\epsilon}}$ are the strain rates. The rate of work done can be written as

$$W = \int \boldsymbol{\sigma}'^{T}\,\dot{\boldsymbol{\epsilon}}\; dV \tag{8.25}$$

The solution to the problem is obtained when the total rate of work done becomes a minimum, i.e.

$$\frac{\partial W}{\partial \mathbf{f}} = \mathbf{0} \tag{8.26}$$

i.e. $$\frac{\partial}{\partial \mathbf{f}} \int \boldsymbol{\sigma}'^{T}\,\dot{\boldsymbol{\epsilon}}\; dV = 0 \tag{8.27}$$

This leads to a set of simultaneous equations of the form,

$$\mathbf{K}\,\mathbf{f} = \mathbf{0} \tag{8.28}$$

where $\mathbf{f}$ are the unknown ψ, u and v at the nodal points.

The stiffness matrix $\mathbf{K}$ involves terms of $\bar{\sigma}$ and $\dot{\bar{\epsilon}}$ and has to be known approximately before the analysis. After the solution new values of $\bar{\sigma}$ and $\dot{\bar{\epsilon}}$ can be used again in equation (8.28) to obtain better values of $\bar{\sigma}$ and $\dot{\bar{\epsilon}}$. The process of iteration can be accelerated by the use of a numerical technique such as the Newton-Raphson method. The strain rates and hence the deviatoric stresses can be

readily obtained from the known values of ξ. The hydrostatic stress not being used directly in the work rate function is not available directly. It may however be possible to obtain the hydrostatic stresses indirectly by using the equilibrium condition at the nodal points.

CHAPTER 9

9 CONCLUSIONS AND DISCUSSION

The finite element method is a powerful tool in the solution of many nonlinear problems. The method is ideally suited for the analysis of elastic, elastic-plastic and large deformation problems. In the displacement method of finite elements used here extensively, approximations are made only in the displacement function assumed for the particular element considered and further approximations are very often unnecessary. The real advantage of the method is its possibility of handling complicated shapes and almost any boundary condition without much difficulty. The disadvantages are of course the large storages and times required by the computer to solve large practical problems. The advantages in most cases seem to outweigh the disadvantages, (which keep on diminishing with the advent of modern high speed digital computers having large core storages) and the method seems feasible for the solution of many practical problems.

The tangential stiffness method has been used for the present analysis due to the combined nature of the nonlinearities. This method is believed to be superior to the alternative initial strain or initial stress methods when large deformations are experienced together with plasticity. Any other forms of nonlinearity can also be incorporated without much difficulty as the overall stiffness matrix is changed in any case after every increment.

For the evaluation of the stiffness of the element two distinct methods have been suggested. First is the 'Cartesian

stiffness' method due to Turner (72) and others. The second method is due to Argyris (4) and is known as the 'natural mode technique'. The former is simpler and easier to program for the case of the triangular element and is adopted here for the plane-stress and the axisymmetric cases. The latter is used to derive the stiffnesses of the plane-strain and three-dimensional TET4 elements.

The effect of plasticity has been taken into account using the Prandtl-Reuss relations and the yield criterion of von-Mises although any other form can be readily substituted by replacing the function f in section (2.3). This has not been attempted in the present work as it is well established that the behaviour of most metals can be very closely represented by the Prandtl-Reuss relations and the von-Mises yield criterion. The nonlinear stress-strain relationship for most metals can be approximated by the law $\bar{\sigma} = \sigma_o (1 + B \bar{\epsilon}_p)^n$ and this is adopted throughout the present analysis, experimental values being used to fit the best possible curve.

Some difficulty was experienced in trying to fit experimental values to the given stress-strain law. There does not seem to be a consistently accurate method which would work for most cases. Several methods have been suggested in Appendix B, even though most of them give different answers for the values of σ_o, B and n. The Gauss-Newton method and the simplex direct search method do not necessarily give a solution to certain experimental data. It seems that good starting values of σ_o, B and n are necessary to obtain an accurate solution from these techniques. A method suggested by Alexander* seems to give at least an approximate answer most

* J.M. Alexander - private communication.

of the time. The results obtained by this method (which minimise the log of the function, but does not require a starting solution), although fairly accurate are not usually the same as obtained by the other methods. An alternative and a somewhat better method would be to get a starting point from the last method and to use the simplex method of direct search to obtain a better solution.

The nonlinearities arising from the large displacements are dealt with in two alternative ways. The first is the usual approach of using the Green's strain tensor to obtain the additional 'Initial displacement' and the 'Initial stress' matrices. The second is to obtain the 'Initial stress' or the 'Geometric matrix' using natural modes. The two methods in the present work have been used intuitively although the first leads to the Lagrangian approach with reference to the initial configuration, and the second to the Eulerian approach with reference to the current configuration. However by properly defining a local co-ordinate system the first method can be used with the Eulerian approach as well, which consequently discards the 'Initial displacement matrix'. 'Initial Load' matrices (19) would be present for both cases, but it has been shown that these vanish for the simplest case of a constant strain triangular element.

The Lagrangian approach gives rise to the Green strain tensor and the Kirchoff stress, while the Eulerian approach gives the Euler strain tensor and the Euler stress. These two strains and stresses can be related in terms of the current and the initial configurations. Both approaches have their own advantages and disadvantages. With large strains together with large displacements, the existing small strain constitutive relations may not be valid and proper constitutive

relations may have to be found. Furthermore the strains and the stresses have to be referred to the proper configuration; the stresses in the Eulerian formulation being also the true stresses. In the Lagrangian formulation the stresses obtained are the Kirchoff's stresses which can be transformed into the true stresses (19).

The methods used for the determination of the proper load increment and allowing more than one element to yield at one time was found to be quite satisfactory. The two methods have been combined together to be more efficient and were used to obtain the solution for most of the problems given here. This was found to be particularly advantageous during the early load increments where the plastic region is still small compared to the elastic region. When the plastic zone region spreads out during subsequent load increments the step size is controlled manually to give the desired deformation within a reasonable number of steps. It was found that fast convergence of the stresses within a load increment was achieved by the use of small load increments.

The iterative technique used for the convergence of the stresses within an increment did not show any convergence or converged slowly for certain cases and for relatively large load increments. A non-iterative technique, the fourth order Runge-Kutta method was used for such cases and was found to take less computational time. For load increments where the iterative method took long to converge (more than 4 iterations), the Runge-Kutta method was found to be computationally superior. The Gauss Siedel iterative method was used to solve the overall stiffness matrix. Sev-

eral other alternative methods have been suggested but it has been found that this method is the fastest available for the solution of a large number of simultaneous equations and is adopted here for all the problems considered.

The program developed was used to obtain the solutions for the two known problems in Chapter 6. The material was assumed to be elastic-plastic, but only small displacements were considered. The results agree well with the existing theoretical and experimental solutions. It was noted that a higher degree of accuracy was obtained using the second mesh idealization for the thick walled cylinder although the same number of elements were used in both cases.

The two plate problems represented good examples of combined nonlinearity. The plates under deformation had three distinct regions. The elastic region near the edge of the plate, the elastic-plastic region in the middle and the distinct large deformation elastic-plastic region near the edge of the hole. The large deformations were localised and did not extend over the whole elastic-plastic region. The finite element solutions obtained agreed well with the theoretical and the experimental results.

An attempt was made to give a solution to the more difficult problem of 'dieless drawing' using the finite element method. The displacement method of finite elements is not capable of giving a complete solution to a steady-state problem in which the forces of deformation remain unchanged. The displacement method provides increments of displacements for increments of the load or vice-versa and also the corresponding increments of the strains

and the stresses. In a steady state problem there are finite displacements for no further increase of the load, and this from the displacement type of approach is not feasible unless the stiffness matrix becomes singular. For such a case there will be an infinite number of solutions in general and hence the solution scheme would fail. However, a steady state type solu - tion may be approached using the displacement method incrementally until no convergence is obtained for further load increments.

The finite element solutions obtained for the dieless drawing problem are not very accurate. Some accuracy is sacrificed in order to save storage and computer time. The use of larger elements and large incremental steps may have resulted in some errors particularly for the stresses. However, the agreement obtained with experimentally obtained profiles during steady state deformation is very good. The strains obtained are also of the same order as the approximate theoretical solution but the stresses are overestimated.

An alternative approximate solution is suggested for this problem. It has been noticed that the solution is very sensitive to change of stress-strain data with temperature. Unless these data have been obtained fairly accurately, the solutions may not be useful at all. The effect of strain-rate should also be taken into account to predict better results as was shown by some of the experiments with stainless steel and titanium. The stainless steel specimens always tend to go into a deep neck without going into the steady state whilst the titanium specimens get into the steady state without much difficulty.

9.1 Suggestions for future work

The finite element method has been used extensively in the solution of problems in all areas of Engineering and Science. With the advent of modern high speed digital computers very complicated problems can be solved economically using this method.

The method suggested here should be useful for stress analysis problems and the analysis of large deformation elastic-plastic problems. The present method may be improved and modified to provide more accurate solutions using lesser computer storages and times. Although some attempt was made to economise on the storage and time, extensive research was not carried out in this direction. The elements too can be improved by assuming higher polynomial displacement functions and using curved edges. The use of three-dimensional elements for nonlinear cases with plasticity and large deformations should be investigated. Although a program was developed for the TET4 element and several trial runs made no proper problem was solved using this program. The limitations of the use of such a program is mainly due to the storage and time limits in the computer.

The displacement method suggested is, however, not very suitable for the solution of steady state problems. As stated in chapter 8.2 a different formulation using the stream function ψ and its derivatives may be more suitable for such an analysis. Several interesting metal flow problems may be solved using the suggested formulation. It would be comparatively easy to obtain a solution for a kinematically admissible velocity field using this method, but whether it is possible to find a direct solution to the

stress field is not very clear, due to the absence of the mean stress in the work rate function. This may be evaluated indirectly, perhaps, by considering the equilibrium of the forces and the stresses at each nodal point.

The displacement method on the other hand is very suitable for unsteady elastic-plastic problems with large deformations. The method would be ideal for instance, for the analysis of stresses around cracks. Here it would be interesting to see the effect of large deformations on the distribution of the stresses. The method would be also applicable for other stress analysis problems.

The problems of forging, indentation and other similar unsteady problems may be solved using this method. The boundary conditions, of course, would present some difficulty especially at the interface where the frictional conditions are unknown. This probably would have to be evaluated experimentally or several runs may be made with varying frictional properties to predict a correct solution.

Another area in which this method may be useful is for the determination of collapse load conditions and break down analysis in bodies and structures. The tangential stiffness method can be used very effectively here, taking into account all the forms of nonlinearities and carrying out the analysis step by step.

Some research has been made into the application of the finite element method to soil mechanics (38). The method suggested here would be very suitable to analyse the plastic deformation of soils, after substituting a suitable yield criterion and flow rule for the particular soil concerned.

LOADING	E_p=220	E_p=0
I	0.617	0.620
II	0.665	0.660
III	0.778	0.770
IV	0.880	0.870
V	0.983	0.960
VI	1.022	0.990

Values of $2\sigma_m/\sigma_o$

Table 1

T ^{o}C	σ_o T/in^2	B	n
800	7.872	25.05	0.2238
900	5.145	24.78	0.1851
1000	2.571	25.95	0.2262
1100	0.953	18.27	0.4689

Table 2

Material Properties of EN 58J Steel

SPECIMEN NO. 101

LOAD ON THE SPECIMEN = 4.80000 TONS

NO.	DISTANCE"	DIAMETER"	TEMPER. °C	T/in² STRESSS	STRAIN	in/s VELOCITY
1	0.0000	1.5000	994.36	2.71624	0.00000	.85000
2	.2000	1.4960	996.78	2.73078	.00534	.85455
3	.4000	1.4940	997.87	2.73810	.00802	.85684
4	.6000	1.4870	1001.79	2.76394	.01741	.86493
5	.8000	1.4760	1007.98	2.80529	.03226	.87787
6	1.0000	1.4620	1013.76	2.85927	.05132	.89476
7	1.2000	1.4360	1020.86	2.96375	.08721	.92745
8	1.4000	1.4140	1024.66	3.05669	.11809	.95654
9	1.6000	1.3840	1027.75	3.19064	.16097	.99846
10	1.8000	1.3550	1029.08	3.32868	.20333	1.04165
11	2.0000	1.3240	1029.05	3.48638	.24962	1.09100
12	2.2000	1.2930	1027.72	3.65555	.29700	1.14394
13	2.4000	1.2520	1024.05	3.89890	.36145	1.22009
14	2.6000	1.2190	1019.53	4.11285	.41487	1.28705
15	2.8000	1.1730	1010.73	4.44175	.49180	1.38997
16	3.0000	1.1240	998.94	4.83746	.57714	1.51380
17	3.2000	1.0770	991.35	5.26889	.66257	1.64881
18	3.4000	1.0280	981.81	5.78315	.75570	1.80974
19	3.6000	.9870	972.37	6.27359	.83710	1.96321
20	3.8000	.9580	964.79	6.65916	.89675	2.08387
21	4.0000	.9370	958.78	6.96099	.94107	2.17832
22	4.2000	.9330	957.58	7.02081	.94963	2.19704

TABLE 3

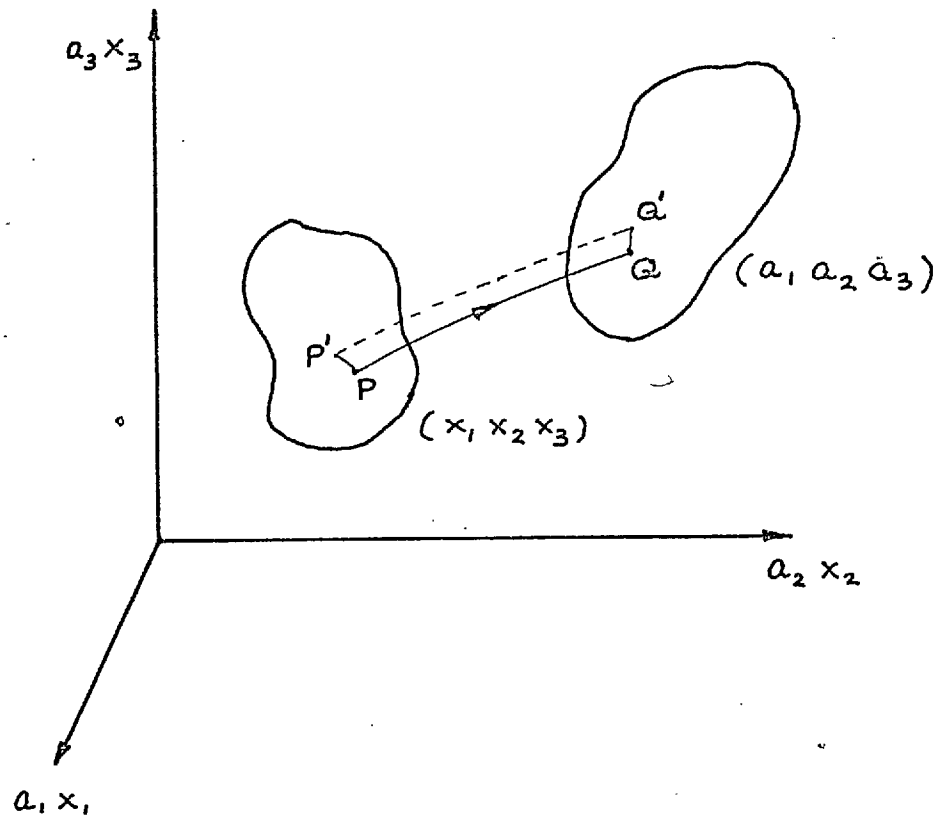


FIG. 1 FINITE DEFORMATION OF A BODY

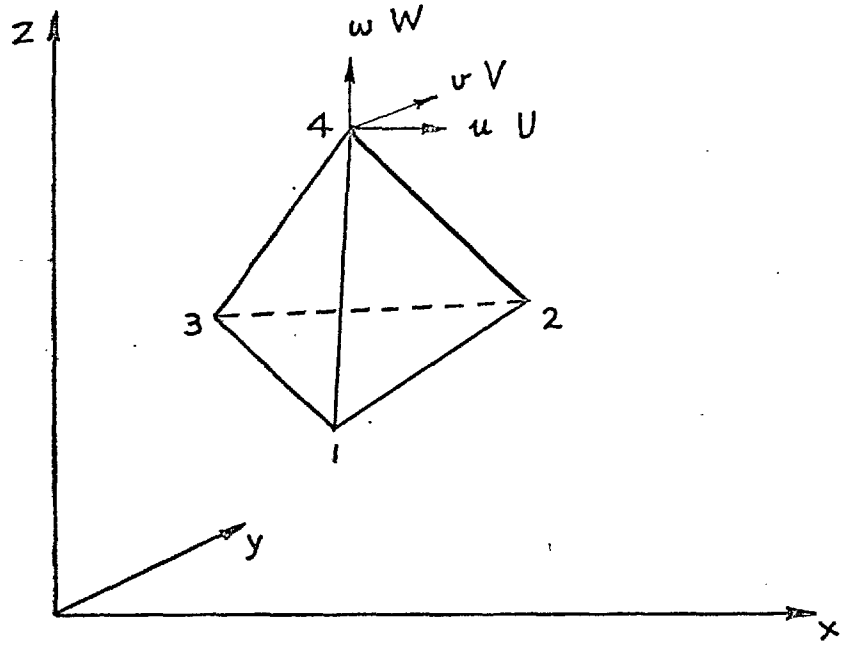


FIG. 2 CARTESIAN DISPLACEMENT AND FORCES TETRAHEDRON WITH 4 N.P.

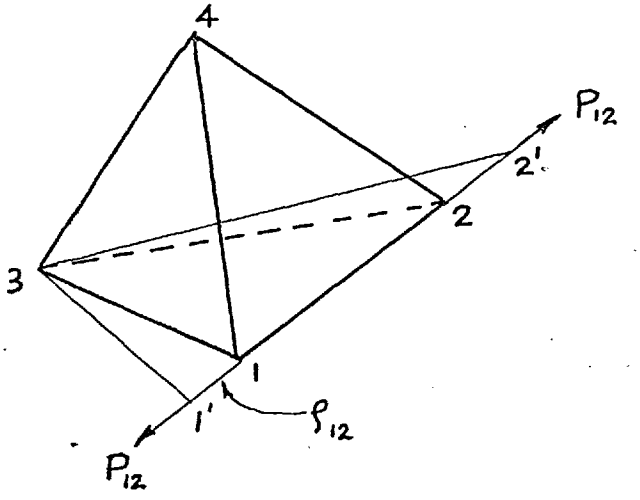


FIG. 3 NATURAL DISPLACEMENT AND FORCES (TET4)

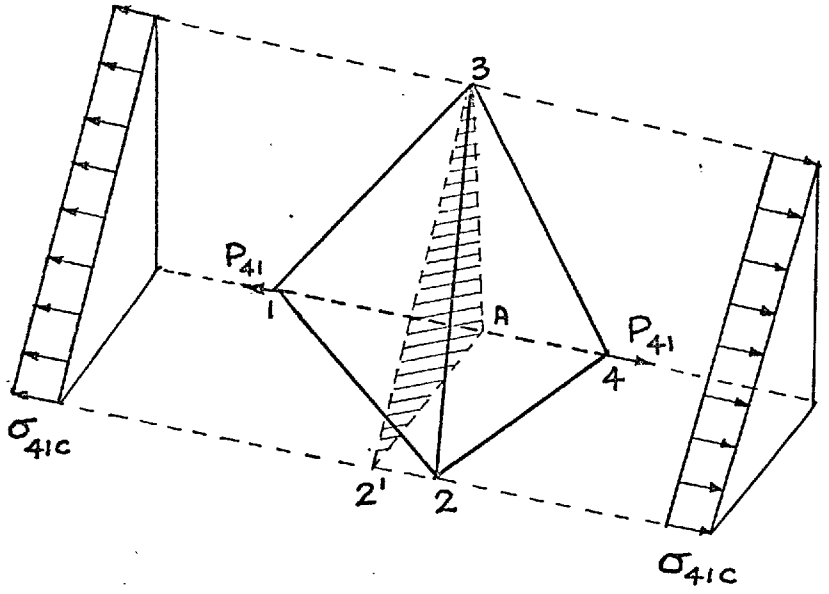


FIG.4 NATURAL COMPONENT STRESSES

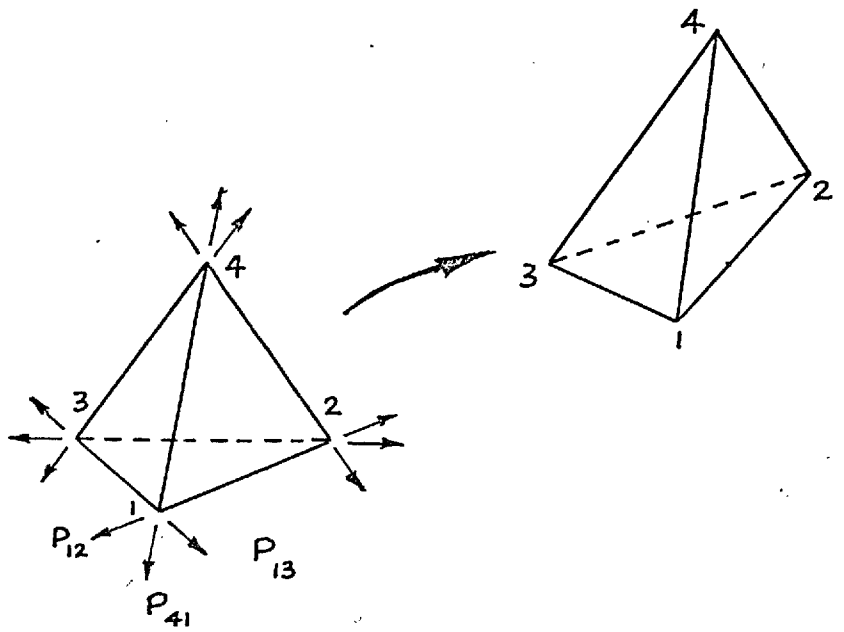


FIG.5 LARGE DEFORMATIONS (TET4)

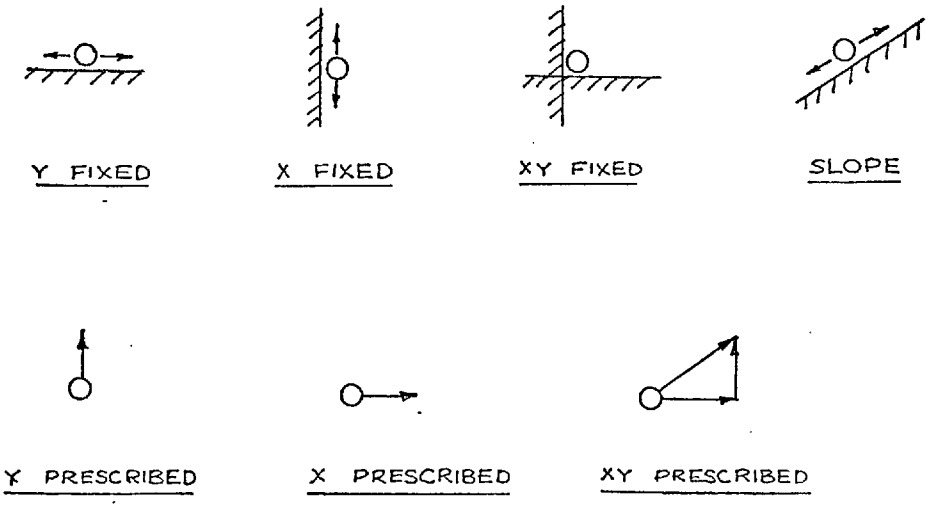


FIG. 6 DISPLACEMENT BOUNDARY CONDITIONS

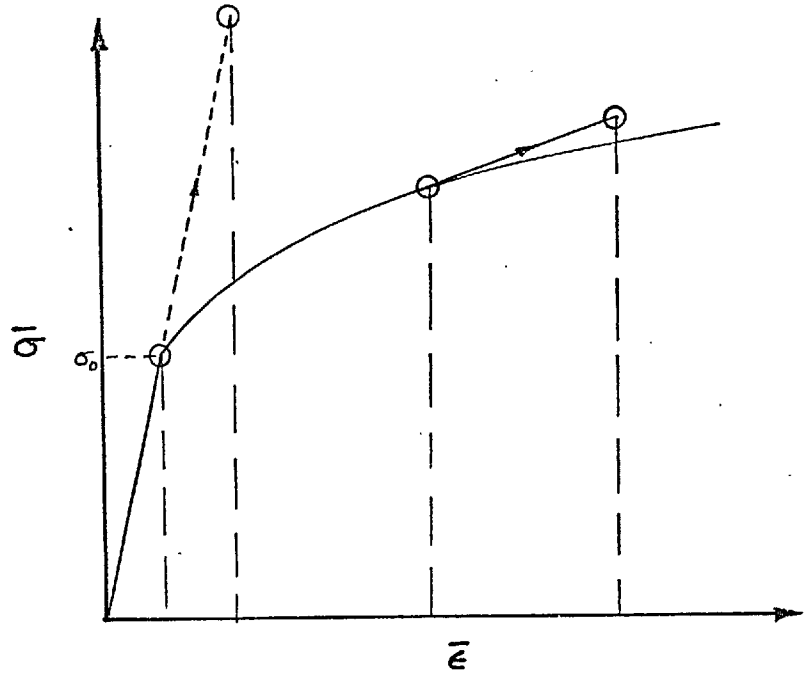
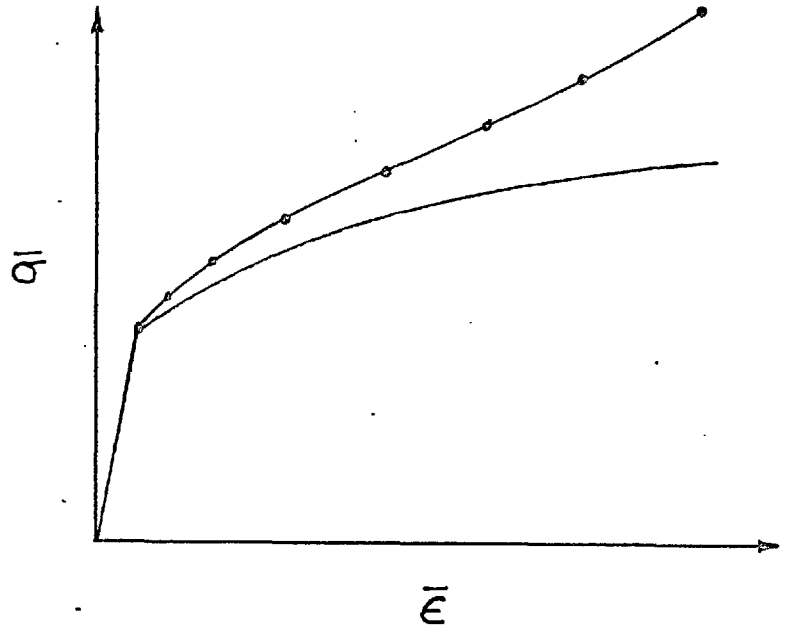
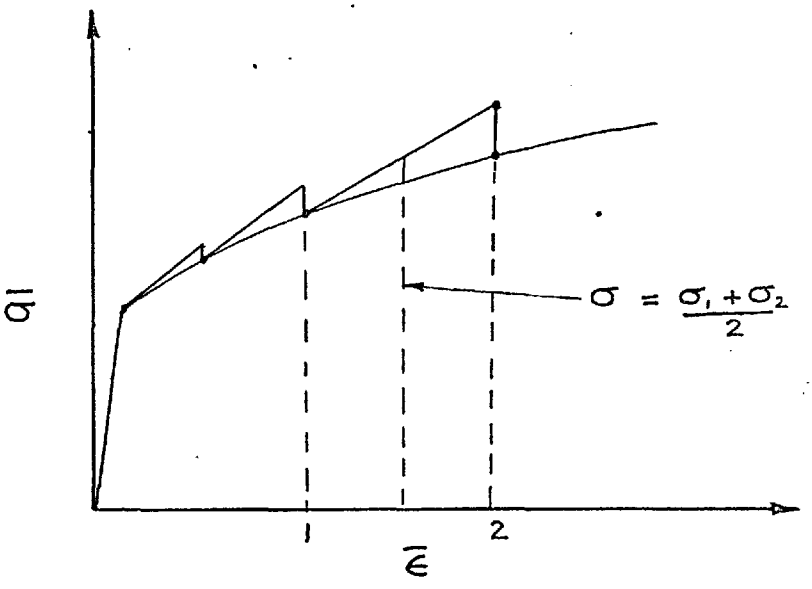


FIG. 7 LARGE LOAD INCREMENTS YIELD INCORRECT RESULTS



(a) ERROR ACCUMULATION DURING SUCCESSIVE INCREMENTS



(b) ITERATION DURING EACH INCREMENT

FIG. 8

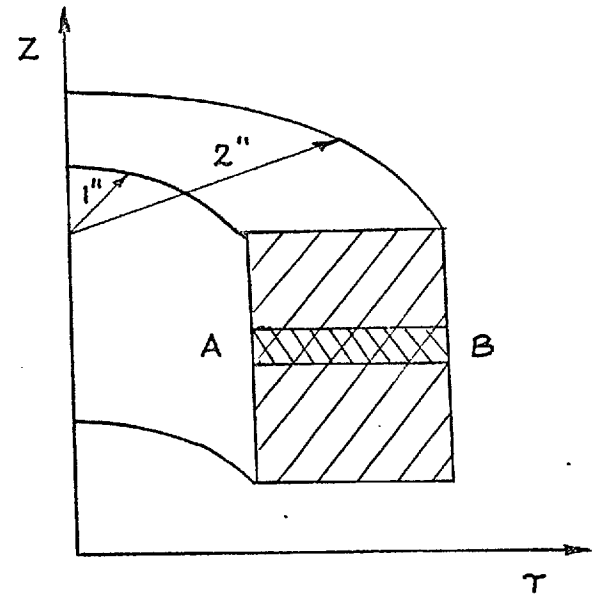
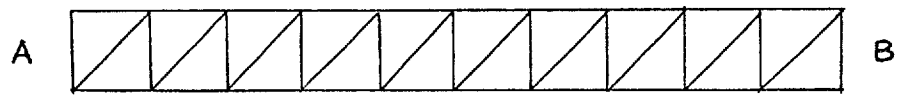
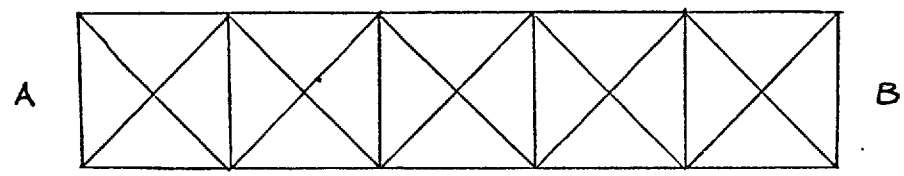


FIG. 9 THICK WALLED CYLINDER



(a) FIRST MESH



(b) SECOND MESH

FIG. 10 FINITE ELEMENT MESH IDEALISATIONS

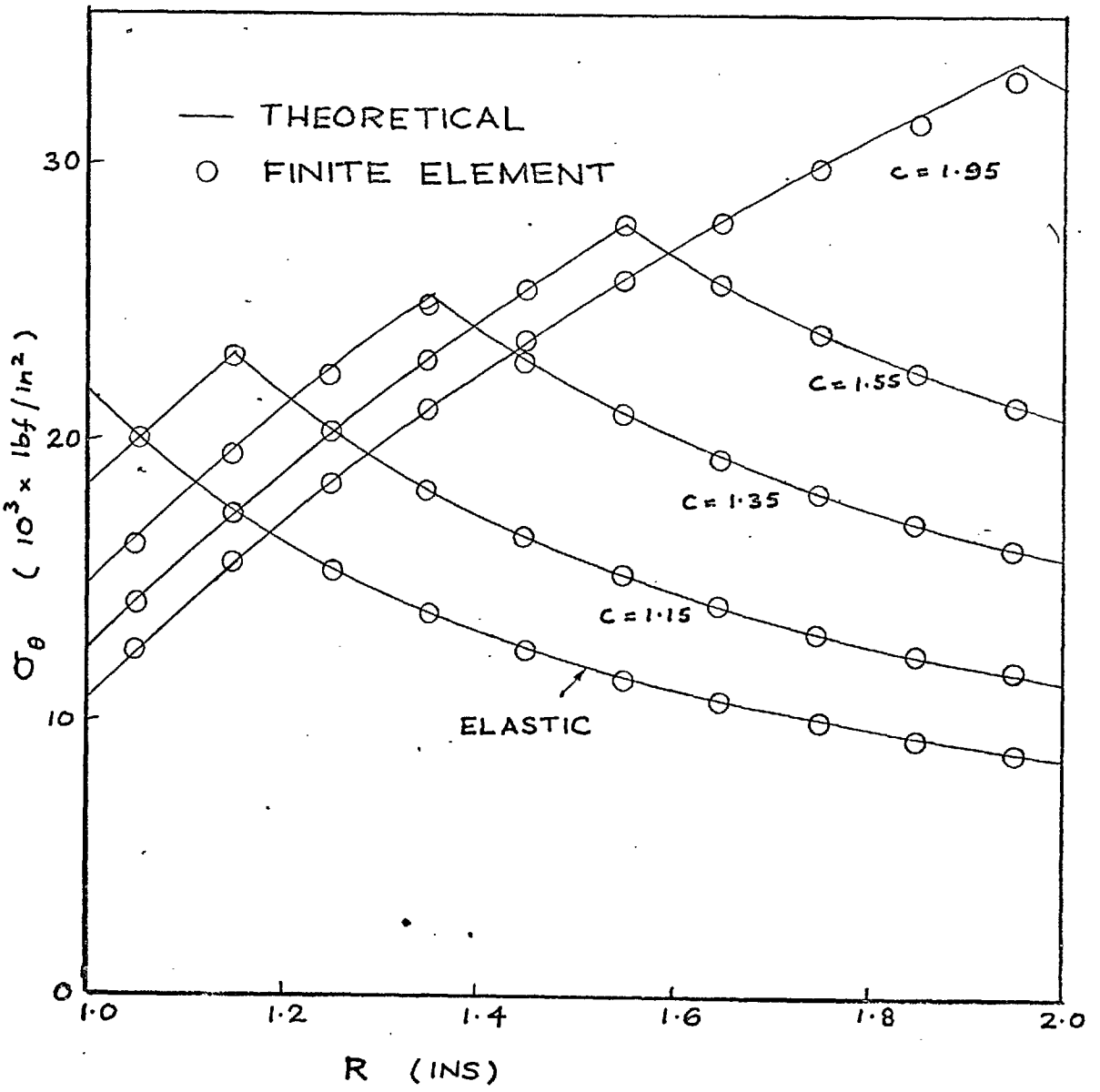


FIG. 11 TANGENTIAL STRESS DISTRIBUTION FOR THE THICK WALLED CYLINDER

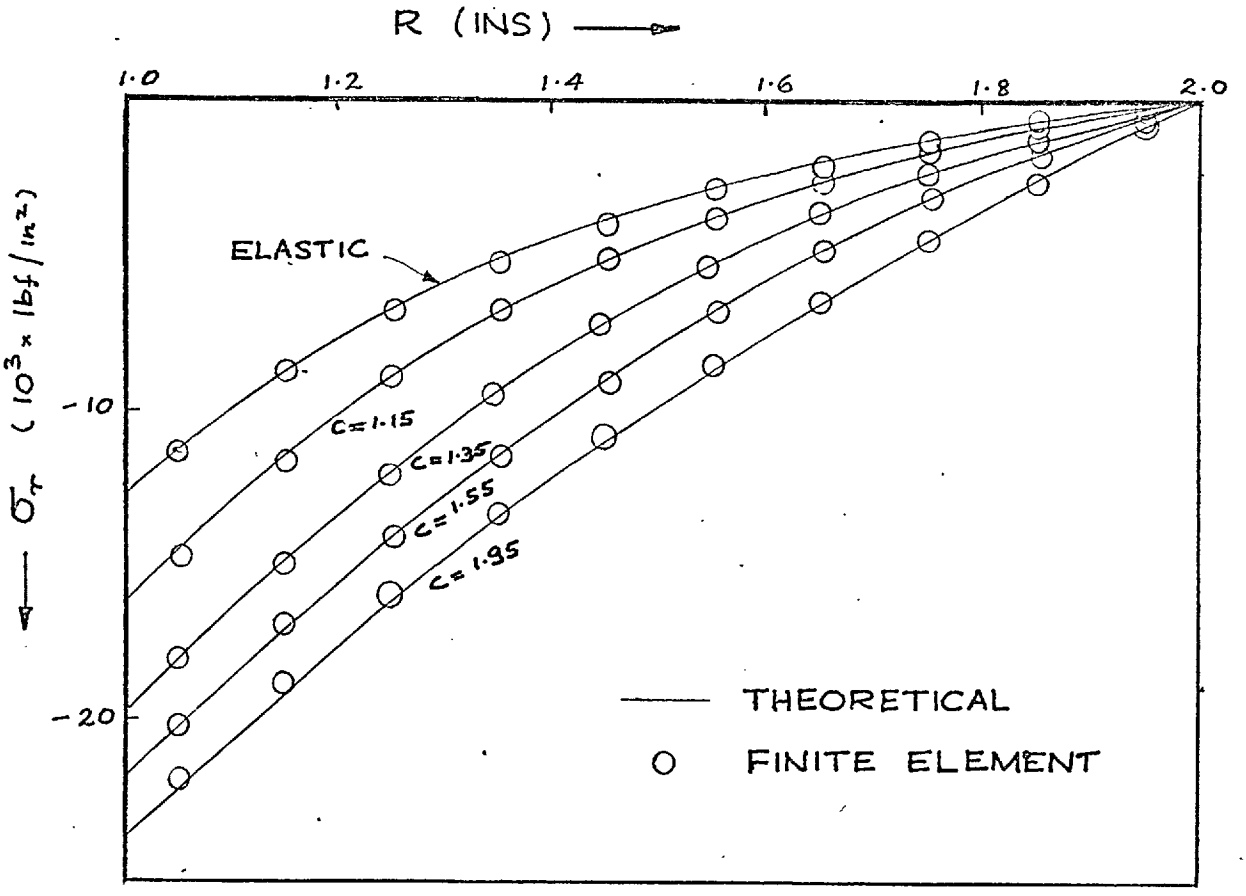


FIG. 12 RADIAL STRESS DISTRIBUTION FOR THE THICK WALLED CYLINDER

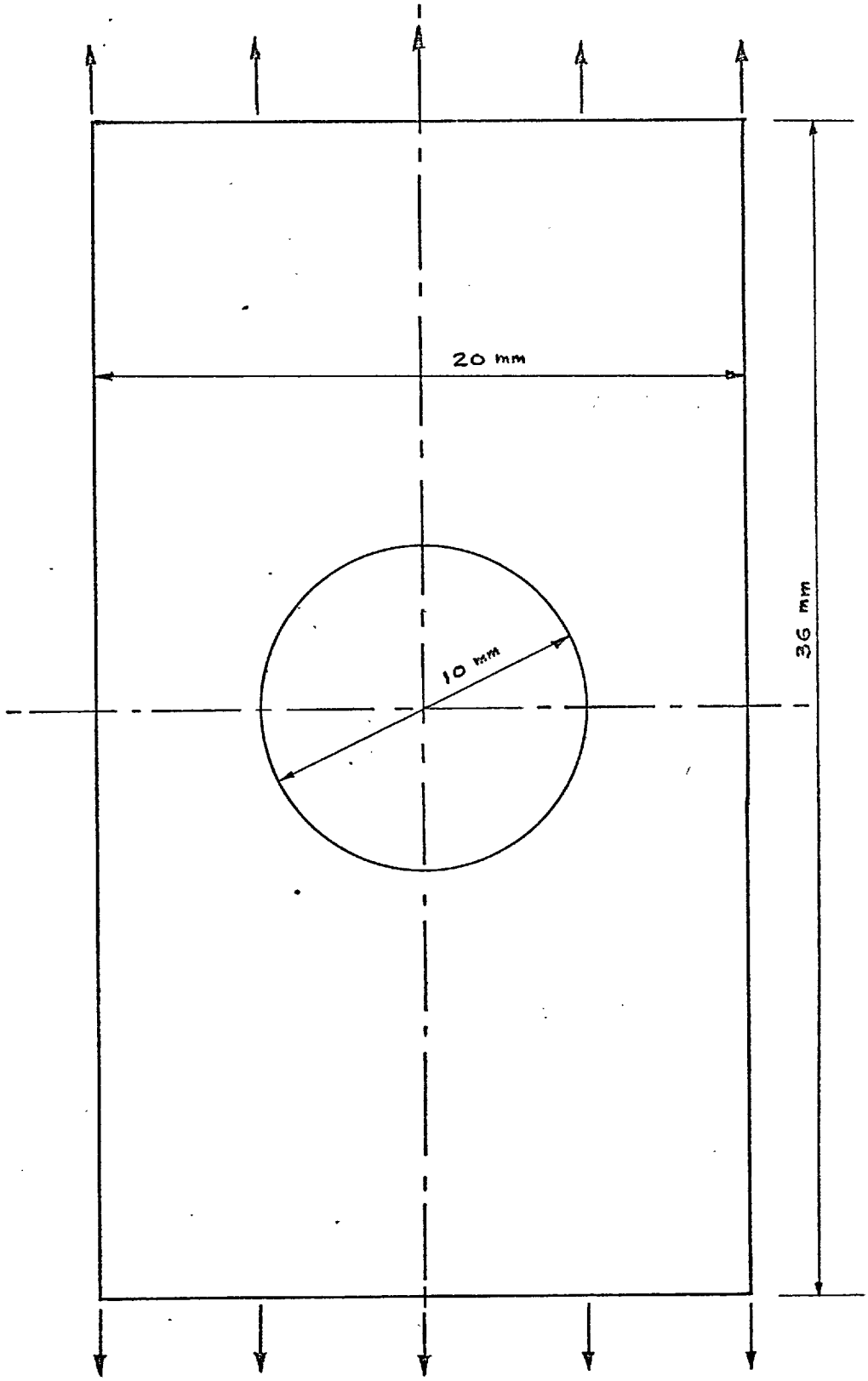


FIG. 13 PERFORATED STRIP UNDER TENSION

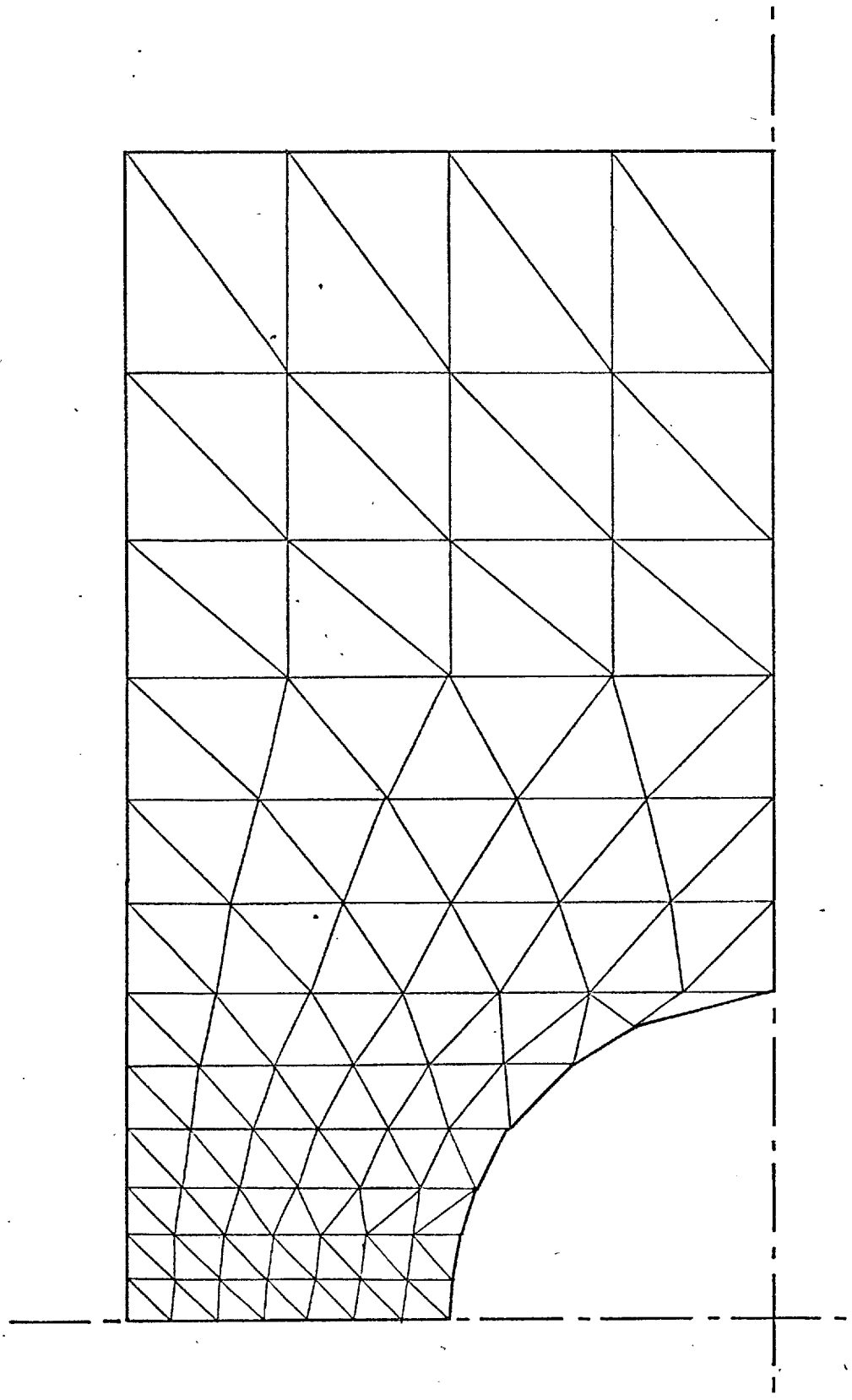


FIG. 14 MESH IDEALISATION FOR THE PERFORATED STRIP

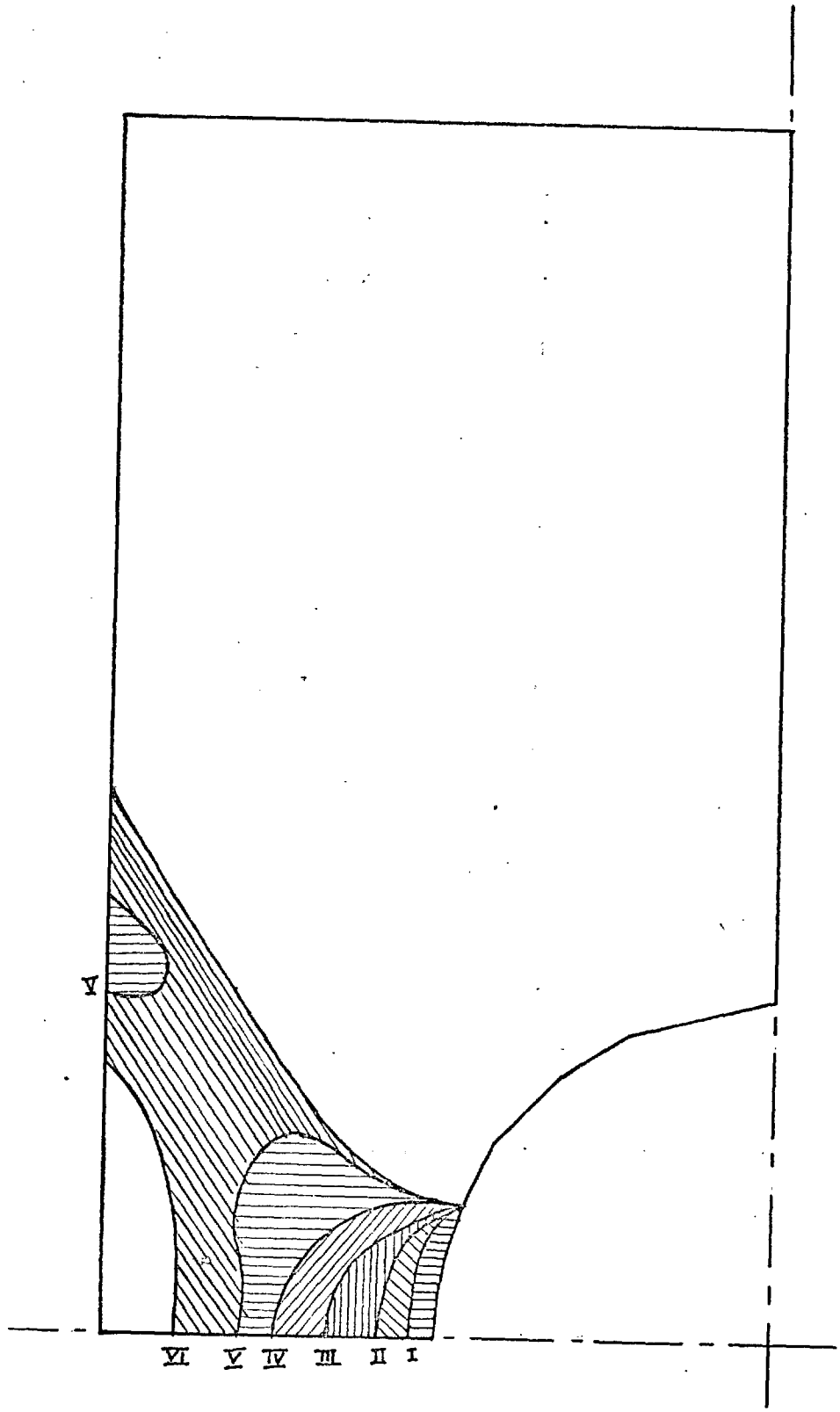


FIG. 15 DEVELOPMENT OF THE ELASTIC PLASTIC BOUNDARY ($E_p \neq 0$)

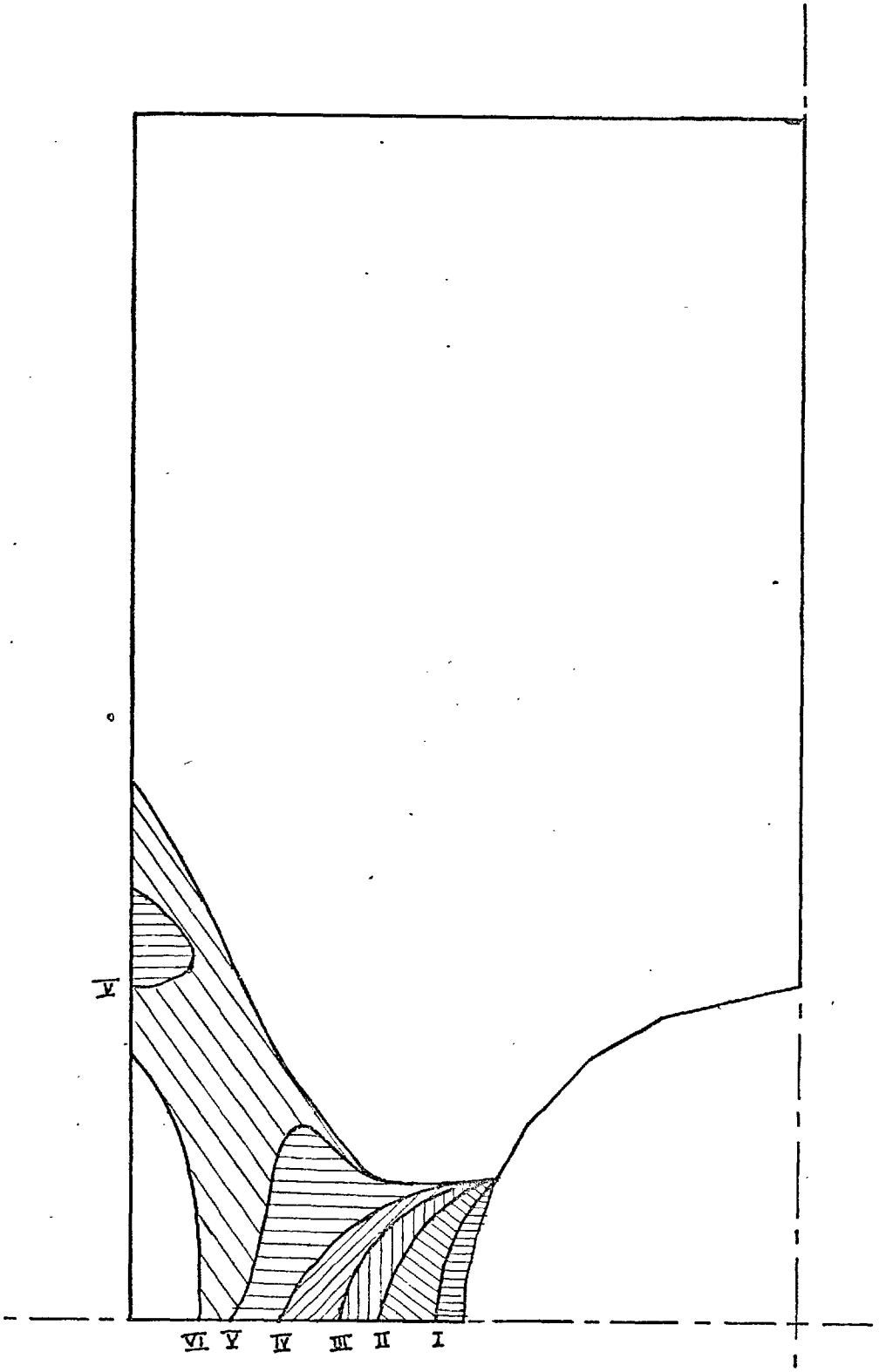


FIG. 16 DEVELOPMENT OF THE ELASTIC PLASTIC BOUNDARY ($E_p = 0$)

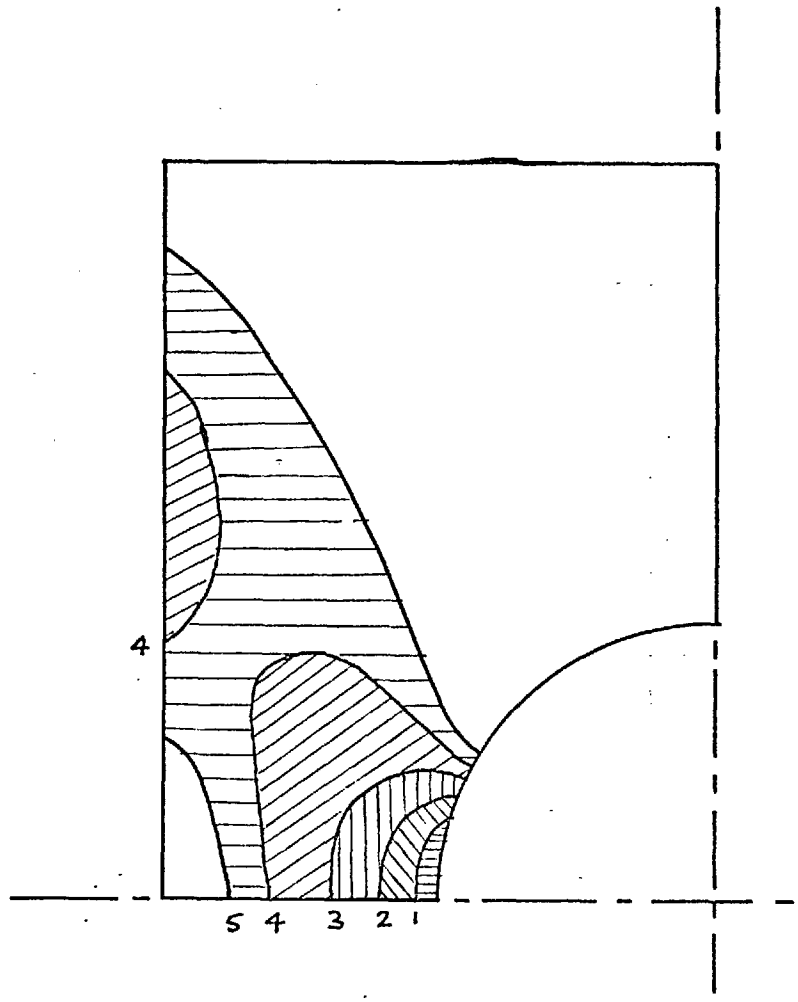
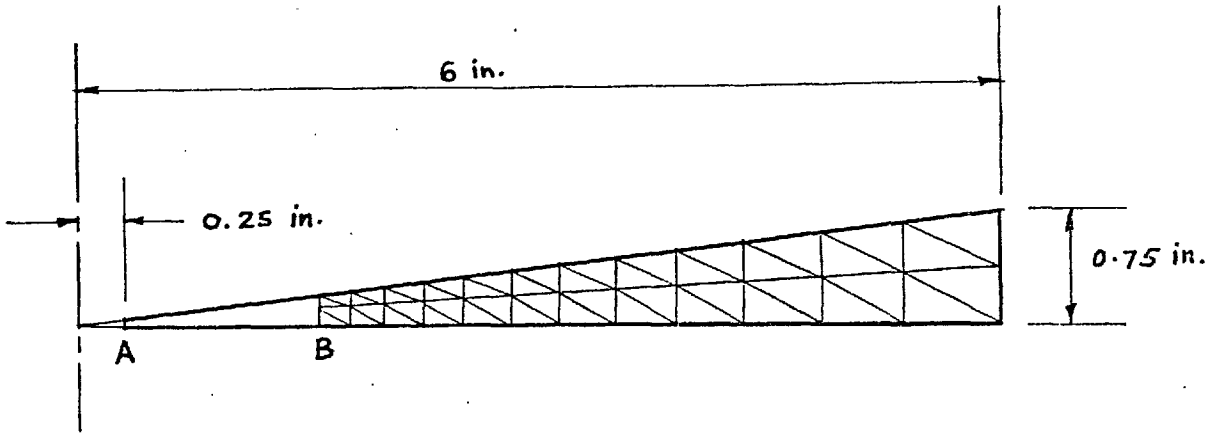


FIG. 17 DEVELOPMENT OF THE ELASTIC PLASTIC BOUNDARY (EXPERIMENTAL REF. 71) LOADING STEPS NOT IDENTICAL TO FIGS. 15, 16



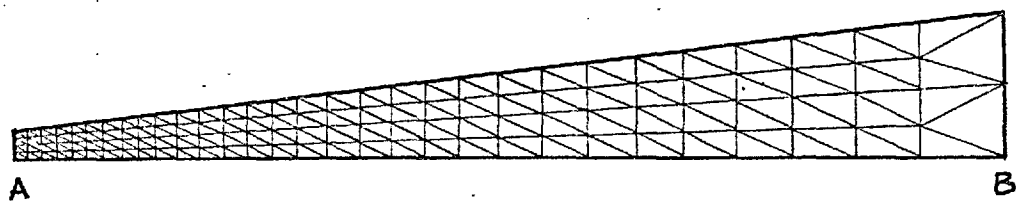


FIG.18 FINITE ELEMENT MESH IDEALIZATION FOR THE CONICAL PLATE

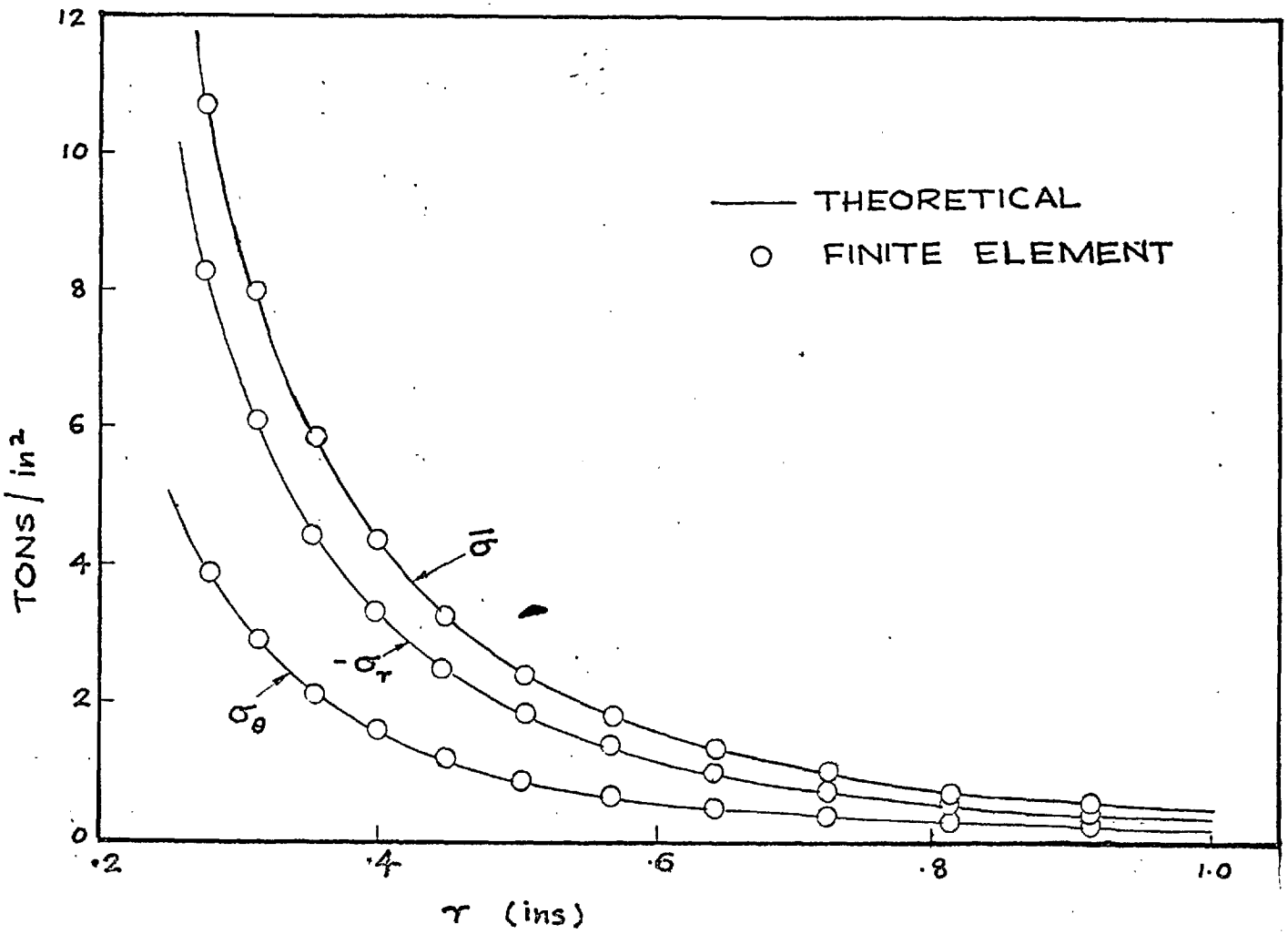


FIG. 19 STRESS DISTRIBUTION FOR THE CONICAL PLATE (ELASTIC)

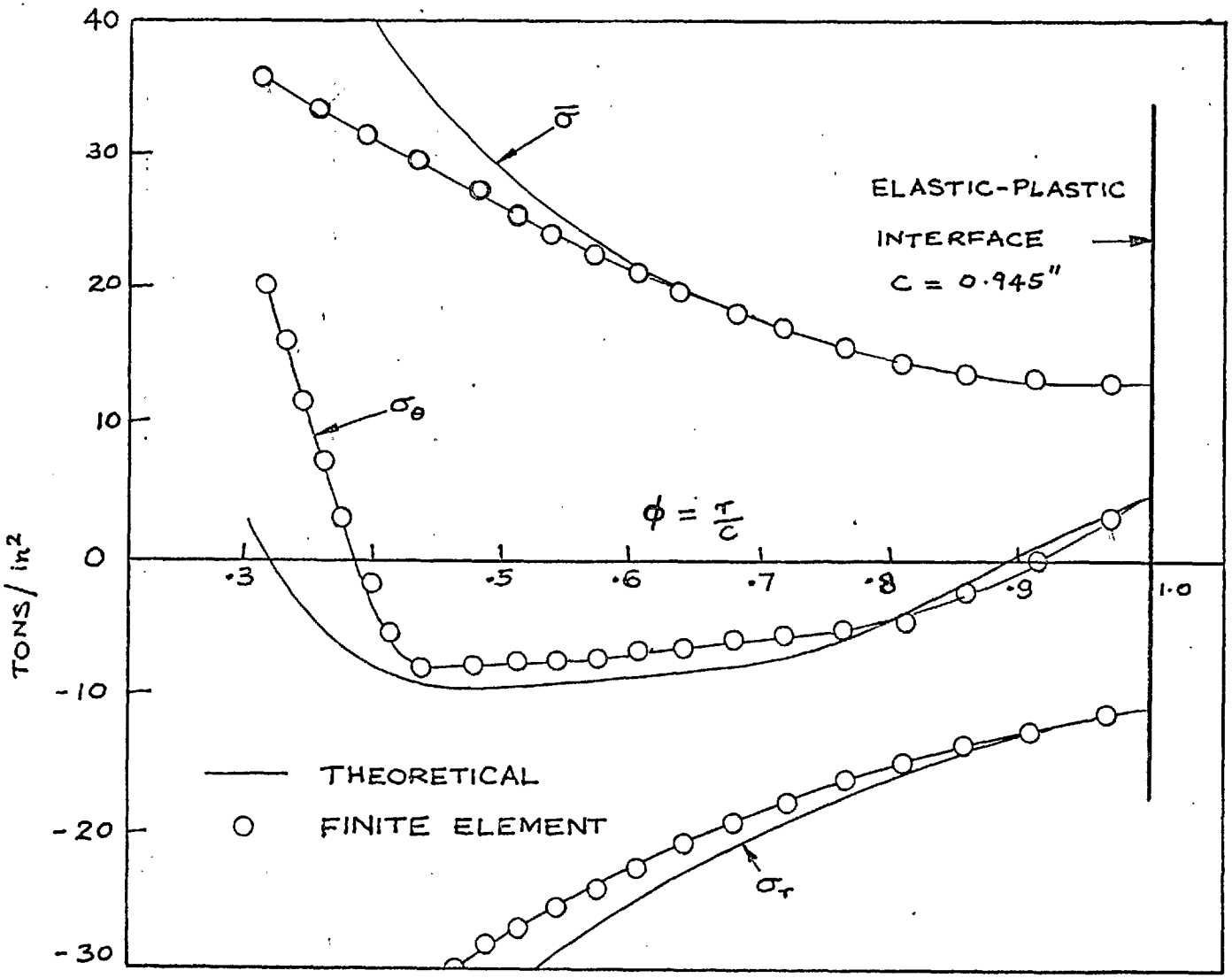


FIG. 20 STRESS DISTRIBUTION FOR CONICAL PLATE (ELASTIC-PLASTIC)

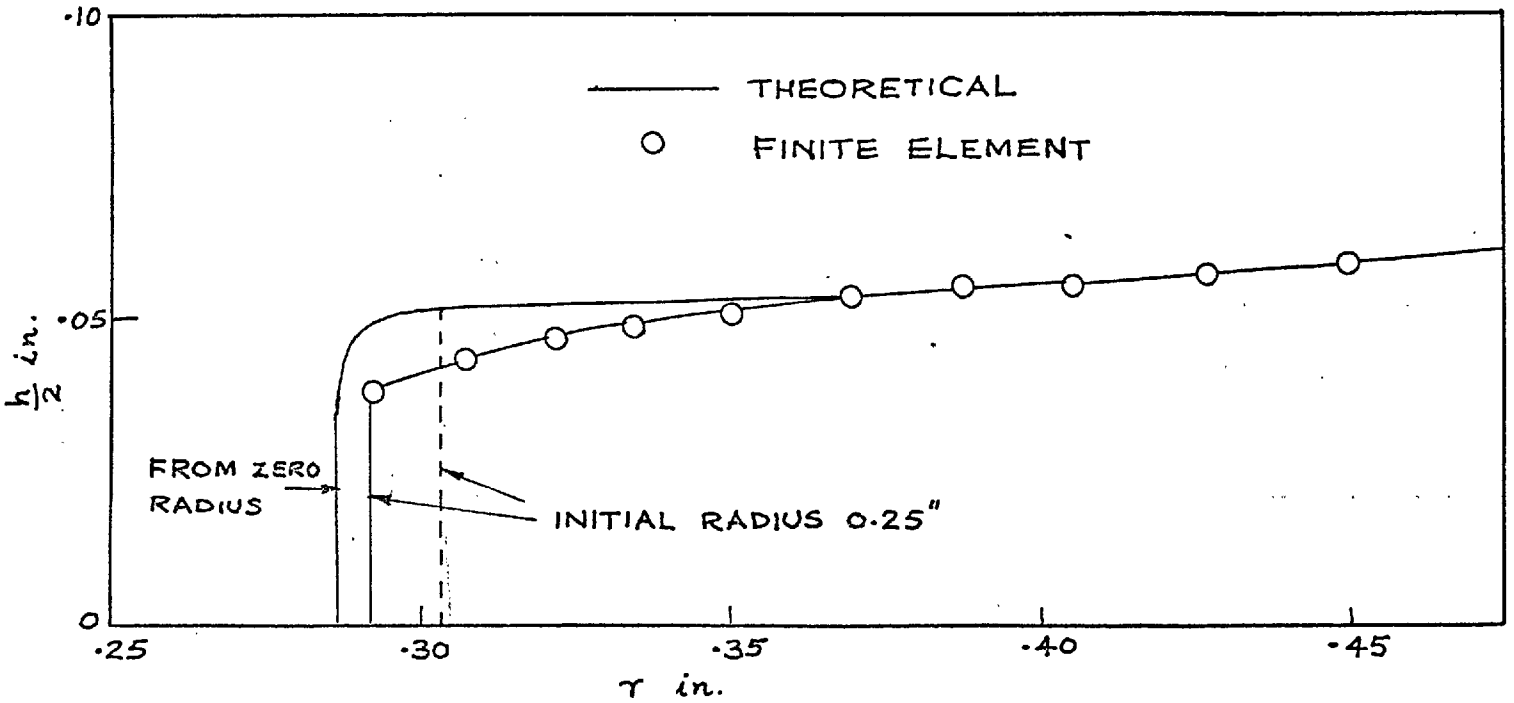


FIG. 21 THICKNESS PROFILE (CONICAL PLATE)

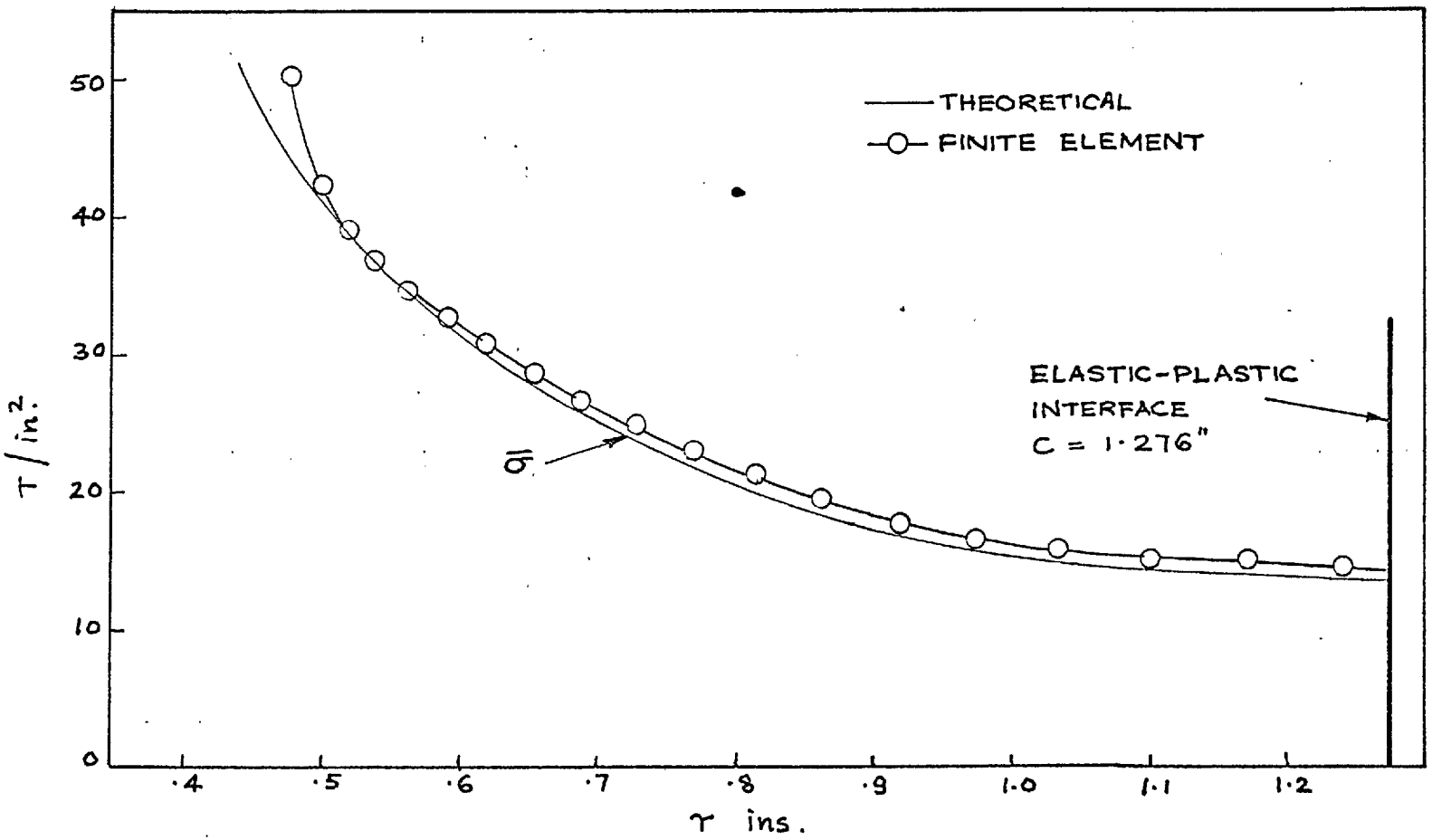


FIG. 22a FINAL STRESS DISTRIBUTION FOR THE CONICAL PLATE

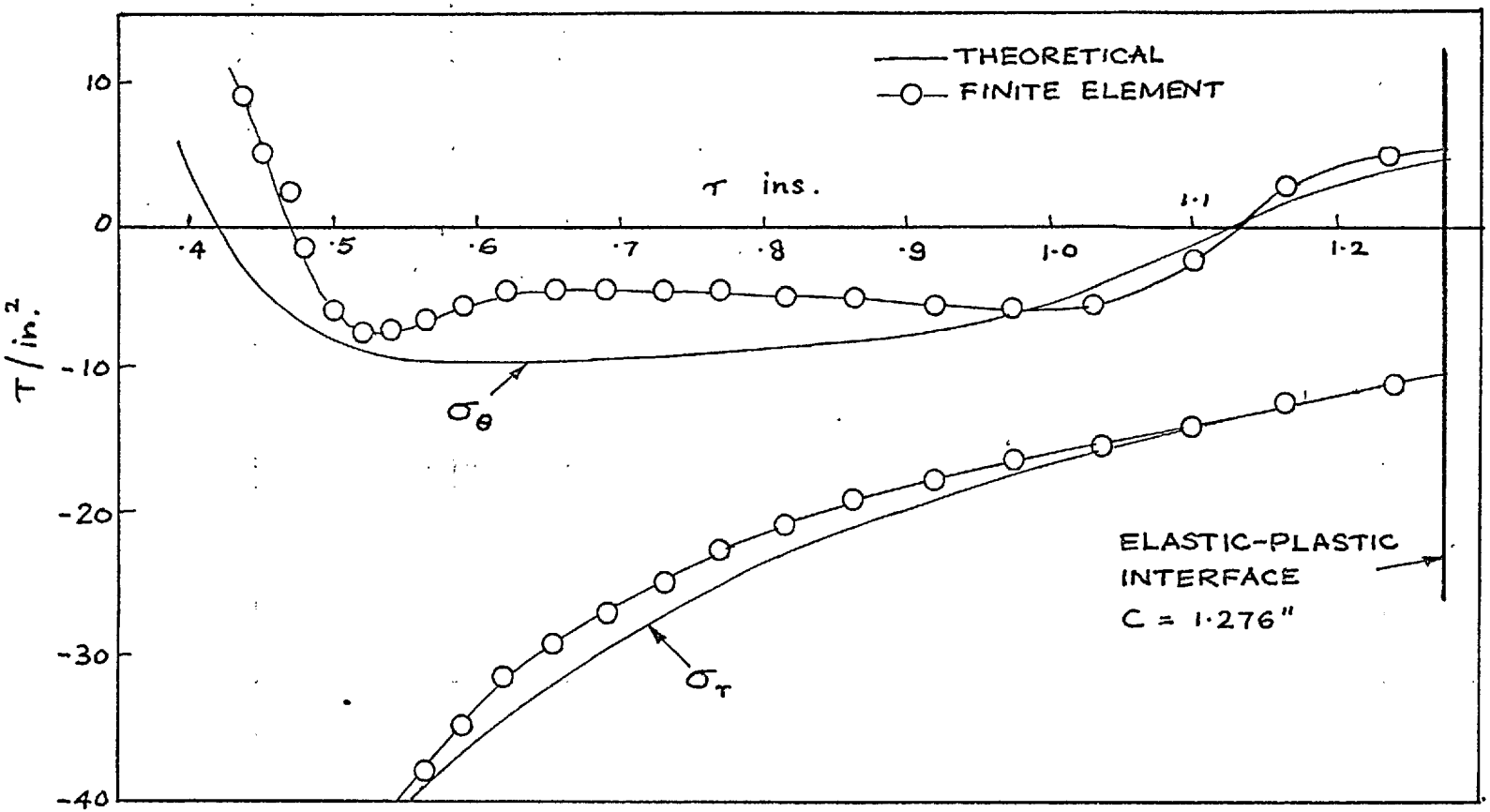


FIG. 22 b FINAL STRESS DISTRIBUTION FOR THE CONICAL PLATE

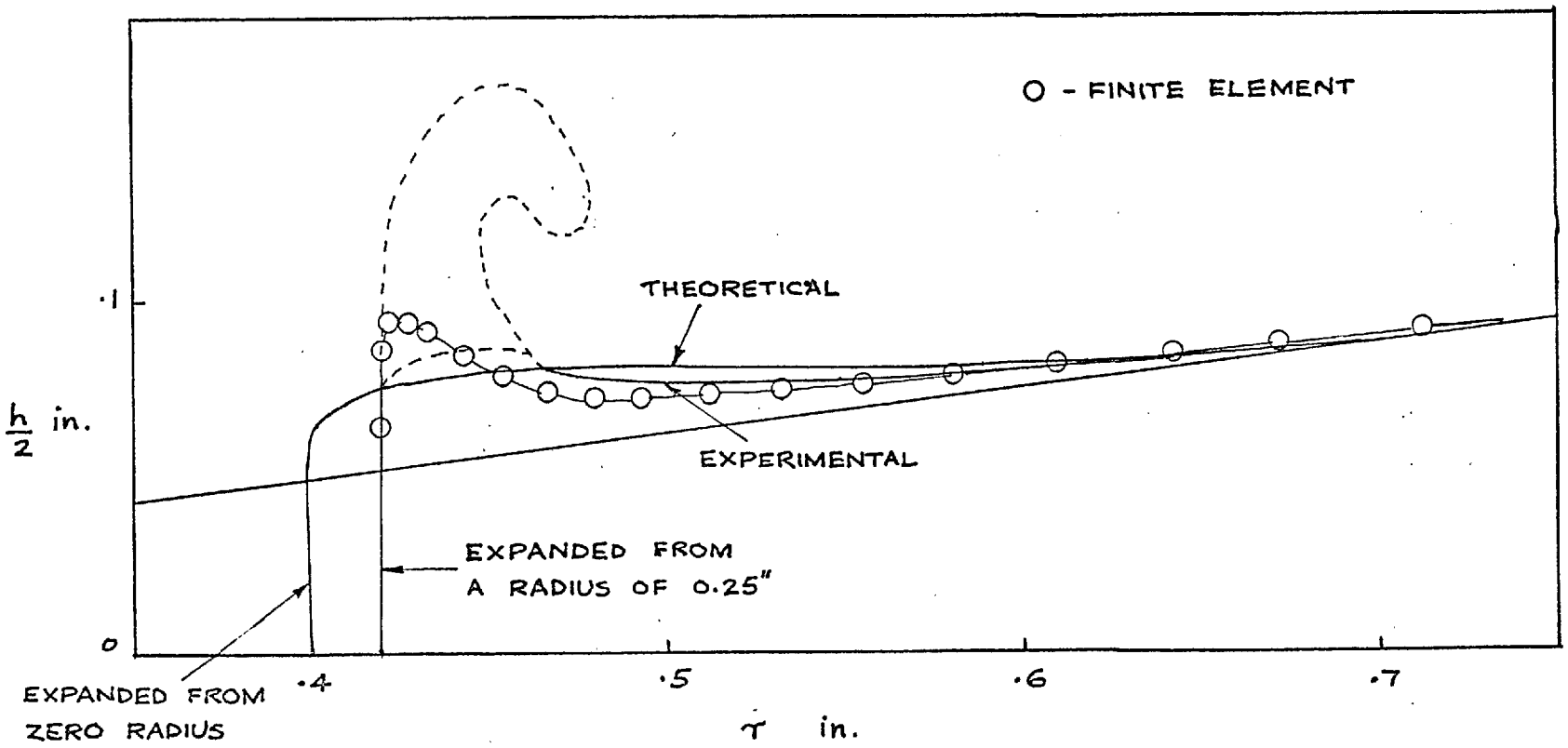


FIG. 23 FINAL THICKNESS PROFILE (CONICAL PLATE)

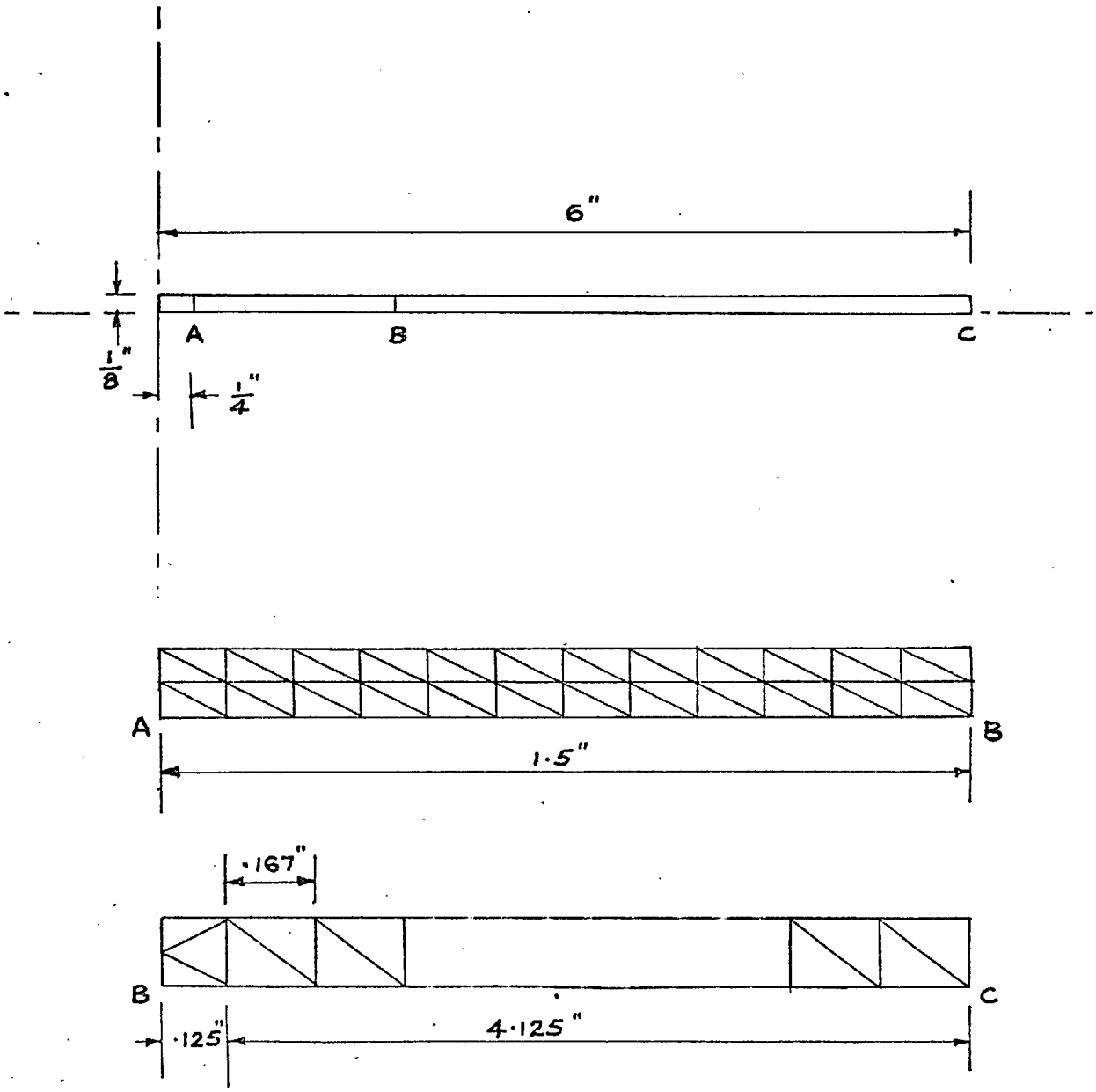


FIG. 24 FINITE ELEMENT MESH IDEALISATION FOR THE FLAT PLATE

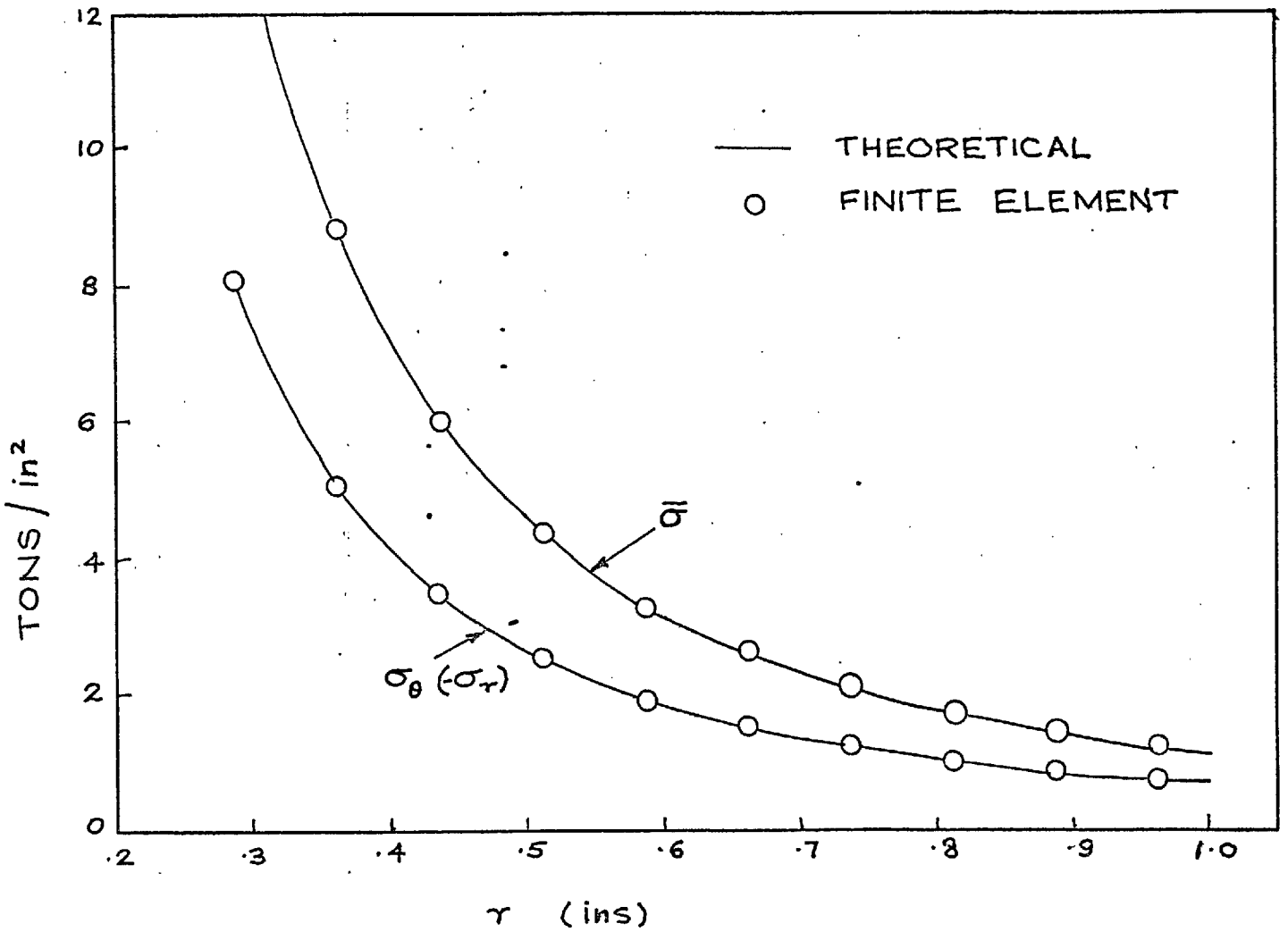


FIG.25 STRESS DISTRIBUTION FOR THE FLAT PLATE (ELASTIC)

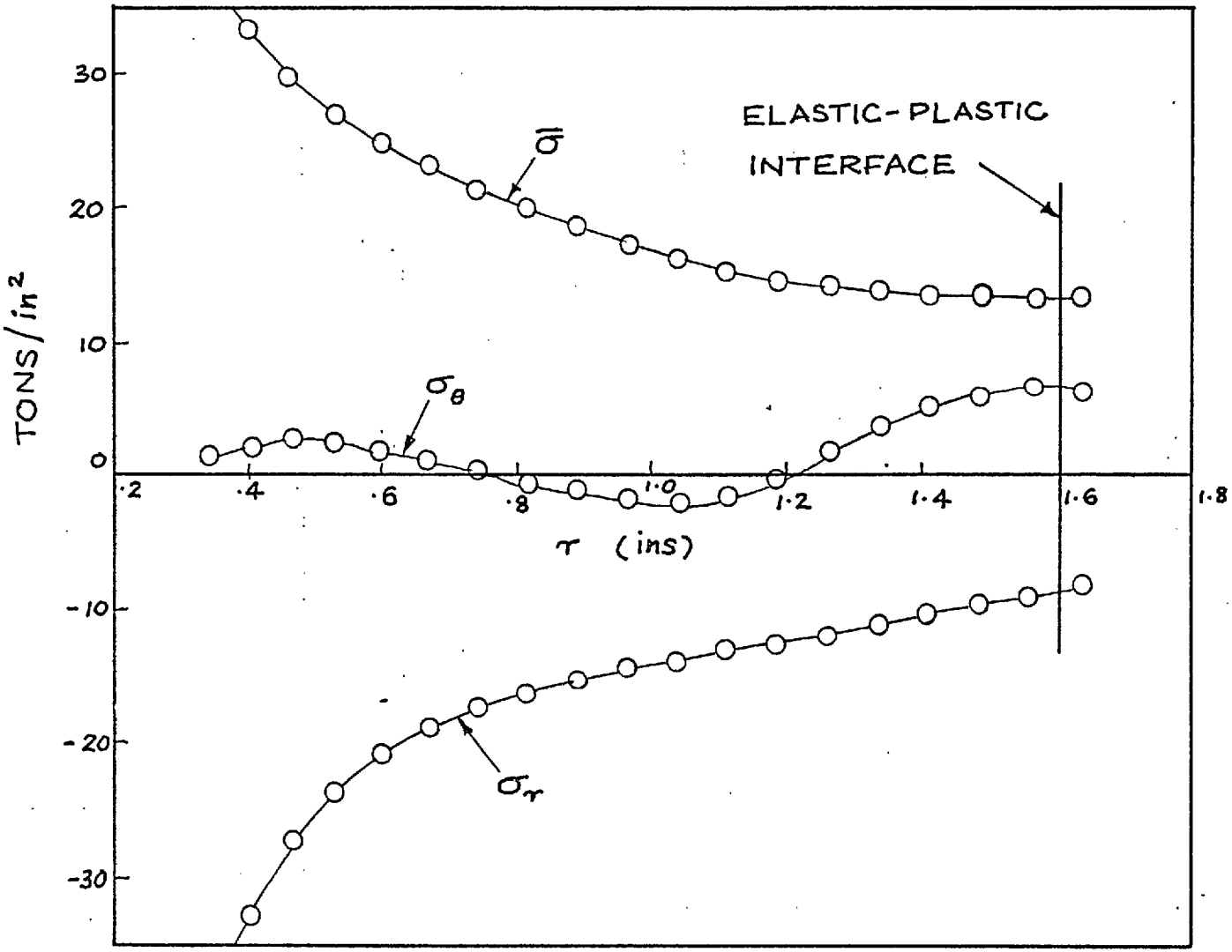


FIG. 26 STRESS DISTRIBUTION FOR FLAT PLATE (ELASTIC-PLASTIC) FINITE ELEMENT

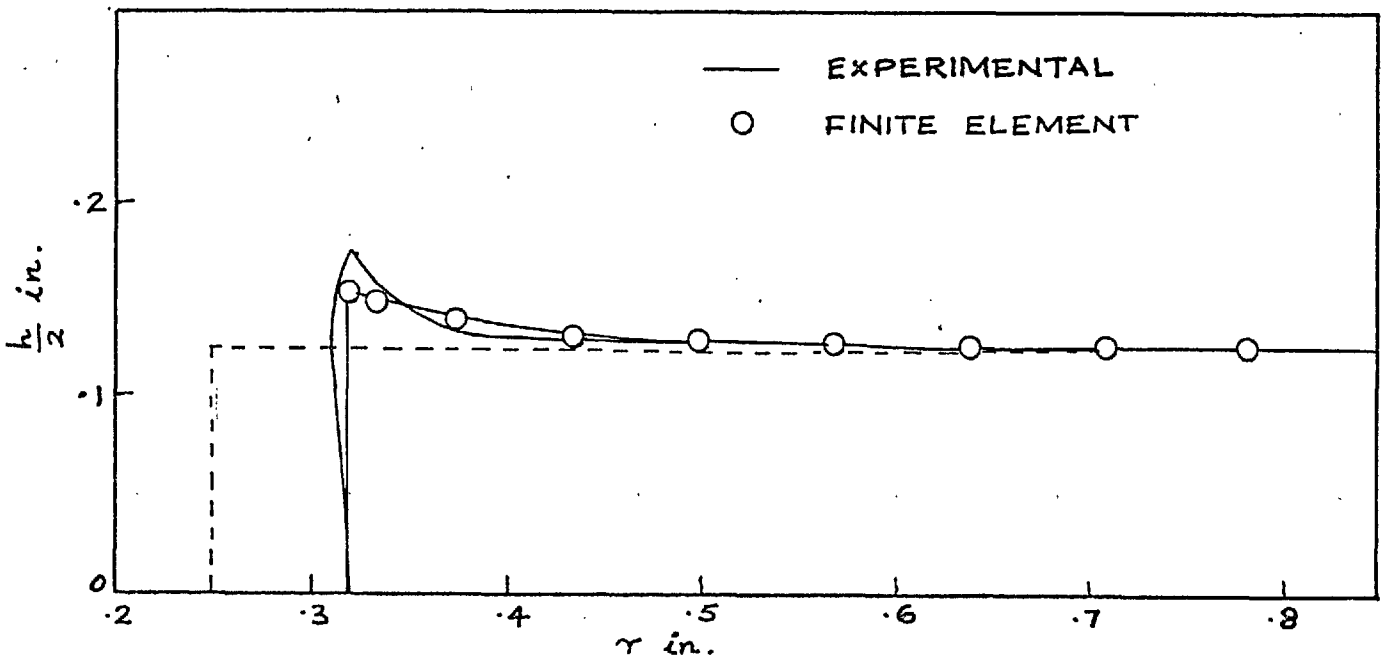


FIG. 27 THICKNESS PROFILE (FLAT PLATE)

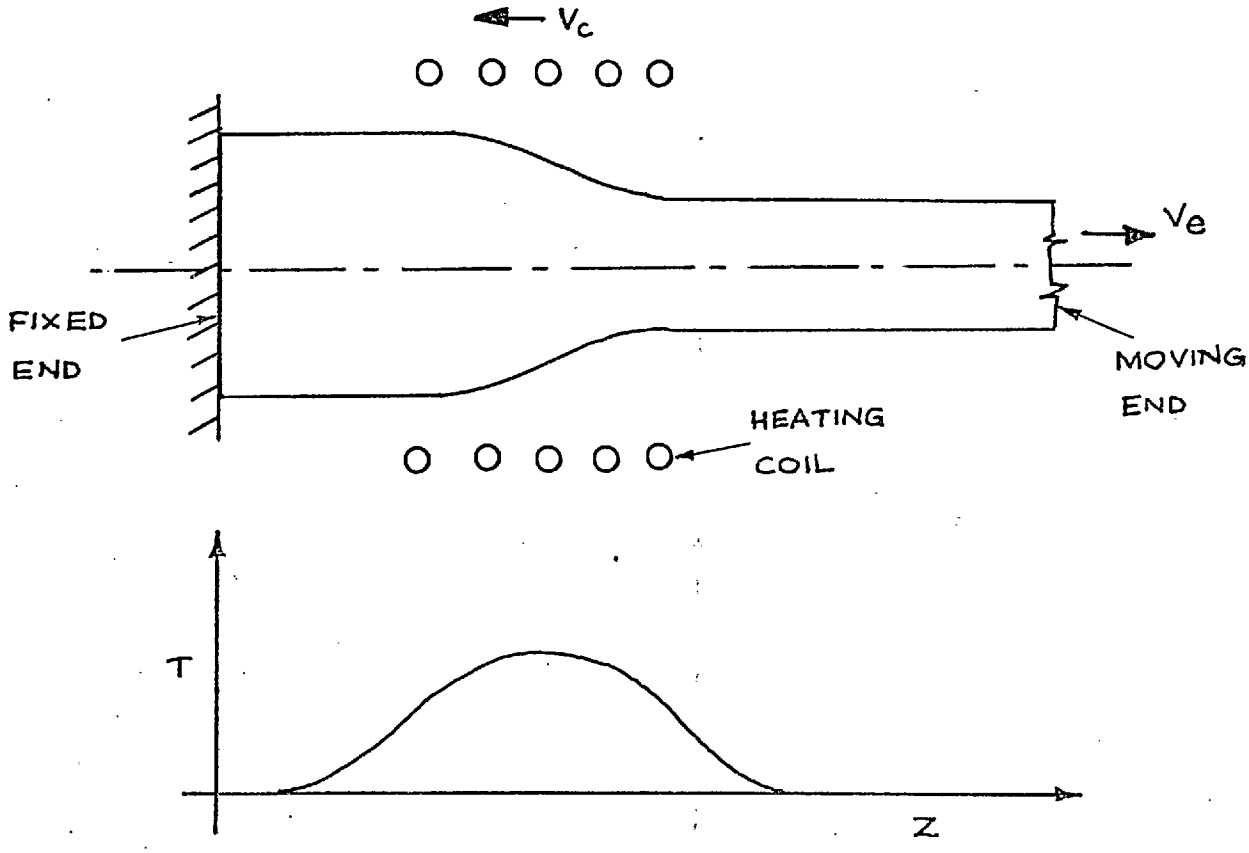


FIG. 28 TYPICAL LAYOUT OF THE DIELESS DRAWING PROCESS

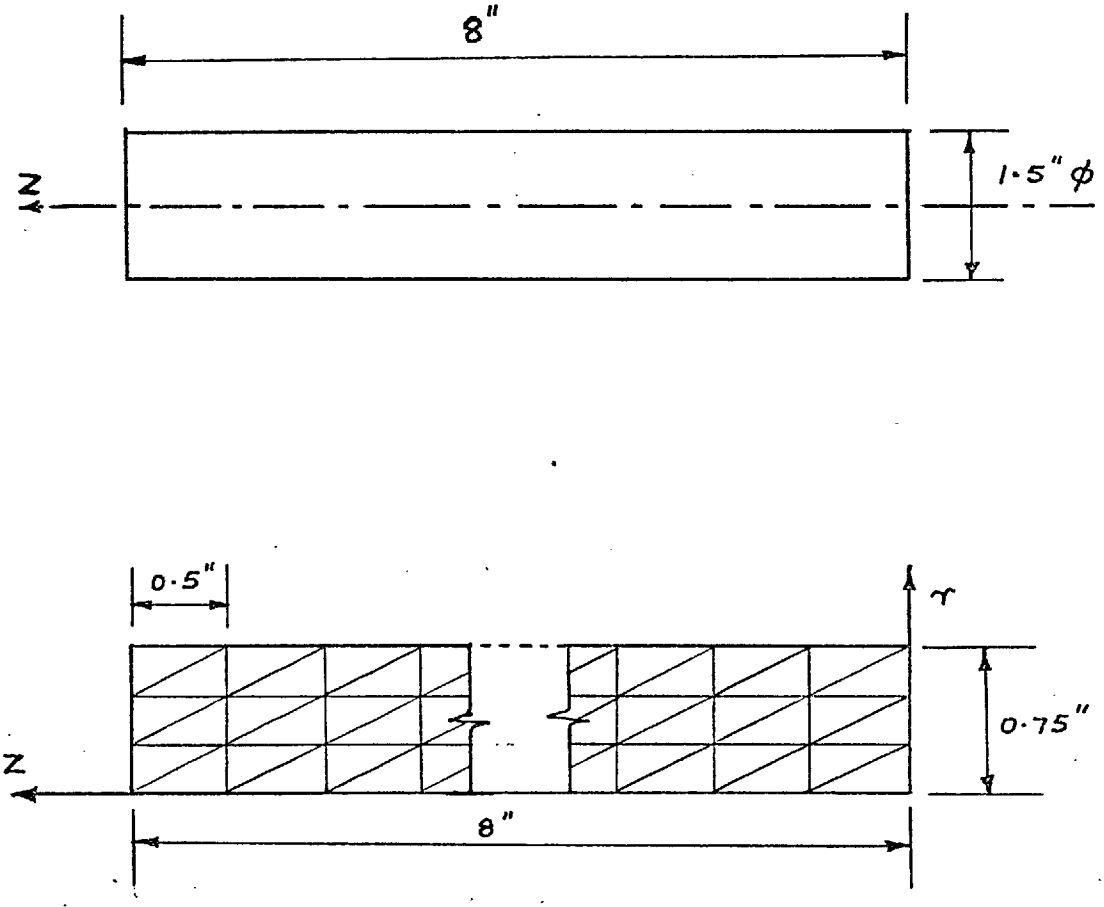


FIG. 29 FINITE ELEMENT MESH IDEALIZATION FOR THE STEEL BAR

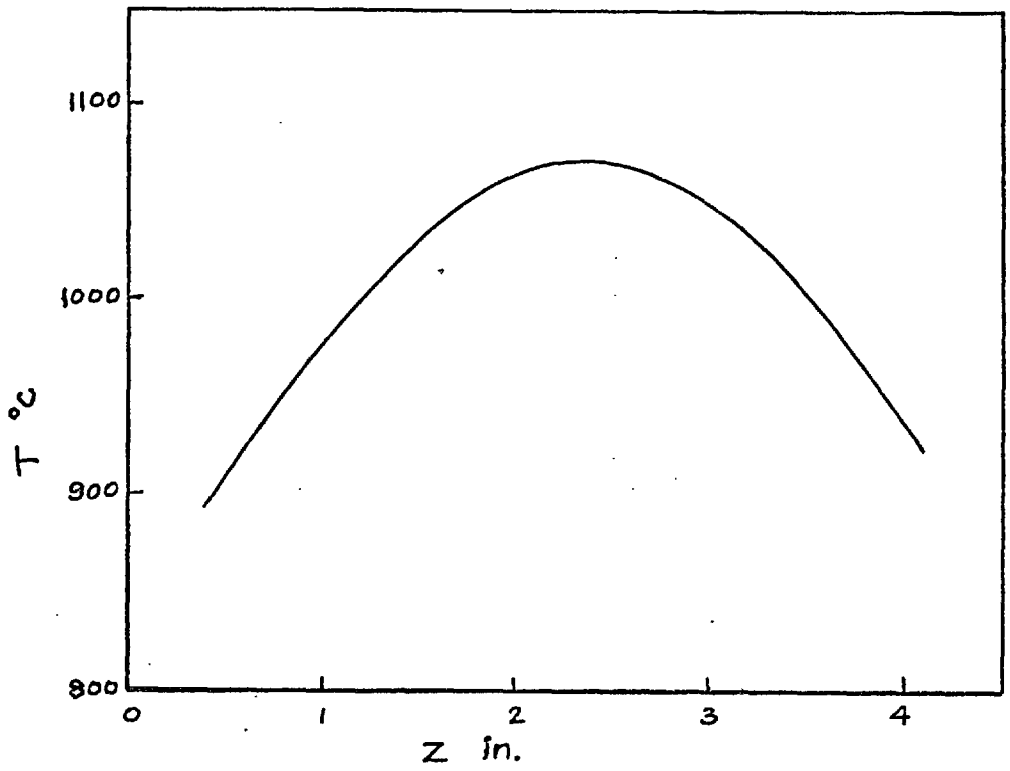


FIG. 30 TEMPERATURE PROFILE (EXPERIMENTAL)

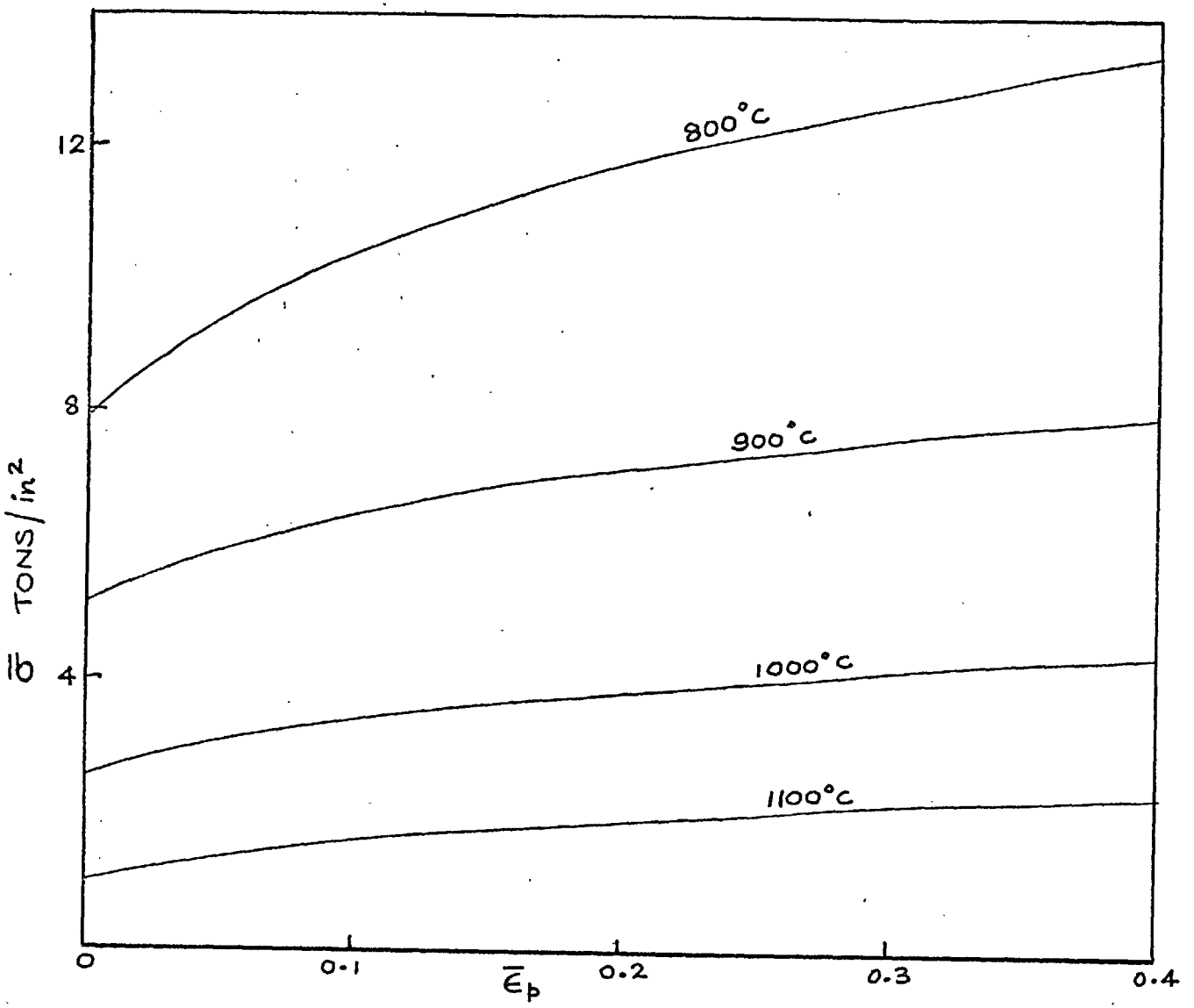
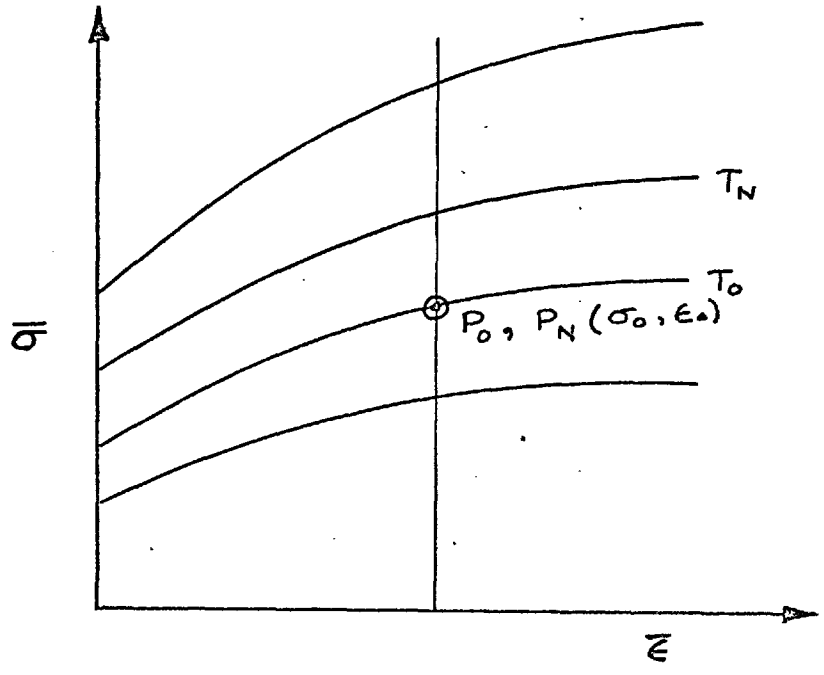


FIG. 31 STRESS-STRAIN CURVES FOR EN58J STEEL



POINT $P_0(\sigma_0, \epsilon_0, T_0)$ IS PLASTIC

POINT $P_N(\sigma_0, \epsilon_0, T_N)$ IS ELASTIC

FIG. 32 TEMPERATURE EFFECT ON UNLOADING

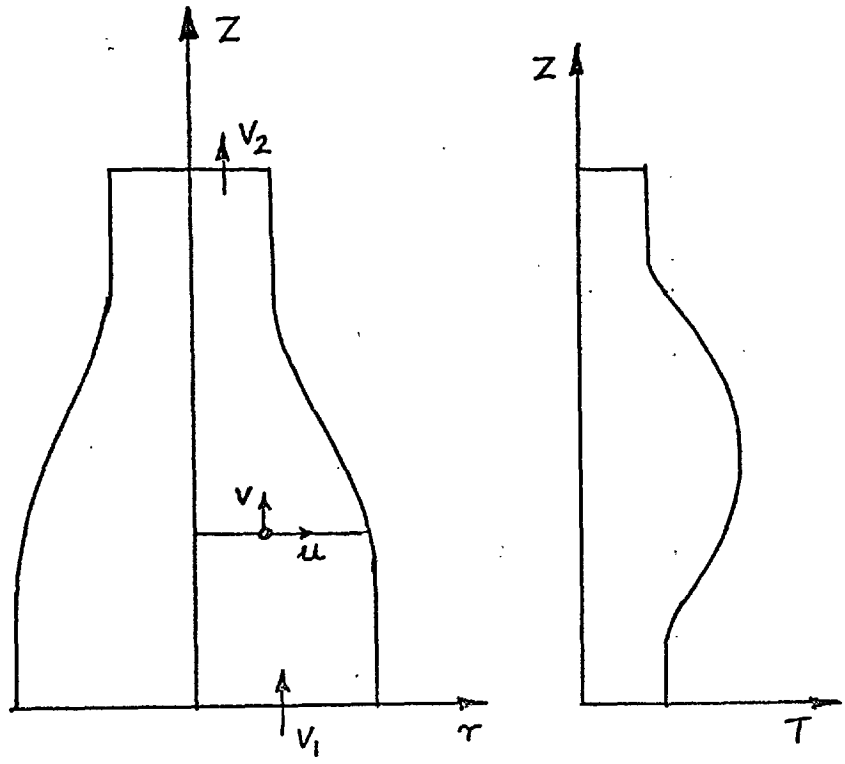


FIG. 33 DIELESS DRAWING PROCESS (FIXED COIL)

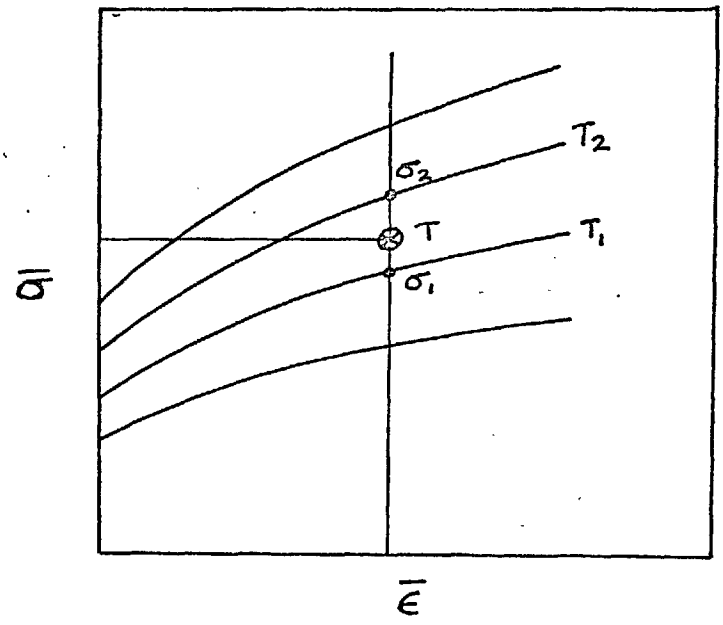


FIG. 34 INTERPOLATION TO EVALUATE THE TEMPERATURE

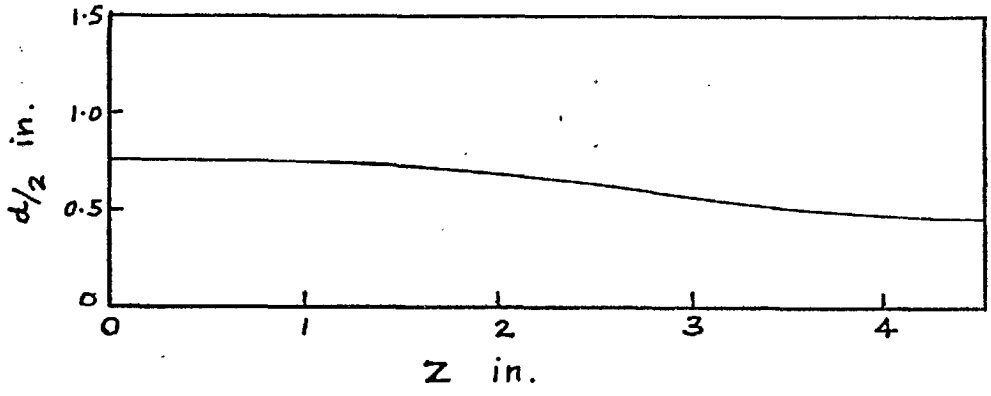


FIG. 35 EXPERIMENTALLY OBTAINED PROFILE

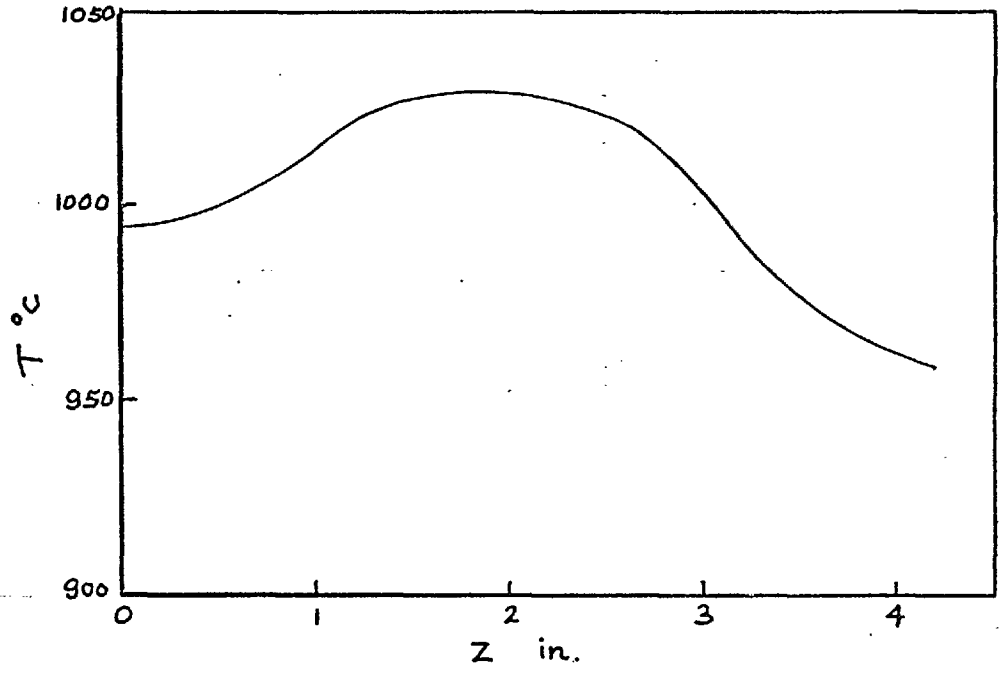


FIG. 36 THEORETICALLY PREDICTED TEMPERATURE DISTRIBUTION

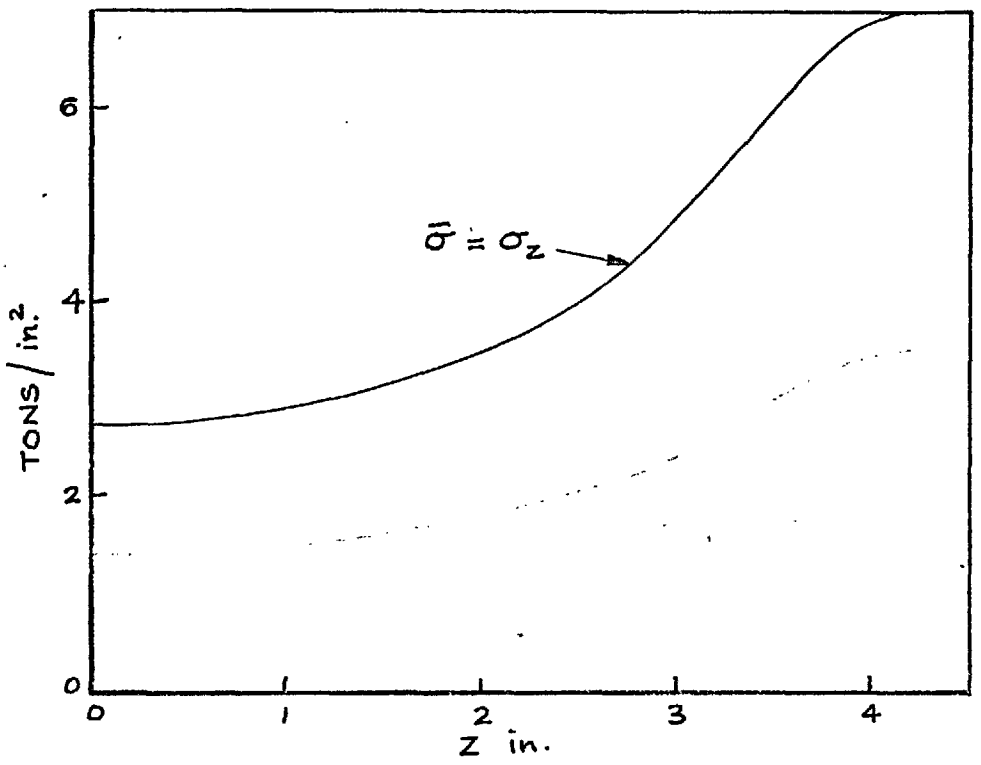


FIG. 37 STRESS DISTRIBUTION (APPROXIMATE THEORY)

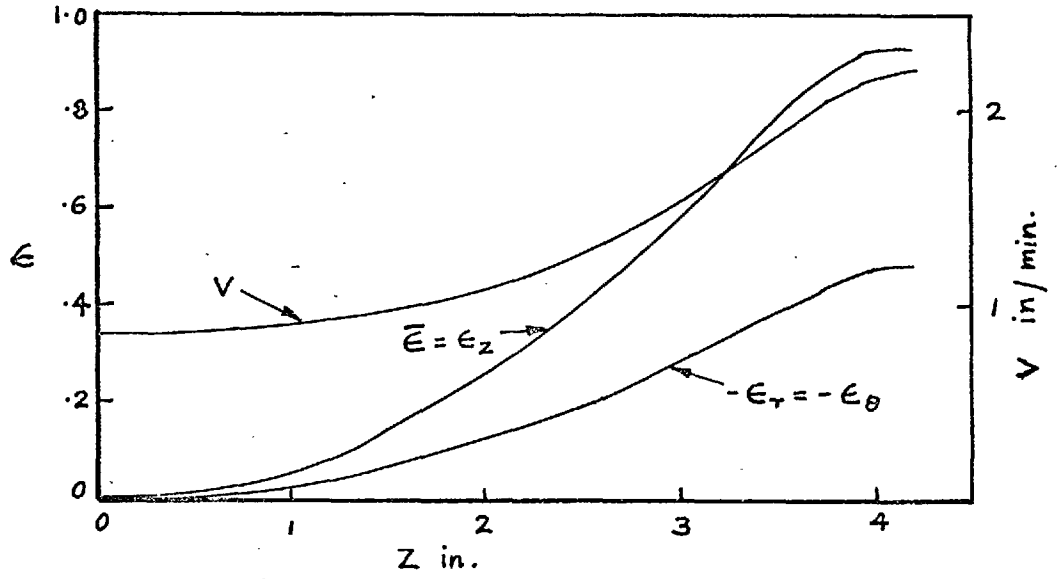


FIG. 38 STRAIN AND VELOCITY DISTRIBUTIONS (APPROXIMATE THEORY)

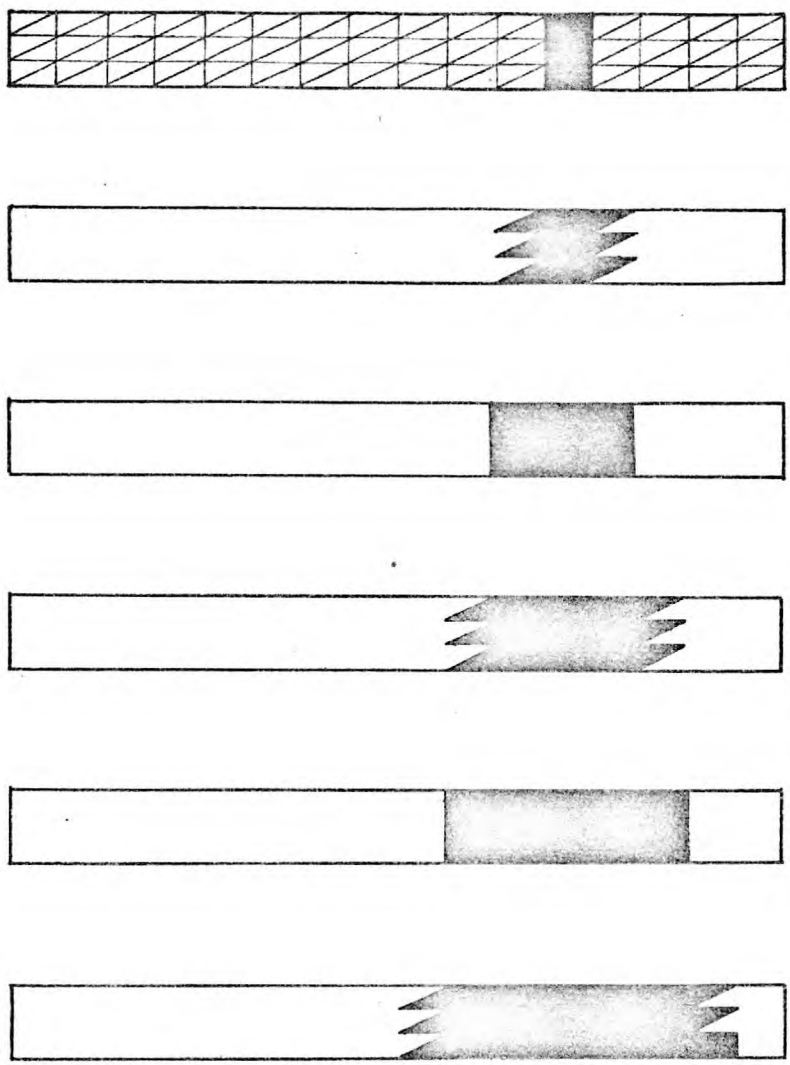


FIG.39 DEVELOPMENT OF THE PLASTIC ENCLAVES (INITIAL STAGES)

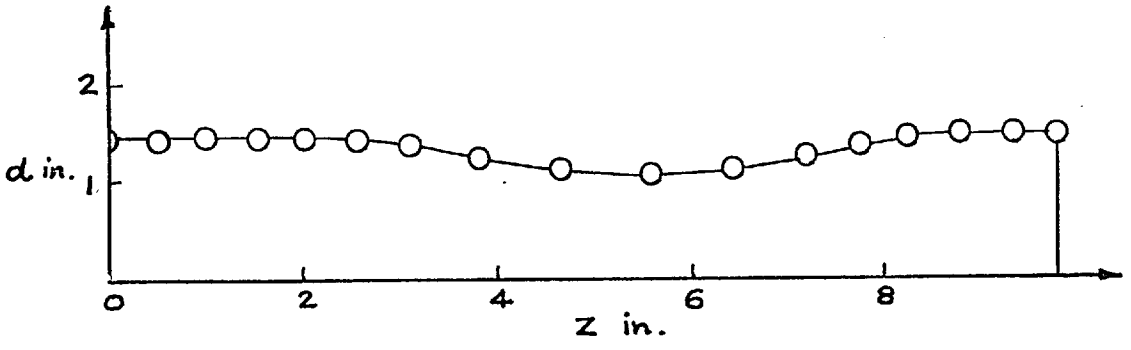


FIG. 40 PROFILE OBTAINED HALF WAY THROUGH DEFORMATION (F.E.M)

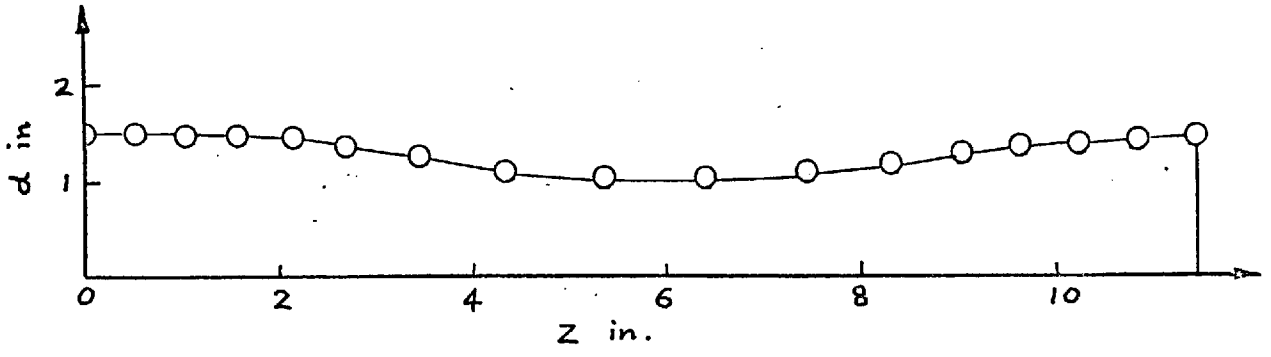


FIG. 41 FINAL PROFILE (FINITE ELEMENT METHOD)

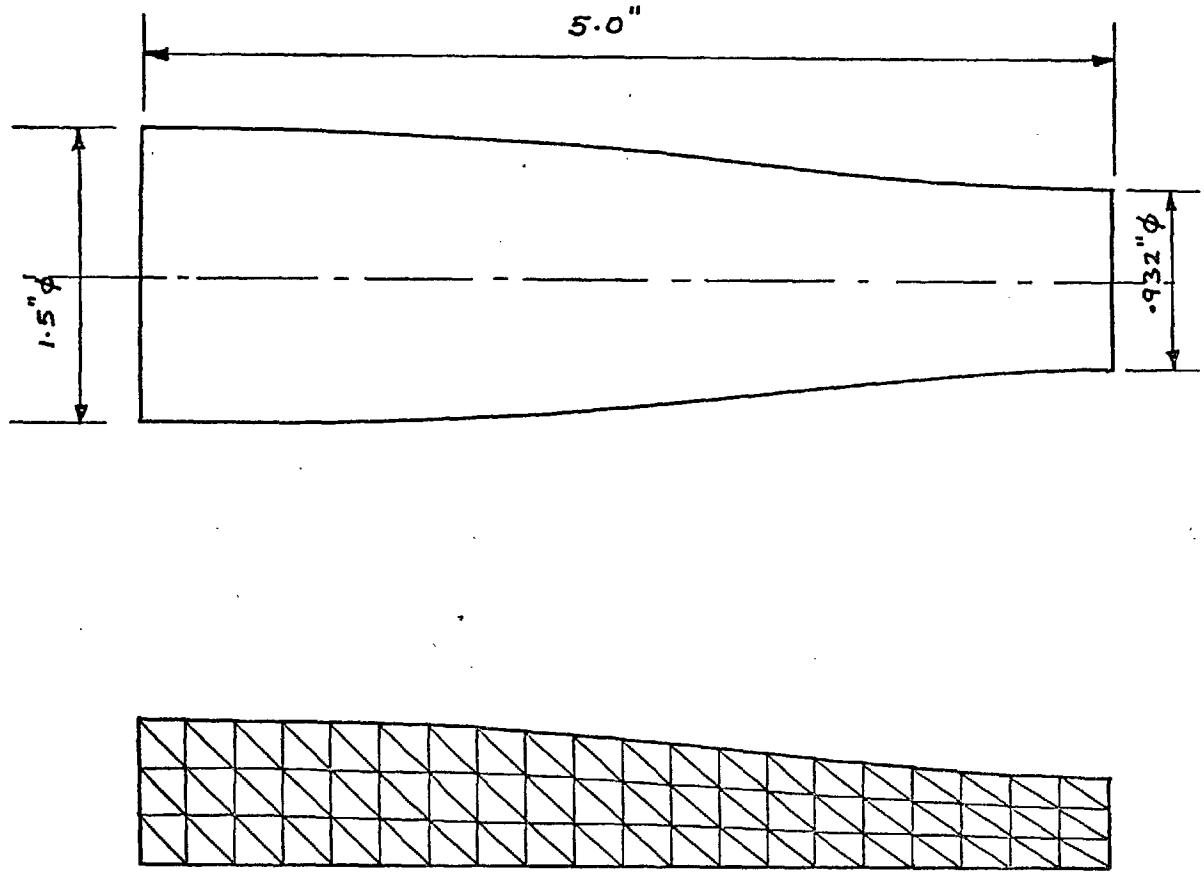


FIG. 42 FINITE ELEMENT MESH IDEALIZATION FOR THE DEFORMED SPECIMEN

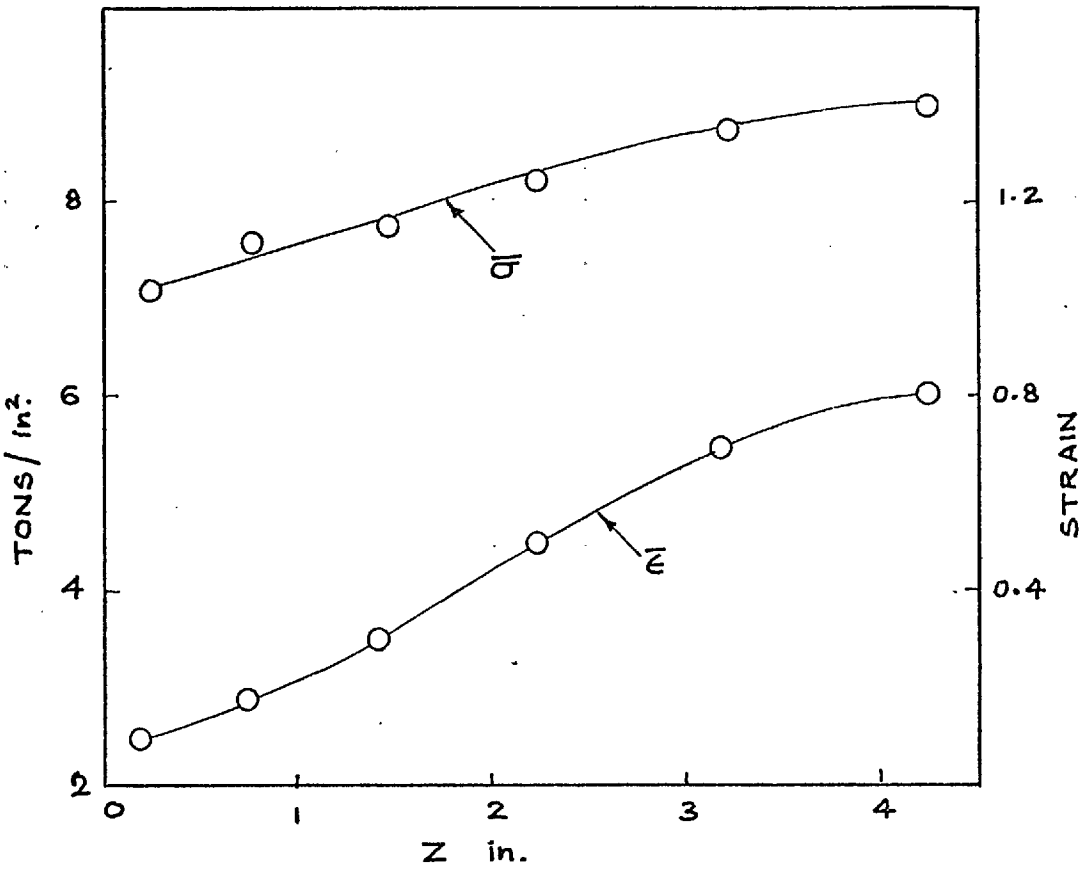


FIG. 44 STRESS AND STRAIN DISTRIBUTIONS (FINITE ELEMENT METHOD)

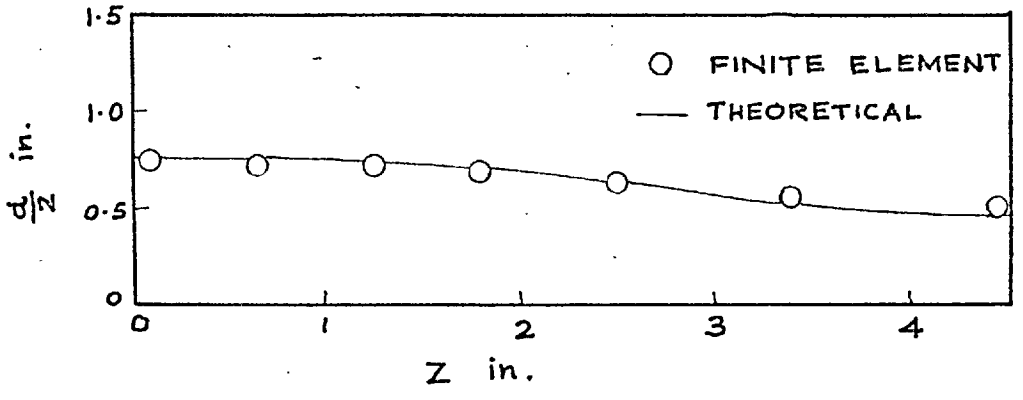


FIG. 43 COMPARISON OF THE PROFILES

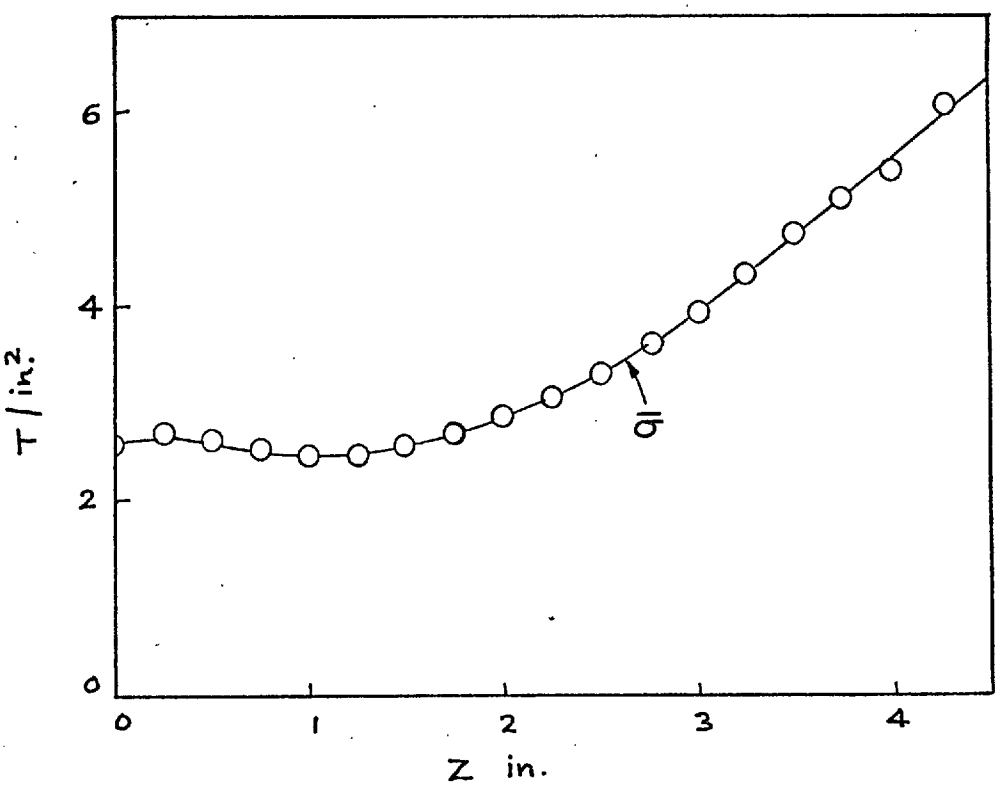


FIG. 45 STRESS DISTRIBUTION (FINITE ELEMENT, THIRD METHOD)

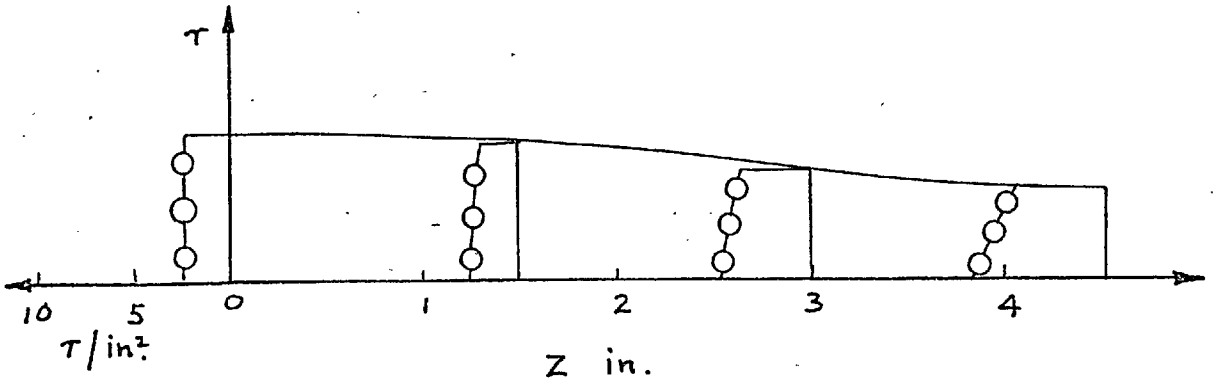


FIG. 46 EQ. STRESS DISTRIBUTION ACROSS THE RADIUS (THIRD METHOD)

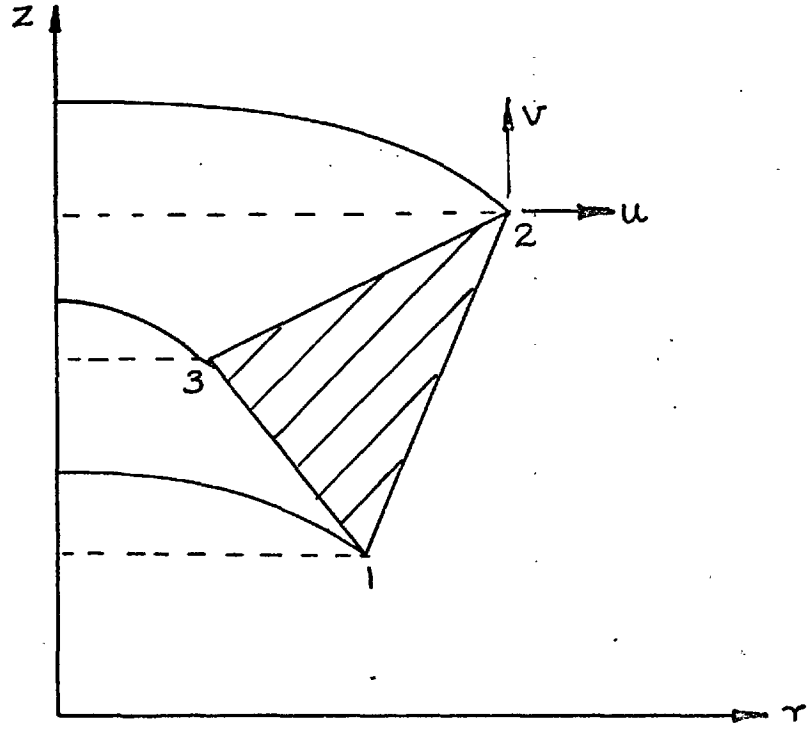


FIG.47 TRIANGULAR ELEMENT (AXISYMMETRIC)

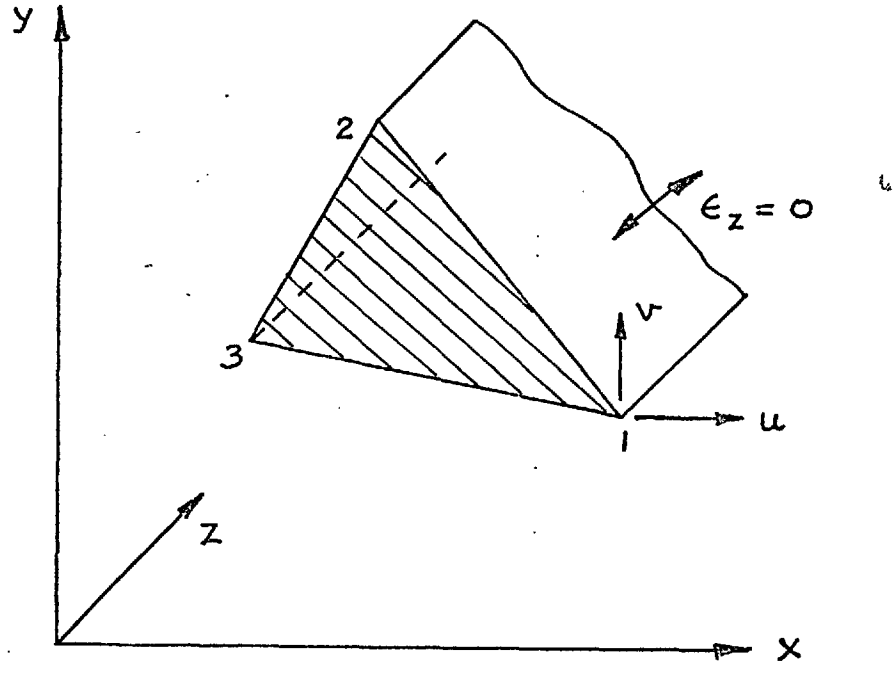


FIG .48 TRIANGULAR ELMENT
(PLANE STRAIN)

REFERENCES

1. Akyuz, F.A. and Merwin, J.E. Solution of nonlinear problems of elastoplasticity by finite element method. AIAA, 6, 1968.

2. Alexander, J.M. and Gunasekera, J.S. On the geometrically similar expansion of a thin infinite plate. Proc. R. Soc. Lond. A.326, p. 361, 1972.

3. Anand, S.C., Lee, S.L. and Rossow, E.C. Finite element analysis of elastic-plastic plane stress problems based upon Tresca's yield criterion, Ingenieur Archiv, 39, 1970.

4. Argyris, J.H. 'Energy theorems and structural analysis', Butterworths, 1960.

5. Argyris, J.H. Three dimensional anisotropic and inhomogenous elastic media, matrix analysis for small and large displacements. Ingenieur Archiv, 34, 1965.

6. Argyris, J.H. Elasto-plastic matrix displacement analysis of three dimensional continua. J.R.Ae.S., 69, 1965.

8. Argyris, J.H. Continua and discontinua . Proc. Conf. Matrix Methods in Struct. Mechs., Ohio, 1965.

9. Argyris, J.H., Buck, K.E., Greiger, I. and Mareczek, G. Application of the matrix displacement method to the analysis of pressure vessels. A.S.M.E., J.Eng. Industry, 1970.

10. Argyris, J.H., Kelsey, S. and Kamel, J. 'Matrix methods of structural analysis'. Pergamon Press, 1964.

11. Argyris, J.H. and Scharpf, D.W. Some general considerations of the natural mode technique. Part I, J.R.Ae.S., 73, 1969.

12. Argyris, J.H. and Scharpf, D.W. Some general considerations of the natural mode technique. Part II, J.R.Ae.S., 73, 1969.

13. Argyris, J.H. and Scharpf, D.W. Methods of elasto-plastic analysis. Symposium of finite element techniques at the Inst. für Statik und Dynamik der Luft und Raumfahrtstrucktionen. University of Stuttgart, 1969.

14. Armen, H., Isakson, G. and Pifko, A. Discrete element methods for the plastic analysis of structures subjected to cyclic loading. Int. J. Num. Methods in Eng., 2, 1970.

15. Bogner, F.K., Fox, R.L. and Schmit, L.A. A cylindrical shell discrete element. AIAA, 5, No. 4, April 1967.

16. Brebbia, C. and Connor, J. Geometrically nonlinear finite element analysis. A.S.C.E., J. of Eng. Mech. Div., 95, April 1969.

17. Bushnell, D. Nonlinear axisymmetric behaviour of shells of revolution. AIAA, 5, No. 3, March 1967.

18. Chan, A.S.L. and Firmin, A. The analysis of cooling towers by the matrix finite element method. J.R.Ae.S., 74, Dec. 1970.

19. Dupuis, G.A. Incremental finite element analysis of large elastic deformation problems. Brown University, May 1971.

20. Ford, H. and Alexander, J.M. 'Advanced Mechanics of Materials'. Longmans, 1963.

21. Fuchs, von G. and Schrem, E. ASKA - A computer system for structural engineers. Symposium on finite element techniques at the Institut für Statik und Dynamik der Luft und Raumfahrt-konstruktionen, June 1969.

22. Fung, Y.C. 'Foundations of solid mechanics'. Prentice Hall, 1965.

23. Gallagher, R.H., Gellatly, R.A., Padlog, J. and Mallet, R.H. A discrete element procedure for thin shell instability analysis. AIAA, 5, No. 1, 1967.

24. Gallagher, R.H. and Padlog, J. Discrete element approach to structural instability analysis. AIAA, 1, June 1963.

25. Gunasekera, J.S. A preliminary study of closed die forging. M.Sc. Thesis, University of London, 1969.

26. Gunasekera, J.S. and Alexander, J.M. Matrix analysis of the large deformation of an elastic-plastic axially symmetric continuum. To be published in the Proceedings of the Symposium on Foundations of Plasticity, Warsaw, Sept. 1972.

27. Green, A.E. and Naghdi, P.M. A general theory of an elastic plastic continuum. Arch. Rat. Mech. Anal. 18, 1965.

28. Green, A.E. and Zerna, W. 'Theoretical Elasticity'. Clarendon Press, 1954.

29. Hartley, H.O. The modified Gauss-Newton method for the fitting of nonlinear regression functions by least squares. Technometrics, 3, No. 2, May 1961.

30. Hartz, B.J. and Nathan, N.D. Finite element formulation of geometrically nonlinear problems of elasticity. Proc. Japan-U.S. Seminar on Matrix Methods of Structural Analysis and Design, Tokyo, 1969.

31. Hibbit, H.D. and Marcal, P.V. Hybrid finite element analysis with particular reference to axisymmetric structures. AIAA, 8th Aerospace Sciences Meeting, New York, Jan. 1970.

32. Hibbit, H.D., Marcal, P.V. and Rice, J.R. A finite element formulation for problems of large strain and large displacement. Int. J. Solids Struct., 6, 1970.

33. Hill, R. 'The mathematical theory of plasticity.' Clarendon Press, 1950.

34. Hsu, T.C. A study of large deformations by matrix algebra. J. of Strain Analysis, 1, No. 4, 1966.

35. Hodge, P.G. (Jr.). Numerical applications of minimum principles in plasticity. Papers for a Conf. held in Cambridge, University Press, March 1968.

37. Holman, D.F. and Miles, G.A. Finite element programs prepared up to the end of 1967. Report No. W/M (4A), Mech. Eng. Lab., English Electric Co., Ltd., Leicester. June 1968.

38. Hwang, C.T. Finite element method for soil deformation. Ph.D. Thesis, McMaster University, Canada. July 1969.

39. Kapur, K.K. and Hartz, B.J. Stability of plates using the finite element method. ASCE, J. Eng. Mech. Div., 92, April 1966.

40. Kawai, T. and Yoshimura, N. Analysis of large deflection of plates by the finite element method. Int. J. for Num. Methods in Eng., 1, 1969.

41. Lee, C.H. and Kobayashi, S. Elastoplastic analysis of plane-strain and axisymmetric flat punch indentation by the finite element method. Int. J. Mech. Sci., 12, 1970.

42. Lee, C.H. and Kobayashi, S. Analysis of axisymmetric upsetting and plane-strain side-pressing of solid cylinders by the finite element method. ASME, J. of Eng. for

Industry, 93, May 1971.

43. Mallet, R.H. and Marcal, P.V. Finite element analysis of nonlinear structures. ASCE, Struct. Div., 94, Sept. 1968.

44. Marcal, P.V. A stiffness method for elastic-plastic problems. Int. J. Mech. Sci., 7, 1965.

45. Marcal, P.V. A note on the elastic-plastic thick walled cylinder with internal pressure in the open and closed condition. Int. J. Mech. Sci., 7, 1965.

46. Marcal, P.V. The effect of initial displacements on problems of large deflection and stability. Brown University, Nov. 1967.

47. Marcal, P.V. Elastic-plastic analysis of pressure vessel components. Proc. 1st Pressure Vessel and Piping Conf., ASME, Sept. 1968.

48. Marcal, P.V. A comparative study of numerical methods of elastic-plastic analysis. AIAA, 6, No. 1, Jan. 1968.

49. Marcal, P.V. Finite element analysis of combined problems of nonlinear material and geometric behaviour. Brown University, March 1969.

50. Marcal, P.V. and King, I.P. Elastic-plastic analysis of two-dimensional stress systems by the finite element method. Int. J. Mech. Sci., 9, 1967.

51. Martin, H.C. Derivation of stiffness matrices for the analysis of large deflection and stability problems. Proc. 1st Conf. on Matrix Methods in Struct. Mech. Ohio, 1966.

52. Nagamatsu, A., Murota, T. and Jimma, T. On the non-uniform deformation of material in axially symmetric compression caused by friction. Part I, Bull. J.S.M.E., 14, No. 70, 1971.

53. Nagamatsu, A., Murota, T. and Jimma, T. On the non-uniform deformation of material in symmetric compression caused by friction. Part II, Bull. J.S.M.E., 14, No. 70, 1971.

54. Nagamatsu, A., Murota, T. and Jimma, T. On the non-uniform deformation of block in plane-strain compression caused by friction. Part I, Bull. J.S.M.E., 13, No. 66, 1970.

55. Nagamatsu, A., Murota, T. and Jimma, T. On the non-uniform deformation of block in plane-strain compression caused by friction. Part II, Bull. J.S.M.E., 13, No. 66, 1970.

56. Nagamatsu, A., Murota, T. and Jimma, T. On the non-uniform deformation of block in plane-strain compression caused by friction. Part III, Bull. J.S.M.E., 14, No. 70, 1971.

57. Nagamatsu, A., Murota, T. and Jimma, T. On the non-uniform deformation of block in plane-strain compression caused by friction. Part IV, Bull. J.S.M.E., 14, No. 70, 1971.

58. Oden, J.T. Numerical formulation of nonlinear elasticity problems. ASCE, Struct. Div., 93, June 1967.

59. Oden, J.T. Finite element applications in nonlinear

structural analysis. Proc. Symp. Application of finite element methods in Civil Eng. ASCE, Nov. 1969.

60. Oden, J.T. and Key, J.E. Numerical analysis of finite axisymmetric deformations of incompressibe elastic solids of revolution. Int. J. Solids Struct., 5, 1970.

61. Oden, J.T. and Sato, T. Finite strains and displacements of elastic membranes by the finite element method. Int. J. Solids Struct., 3, 1967.

62. Pope, G.G. The application of the matrix displacement method in plane elasto-plastic problems. Proc. Conf. held at Wright-Patterson Air Force Base, Ohio, Oct. 1965.

63. Pope, G.G. A discrete element method for the analysis of plane elasto-plastic stress problems. Aero. Quart., 17, p. 83, Feb. 1966.

64. Popov, E.P., Khojastch-Bakht, M. and Sharifi, P. Elastic-plastic analysis of some pressure vessel heads. ASME, J. Eng. Indus., 93, 1970.

65. Prager, W. 'Introduction to mechanics of continua'. Ginn and Co., 1961.

66. Schmit, L.A., Bogner, F.K. and Fox, R.L. Finite deflection structural analysis using plate and shell discrete elements. AIAA, 6, No. 5, 1968.

67. Shabaik, A.H. Prediction of the geometry changes of the free boundary during upsetting by the slip line theory. ASME Winter Annual Meeting, N.Y. Report 70-38, March 1970.

68. Shabaik, A.H. and Thomsen, E.G. A theoretical method for the analysis of metal working problems. ASME, J. Eng.

Industry, 90, 1968.

69. Siddal, J.N. 'Analytical decision making in engineering design'. New York, Prentice Hall, 1971.

70. Sokolnikoff, I.S. 'Mathematical theory of elasticity'. McGraw Hill, 1946.

71. Theokaris, P.S. and Marketos, E. Elastic-plastic analysis of perforated thin strips of a strain hardening material. J. Mech. Phys. Solids, 12, 1964.

72. Turner, M.J., Clough, R.W., Martin, H.C. and Topp, L. Stiffness and deflection analysis of complex structures. J. Aero. Sci., 23, No. 9, 1956.

73. Turner, M.J., Dill, E.H., Martin, H.C. and Melosh, R.J. Large deflection of structures subjected to heating and external loads. J. Aero Space Sci., 27, 1960.

74. Washizu, K. 'Variational methods in elasticity and plasticity'. Pergamon Press, 1968.

75. Webster, G.A. and Ellison, E.G. Iterative procedures for elastic, plastic and creep deformation in beams. J. Mech. Eng. Sci., 9, No. 2, 1967.

76. Wilson, E.L. Structural analysis of axisymmetric solids. AIAA, 3, No. 12, 1965.

77. Wissmann, J.W. Nonlinear structural analysis; Tensor formulation. Proc. 1st Conf. on Matrix Methods in Struct. Mech., Ohio, Oct. 1965.

78. Yamada, Y., Yoshimura, N. and Sakurai, T. Plastic stress-strain matrix and its application for the solution of elastic-plastic problems by the finite element method. Int. J. Mech. Sci., 10, 1968.

79. Zienkiewicz., O.C. 'The finite element method in Engineering Science'. McGraw Hill, 1971.

80. Zienkiewicz., O.C., Valliappan, S. and King, I.P. Elasto-plastic solutions of engineering problems. 'Initial Stress' finite element approach. Int. J. Num. Methods, 1, 1969.

81. Zudans, Z. Finite element incremental elastic-plastic analysis of pressure vessels. ASME, J. Eng. Industry, 92, p. 293, 1970.

82. Murray, D.W. and Wilson, E.L. An approximate nonlinear analysis of thin plates. Proc. 2nd Conf. on Matrix Methods in Struct. Mechanics. Dec. 1969.

83. Argyris, J.H. Recent Advances in Matrix Methods of Structural Analysis. Progress in Aeronautical Sciences. Vol. 4, 1963.

Proc. R. Soc. Lond. A. **326**, 361–373 (1972)
Printed in Great Britain

On the geometrically similar expansion of a hole in a thin infinite plate

BY J. M. ALEXANDER AND J. S. GUNASEKERA
Department of Mechanical Engineering, Imperial College, London, S.W. 7

(*Communicated by H. Ford, F.R.S. – Received* 20 *May* 1971)

The problem is considered of expanding a central cylindrical hole from zero radius in a thin infinite plate of conical profile such that, initially, thickness is proportional to radius, chosen so that geometrical similarity is maintained. A previously incorrect theory is modified by using a matrix formulation of the equations suitable for iterative solution on the digital computer, and the predicted profile of the plate is compared with that found from an experiment performed on a finite mild steel plate of conical profile. The Prandtl–Reuss relations for the large deformation elastic–plastic flow of a work-hardening material obeying the Maxwell (von Mises) yield criterion are used.

Apart from the intrinsic interest of obtaining a complete solution to a problem of this type, the solution will be used to provide a valid model against which to test solutions obtained by finite element methods for large deformation elastic–plastic analysis.

Notation

a	current radius of hole
B	constant, $= E_{p0}/n\sigma_0'$, in empirical stress–strain relation $\bar{\sigma} = \sigma_0(1 + B\bar{\epsilon}_p)^n$
c	current radius of elastic–plastic interface
E	Young modulus
E_p	plastic tangent modulus, $= d\bar{\sigma}/d\bar{\epsilon}_p$
H	$= h/r$
h	current thickness of plate at radius r
h_0	initial thickness of plate at radius r_0
l	current gauge length in tensile test
l_0	initial gauge length in tensile test
m	$2 \tan \frac{1}{2}\alpha$
n	constant in empirical relation $\bar{\sigma} = \sigma_0(1 + B\bar{\epsilon}_p)^n$
N	number of experimental points for curve fitting
r	current radius to any element
r_0	initial radius to any element
t	time
u	outward radial displacement of any element
v	outward radial velocity of any element defined by $v = du/dc$, i.e. c used as the time scale
α	angle generating surfaces of the plate in which $h_0 = mr_0$
β	$\frac{3}{2} + \sqrt{(\frac{5}{4} - \nu)}$
$\epsilon_r, \epsilon_\theta, \epsilon_z$	radial, circumferential and axial logarithmic strains
$\bar{\epsilon}_p$	effective or equivalent plastic strain, $= \ln (l/l_0 - \bar{\sigma}/E)$

$\bar{\epsilon}_{p,i}$ equivalent plastic strain (observed)
$\delta\lambda$ incremental parameter in the Prandtl–Reuss relations, $= \frac{3}{2}d\bar{\epsilon}_p/\bar{\sigma}$
ν Poisson ratio
σ hydrostatic component of the stresses, $= \frac{1}{3}(\sigma_r + \sigma_\theta + \sigma_z)$
$\sigma_r, \sigma_\theta, \sigma_r$ radial, circumferential and axial stresses
$\sigma'_r, \sigma'_\theta, \sigma'_z$ radial, circumferential and axial deviatoric stresses, e.g. $\sigma'_r = \sigma_r - \sigma$
$\bar{\sigma}$ effective or equivalent flow or yield stress
$\bar{\sigma}_i$ equivalent yield stress (observed)
σ_0 initial yield stress
ϕ $= r/c$

Notes

Dots denote time derivatives with respect to c, thus

$$\dot{\epsilon}_r = \frac{d\epsilon_r}{dc} = \frac{\partial}{\partial r}\left(\frac{du}{dc}\right) = \frac{\partial v}{\partial r}$$

$$\dot{\epsilon}_\theta = \frac{1}{r}\frac{du}{dc} = \frac{v}{r}$$

$$\dot{h} = \frac{dh}{dc}, \quad \text{for example.}$$

Incremental quantities denoted thus: $\delta\epsilon_r, \delta\sigma_r, \delta\lambda$ etc.
Matrix quantities as defined in the text $\boldsymbol{A}$, $\boldsymbol{b}$, $\boldsymbol{x}$
Transposed matrices denoted thus: x^T

Introduction

This problem was first considered by Alexander & Ford (1954) as part of a general investigation of the process of expanding a tube into a boiler plate. Although the actual geometry of the plate is more closely represented by considering it to be a thin plate of constant thickness, such a plate could not maintain the geometrical similarity necessary to enable the benefits of deriving a one-dimensional solution in which all variables may be postulated to be functions of the single parameter $\phi = r/c$ as originally suggested by Hill (1949). For this reason a conical plate of initial profile $h_0 = mr_0$ was considered by Alexander & Ford (1954) with the restriction that the angle $\alpha = 2\tan^{-1}\frac{1}{2}m$ should be small enough that plane stress conditions of axial symmetry could be assumed (see figure 1).

The problem has been considered by many investigators. Taylor (1948), Hill (1949) obtained solutions for the plastic straining of a flat sheet using the criterion of von Mises for a non-work-hardening, rigid plastic material. Hodge & Sankaranarayanan (1958) extended the solution for isotropic hardening materials, using Tresca's yield criterion.

Two papers by Nordgren & Naghdi (1963*a*, *b*) deal with twisting and expansion of a hole in an elastic–plastic plate and a rigid-plastic plate respectively. The former deals with infinitesimal strains while the latter includes the effect of finite strains.

Rogers (1967) obtained a complete analytical solution for an elastic–plastic non-hardening material obeying Tresca's yield criterion and the associated flow rule.

Several papers by Chern & Nemat-Nasser (Nemat-Nasser 1968; Chern 1969; Chern & Nemat-Nasser 1969, 1970) analyse the problem of expansion and twisting of a hole in a plate for a number of conditions. Nemat-Nasser (1968), Chern (1969) used Tresca's yield criterion and assumed the material to be rigid-plastic with isotropic strain-hardening and kinematic hardening respectively. Chern & Nemat-Nasser (1969) then used the yield criterion of von Mises and its associated flow rule

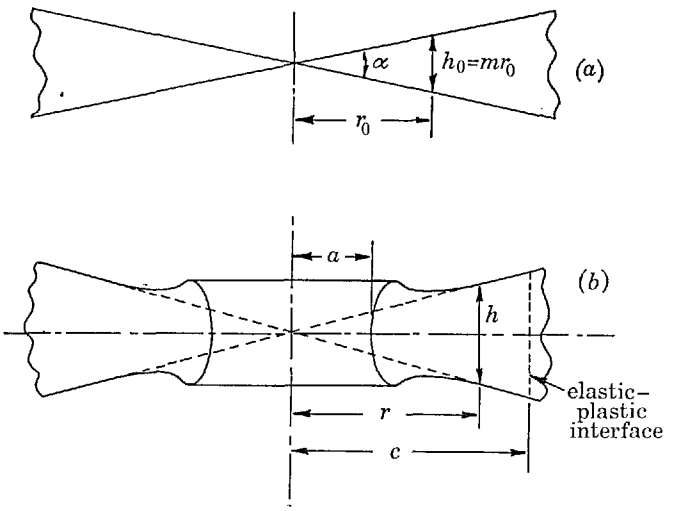


FIGURE 1. (*a*) Initial profile of conical plate; $m = 2\tan\frac{1}{2}\alpha$.
(*b*) Deformed profile; $\phi = r/c$, $H = h/r$.

for a rigid-plastic material. Finally, Chern & Nemat-Nasser (1970) assumed the material to be rigid-plastic for finite and elastic–plastic for infinitesimal deformations.

Chakrabarty (1971) has obtained an analytical solution using Tresca's yield criterion and the associated flow rule for a linearly work-hardening material, but the solution is restricted to be only for infinitesimal strains.

The present solution attempts to cover all the conditions considered in the other papers together and hence is valid for finite strains and for elastic–plastic materials with isotropic hardening and obeying the yield criterion of von Mises and the Prandtl–Reuss relations.

Rogers (1967) pointed out that for a geometrically similar solution the dimensionless parameter $H = h/r$ must be considered as a function of $\phi = r/c$, and not the actual thickness h as incorrectly formulated by Alexander & Ford (1954). By adopting a plate of initial profile $h_0 = mr_0^n$ he obtained solutions for plates of various profile, including the flat plate ($n = 0$). However, only the plate of conical profile ($n = 1$) can satisfy the condition of geometrical similarity, so attention will be restricted to that case in the present paper.

Theory

The initial geometry of the plate (figure 1) is defined by the equation

$$h_0 = mr_0, \quad \text{where} \quad m = 2\tan\tfrac{1}{2}\alpha. \tag{1}$$

For geometrical similarity it is convenient to express all variables as functions of the single dimensionless independent variable.

$$\phi = r/c. \tag{2}$$

If α is sufficiently small, plane stress conditions can be assumed so that σ_r, σ_θ and σ_z are all principal stresses with σ_z zero. For an annular section of the plate equilibrium of the stresses requires

$$\frac{\partial}{\partial r}(h\sigma_r) + \frac{h}{r}(\sigma_r - \sigma_\theta) = 0. \tag{3}$$

All the dependent variables in the geometrically similar solution are dependent on ϕ only, with the exception of h (which is also dependent on c as pointed out by Rogers (1967)) so that the following transformation relations introduced by Hill (1950) can be used, where v is the outward radial velocity of any element, c being used as the time scale in place of time t and u is radial displacement

$$v = \frac{\mathrm{d}u}{\mathrm{d}t} = \frac{\mathrm{d}u}{\mathrm{d}c}; \tag{4}$$

if $\mathrm{d}c/\mathrm{d}t$ is conveniently taken as unity

$$\frac{\partial}{\partial r} = \frac{\partial\phi}{\partial r}\frac{\mathrm{d}}{\mathrm{d}\phi} = \frac{1}{c}\frac{\mathrm{d}}{\mathrm{d}\phi}, \tag{5}$$

$$\frac{\partial}{\partial c} = \frac{\partial\phi}{\partial c}\frac{\mathrm{d}}{\mathrm{d}\phi} = -\frac{r}{c^2}\frac{\mathrm{d}}{\mathrm{d}\phi} = -\frac{\phi}{c}\frac{\mathrm{d}}{\mathrm{d}\phi}, \tag{6}$$

since $\phi = r/c$. The total differential $\delta\phi$ can be expressed as

$$\delta\phi = \frac{\partial\phi}{\partial r}\delta r + \frac{\partial\phi}{\partial c}\delta c = \frac{1}{c}\delta r - \frac{\phi}{c}\delta c.$$

Thus

$$\frac{\mathrm{d}\phi}{\mathrm{d}c} = \frac{1}{c}\frac{\mathrm{d}r}{\mathrm{d}c} - \frac{\phi}{c} = \frac{v-\phi}{c}$$

and

$$\frac{\mathrm{d}}{\mathrm{d}c} = \frac{\mathrm{d}}{\mathrm{d}\phi}\frac{\mathrm{d}\phi}{\mathrm{d}c};$$

hence

$$\frac{\mathrm{d}}{\mathrm{d}c} = \frac{v-\phi}{c}\frac{\mathrm{d}}{\mathrm{d}\phi}. \tag{7}$$

Although the current thickness h at any radius r is dependent on both ϕ and c, it is possible to define a dimensionless thickness which is independent of c, namely

$$H = h/r \tag{8}$$

to which the transformation relations (5), (6), (7) can be applied.

The principal strain–rate–displacement relations are

$$\dot{\epsilon}_r = \frac{\partial v}{\partial r}, \quad \dot{\epsilon}_\theta = \frac{v}{r}, \quad \dot{\epsilon}_z = \frac{\dot{h}}{h}. \tag{9}$$

The Prandtl–Reuss relations, with $\sigma_z = 0$, may be written as

$$\delta\epsilon_r = (1/E)(\delta\sigma_r - \nu\delta\sigma_\theta) + \sigma_r'\delta\lambda \tag{10}$$

$$\delta\epsilon_\theta = (1/E)(\delta\sigma_\theta - \nu\delta\sigma_r) + \sigma_\theta'\delta\lambda \tag{11}$$

$$\delta\epsilon_z = -(\nu/E)(\delta\sigma_r + \delta\sigma_\theta) + \sigma_z'\delta\lambda, \tag{12}$$

where $\delta\lambda = \frac{3}{2}\delta\bar{\epsilon}_p/\bar{\sigma}$.

Addition of these equations gives the compressibility relation

$$\delta\epsilon_r + \delta\epsilon_\theta + \delta\epsilon_z = \{(1-2\nu)/E\}(\delta\sigma_r + \delta\sigma_\theta). \tag{13}$$

The Maxwell (von Mises) criterion of yielding, with $\sigma_z = 0$, is

$$\bar{\sigma}^2 = \tfrac{3}{2}(\sigma_r'^2 + \sigma_\theta'^2 + \sigma_z'^2) = \sigma_r^2 + \sigma_\theta^2 - \sigma_r\sigma_\theta. \tag{14}$$

The differential form of this is

$$2\bar{\sigma}\delta\bar{\sigma} = (2\sigma_r - \sigma_\theta)\delta\sigma_r + (2\sigma_\theta - \sigma_r)\delta\sigma_\theta. \tag{15}$$

The tangent modulus is defined as

$$E_p = \mathrm{d}\bar{\sigma}/\mathrm{d}\bar{\epsilon}_p. \tag{16}$$

To obtain a numerical solution to the problem it is necessary to write these equations in incremental form. Dividing equations (10), (11) and (12) by δc to form the total differential components $\dot{\epsilon}_r$, $\dot{\epsilon}_\theta$ and $\dot{\epsilon}_z$ and substituting relation (9) we obtain

$$\frac{\partial v}{\partial r} = \frac{1}{E}\left(\frac{\mathrm{d}\sigma_r}{\mathrm{d}c} - \nu\frac{\mathrm{d}\sigma_\theta}{\mathrm{d}c}\right) + \frac{3}{2}\frac{\sigma_r'}{\bar{\sigma}}\frac{\mathrm{d}\bar{\epsilon}_p}{\mathrm{d}c}, \tag{10a}$$

$$\frac{v}{r} = \frac{1}{E}\left(\frac{\mathrm{d}\sigma_\theta}{\mathrm{d}c} - \nu\frac{\mathrm{d}\sigma_r}{\mathrm{d}c}\right) + \frac{3}{2}\frac{\sigma_\theta'}{\bar{\sigma}}\frac{\mathrm{d}\bar{\epsilon}_p}{\mathrm{d}c}, \tag{11a}$$

$$\frac{1}{h}\frac{\mathrm{d}h}{\mathrm{d}c} = -\frac{\nu}{E}\left(\frac{\mathrm{d}\sigma_r}{\mathrm{d}c} + \frac{\mathrm{d}\sigma_\theta}{\mathrm{d}c}\right) + \frac{3}{2}\frac{\sigma_z'}{\bar{\sigma}}\frac{\mathrm{d}\bar{\epsilon}_p}{\mathrm{d}c}. \tag{12a}$$

Substituting $h = Hr$, i.e. $h = H\phi c$

we have

$$\frac{1}{h}\frac{\mathrm{d}h}{\mathrm{d}c} = \frac{1}{H}\frac{\mathrm{d}H}{\mathrm{d}c} + \frac{1}{\phi}\frac{\mathrm{d}\phi}{\mathrm{d}c} + \frac{1}{c} = \frac{1}{H}\frac{v-\phi}{c}\frac{\mathrm{d}H}{\mathrm{d}\phi} + \frac{v}{c\phi}. \tag{16}$$

Now, using transformations (5) and (7) we can reduce (10*a*), (11*a*) and (12*a*) to the following relations

$$\frac{1}{v-\phi}\frac{\mathrm{d}v}{\mathrm{d}\phi} = \frac{1}{E}\left\{\frac{\mathrm{d}\sigma_r}{\mathrm{d}\phi} - \nu\frac{\mathrm{d}\sigma_\theta}{\mathrm{d}\phi}\right\} + \frac{2\sigma_r - \sigma_\theta}{2\bar{\sigma}}\frac{\mathrm{d}\bar{\epsilon}_\mathrm{p}}{\mathrm{d}\phi}, \tag{10b}$$

$$\frac{1}{v-\phi}\frac{v}{\phi} = \frac{1}{E}\left\{\frac{\mathrm{d}\sigma_\theta}{\mathrm{d}\phi} - \nu\frac{\mathrm{d}\sigma_r}{\mathrm{d}\phi}\right\} + \frac{2\sigma_\theta - \sigma_r}{2\bar{\sigma}}\frac{\mathrm{d}\bar{\epsilon}_\mathrm{p}}{\mathrm{d}\phi}, \tag{11b}$$

$$\frac{1}{v-\phi}\frac{v}{\phi} + \frac{1}{H}\frac{\mathrm{d}H}{\mathrm{d}\phi} = -\frac{\nu}{E}\left\{\frac{\mathrm{d}\sigma_r}{\mathrm{d}\phi} + \frac{\mathrm{d}\sigma_\theta}{\mathrm{d}\phi}\right\} - \frac{\sigma_r + \sigma_\theta}{2\bar{\sigma}}\frac{\mathrm{d}\bar{\epsilon}_\mathrm{p}}{\mathrm{d}\phi}. \tag{12b}$$

In terms of H, the equilibrium equation (3) is

$$\frac{\partial}{\partial r}(Hr\sigma_r) + H(\sigma_r - \sigma_\theta) = 0,$$

or

$$\phi\sigma_r\frac{\mathrm{d}H}{\mathrm{d}\phi} + \phi H\frac{\mathrm{d}\sigma_r}{\mathrm{d}\phi} + H(2\sigma_r - \sigma_\theta) = 0. \tag{3a}$$

The incremental forms of these equations which can be used for a solution are most conveniently written in matrix form by defining an unknown 6×1 column matrix

$$\boldsymbol{x} = [\delta\sigma_r \quad \delta\sigma_\theta \quad \delta\bar{\sigma} \quad \delta\bar{\epsilon}_\mathrm{p} \quad \delta v \quad \delta H]^T. \tag{17}$$

The equations are displayed in (18).

(The equation number from which each incremental equation of the matrix has been derived is shown on the appropriate line.)

$$\left[\begin{array}{cccccc}
\frac{1}{E} & -\frac{\nu}{E} & 0 & \frac{2\sigma_r-\sigma_\theta}{2\bar{\sigma}} & \frac{-1}{v-\phi} & 0 \\
-\frac{\nu}{E} & \frac{1}{E} & 0 & \frac{2\sigma_\theta-\sigma_r}{2\bar{\sigma}} & 0 & 0 \\
\frac{\nu}{E} & \frac{\nu}{E} & 0 & \frac{\sigma_r+\sigma_\theta}{2\bar{\sigma}} & 0 & \frac{1}{H} \\
(2\sigma_r-\sigma_\theta) & (2\sigma_\theta-\sigma_r) & -2\bar{\sigma} & 0 & 0 & 0 \\
H & 0 & 0 & 0 & 0 & \sigma_r \\
0 & 0 & 1 & -E_\mathrm{p} & 0 & 0
\end{array}\right]
\left[\begin{array}{c}
\delta\sigma_r \\ \delta\sigma_\theta \\ \delta\bar{\sigma} \\ \delta\bar{\epsilon}_\mathrm{p} \\ \delta v \\ \delta H
\end{array}\right]
=
\left[\begin{array}{c}
0 \\ \frac{v}{v-\phi}\frac{\delta\phi}{\phi} \\ \frac{-v}{v-\phi}\frac{\delta\phi}{\phi} \\ 0 \\ H(\sigma_\theta-2\sigma_r)\frac{\delta\phi}{\phi} \\ 0
\end{array}\right]
\begin{array}{l}
(10b) \\ (11b) \\ (12b) \\ (15) \\ (3a) \\ (16)
\end{array}
\tag{18}$$

These equations can be written compactly in the form

$$\boldsymbol{A}\boldsymbol{x} = \boldsymbol{b}, \tag{19}$$

where $\boldsymbol{A}$ is the 6×6 matrix on the left of (18) and $\boldsymbol{b}$ is the 6×1 matrix on the right of (18).

The set of six nonlinear simultaneous equations can be solved iteratively using a suitable numerical procedure. The solution to the problem at $\phi = 1$ (i.e. at the elastic–plastic boundary) is known and hence the solution at a point $\phi + \delta\phi$ may be

obtained iteratively using equation (19) until the required degree of convergence is obtained. The solution procedure is repeated for other successive points until the edge of the hole is reached.

In the present solution, stepwise linearity is assumed for the set of nonlinear equations and therefore very close steps are chosen (initially $\delta\phi = 0.01$) to obtain sufficiently accurate results. (An alternative method of solution using the fourth-order Runge–Kutta process was used to solve the simultaneous equations and was found to give results in close agreement with the above solution.)

At the edge of the hole for geometrical similarity to be maintained, the ratio a/c must be constant for all values of c so that the velocity there

$$v = \frac{\mathrm{d}a}{\mathrm{d}c} = \frac{a}{c} = \phi_a \text{ (a constant)}$$

and the solution is completed when the velocity v becomes equal to ϕ. The distortion is so great at the edge of the hole that some of the assumptions made in the solution are obviously violated there (for example that σ_r and σ_z remain principal stresses through the thickness of the plate).

In the elastic region the stresses and strains are given by the equations (Alexander & Ford 1954).

$$\sigma_r = -\frac{\sigma_0}{\sqrt{(2-\nu)}}\phi^{-\beta}, \tag{20}$$

$$\sigma_\theta = \frac{\beta-2}{\sqrt{(2-\nu)}}\sigma_0\phi^{-\beta}, \tag{21}$$

$$\sigma_z = 0, \tag{22}$$

$$\epsilon_r = \frac{(2-\beta)\nu-1}{\sqrt{(2-\nu)}}\frac{\sigma_0}{E}\phi^{-\beta}, \tag{23}$$

$$\epsilon_\theta = \frac{\beta-2+\nu}{\sqrt{(2-\nu)}}\frac{\sigma_0}{E}\phi^{-\beta}, \tag{24}$$

$$\epsilon_z = \frac{\nu(3-\beta)}{\sqrt{(2-\nu)}}\frac{\sigma_0}{E}\phi^{-\beta}, \tag{25}$$

$$v \simeq \frac{(1+\nu)(\beta-1)}{\sqrt{(2-\nu)}}\frac{\sigma_0}{E}\phi^{1-\beta}, \tag{26}$$

where

$$\beta = \tfrac{3}{2} + \sqrt{(\tfrac{5}{4}-\nu)}. \tag{27}$$

To determine the variation of thickness with ϕ the relationship on the left-hand side of equations (11*b*) and (12*b*) may be used, namely

$$\frac{\mathrm{d}\epsilon_z}{\mathrm{d}\phi} = \frac{1}{v-\phi}\frac{v}{\phi} + \frac{1}{H}\frac{\mathrm{d}H}{\mathrm{d}\phi} = \frac{\mathrm{d}\epsilon_\theta}{\mathrm{d}\phi} + \frac{1}{H}\frac{\mathrm{d}H}{\mathrm{d}\phi}. \tag{28}$$

This equation may be integrated directly, with the boundary condition that as $\phi \to \infty$, ϵ_z and $\epsilon_\theta \to 0$ and $H \to h_0/r_0 = m$, to give

$$H = m\exp(\epsilon_z - \epsilon_\theta). \tag{29}$$

Thus
$$h/mc = \phi \exp(\epsilon_z - \epsilon_\theta) \tag{29a}$$
gives the thickness in a form which reveals its functional dependence on ϕ and its linear proportionality to both m and c. This result can also be obtained in a more direct way by noting that,
$$\epsilon_z = \ln\frac{h}{h_0} = \ln\frac{h}{mr_0} = \ln\frac{h}{m(r-u)}$$
and that,
$$r - u = r\exp(-\epsilon_\theta).$$
Hence,
$$h/mr = \exp(\epsilon_z - \epsilon_\theta),$$
and
$$h/mc = \phi\exp(\epsilon_z - \epsilon_\theta),$$
(29a)
as before.

The circumferential strain distribution may be obtained from the equation (derived from equations (9))
$$\frac{d\epsilon_\theta}{d\phi} = \frac{1}{v-\phi}\frac{v}{\phi},$$
$$d\epsilon_\theta = \frac{v}{v-\phi}\frac{d\phi}{\phi}.$$
(30)

Hence
$$\epsilon_0 = (\epsilon_\theta)_{\phi=1} + \int_1^\phi \frac{v}{v-\phi}\frac{d\phi}{\phi}$$
can be determined by numerical integration from the known value of ϵ_θ at the elastic–plastic boundary ($\phi = 1$).

Stress–strain curve

A stress–strain curve of the form
$$\bar{\sigma} = \sigma_0(1 + B\bar{\epsilon}_p)^n. \tag{31}$$
was assumed in this analysis.

Thus the plastic tangent modulus may be written as
$$E_p = d\bar{\sigma}/d\bar{\epsilon}_p = \sigma_0 nB(1 + B\bar{\epsilon}_p)^{n-1}. \tag{32}$$

Experimental values for the stress–strain curve of the mild steel plate used were obtained from a series of Cook & Larke (1954) compression tests on specimens of varying height/diameter ratios. The parameters σ_0, n and B were obtained by minimizing the expression
$$R = \sum_{i=1}^{i=N} \{\bar{\sigma}_i - \sigma_0(1 + B\bar{\epsilon}_{pi})^n\}^2 \tag{33}$$
to obtain the best least squares fit. This was conveniently effected using the Simplex method of direct research described by Siddall (1971).

Theoretical results

Using the method just described the following values were determined for the parameters of the stress–strain curve:

$$\sigma_0 = 13.3\,\text{tonf/in}^2 \quad (20.95\,\text{kgf/mm}^2),$$

$$B = 132.763,$$

$$n = 0.269237.$$

A plot of the stress–strain curve is shown in figure 2.

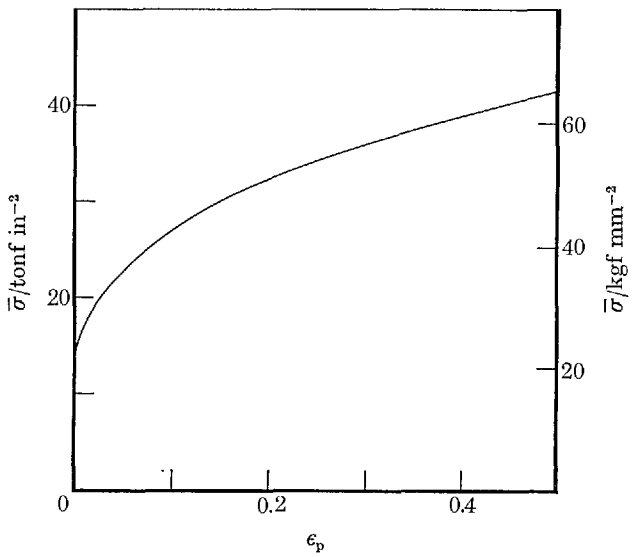


FIGURE 2. Stress–strain curve for the mild steel plate.

With these values the empirical relation (equation (31)) was used in the theory and the results tabulated in table 1 were obtained. In this table only every fifth line of the actual computer print-out has been reproduced, to save space. In fact, increments $\delta\phi$ of 0.01 were used from $\phi = 1.00$ to $\phi = 0.32$, of 0.001 from $\phi = 0.32$ to 0.307, of 0.0001 from $\phi = 0.307$ to 0.3058. These increments were arranged to be reduced wherever the number of iterations required to obtain a solution became excessively large.

In figure 3 are plotted the distributions of stress obtained from the theoretical solution, while the theoretical thickness profile is shown in figure 4.

Experimental results

A mild steel plate of the conical profile under discussion was manufactured, the outside diameter being 12 in (305 mm) and the edge thickness $1\frac{1}{2}$ in (38.1 mm).

TABLE 1. SOLUTION FOR STRESS–STRAIN CURVE $\bar{\sigma} = 13.3\,(1+132.763\bar{\epsilon}_p)^{0.269237}$; 1 tonf in^{-2} = 1.575 kgf mm^{-2}

ϕ	σ_r / tonf in^{-2}	σ_θ / tonf in^{-2}	$\bar{\sigma}$ / tonf in^{-2}	$\bar{\epsilon}_p$	v	H	ϵ_θ
1.00000	−10.206300	4.844700	13.300000	0.0	0.00163000	0.99947529	0.00065888
0.95000	−11.529863	3.227018	13.429903	0.00027689	0.00195773	0.94940981	0.00075323
0.90000	−12.976834	1.219547	13.620398	0.00069629	0.00240502	0.89938958	0.00088059
0.85000	−14.547970	−1.319924	13.927932	0.00140778	0.00308236	0.84949040	0.00105916
0.80000	−16.230925	−4.464035	14.516163	0.00289258	0.00432500	0.79998289	0.00132829
0.75000	−18.023121	−6.931278	15.740271	0.00655047	0.00702293	0.75166204	0.00179395
0.70000	−20.054669	−7.641337	17.525386	0.01345841	0.01168627	0.70473147	0.00268589
0.65000	−22.465637	−8.146013	19.694184	0.02484853	0.01878078	0.65908978	0.00438218
0.60000	−25.342260	−8.735636	22.292702	0.04378582	0.02954658	0.61530740	0.00757666
0.55000	−28.765952	−9.353810	25.410752	0.07593446	0.04593704	0.57436467	0.01365135
0.50000	−32.809924	−9.844106	29.158481	0.13162465	0.07070501	0.53764828	0.02552051
0.45000	−37.532372	−9.890455	33.691122	0.23051119	0.10729101	0.50690136	0.04985291
0.40000	−43.014116	−8.881424	39.330284	0.41551758	0.15927488	0.48391760	0.10436596
0.35000	−49.664752	−5.471204	47.165662	0.82348655	0.22926624	0.46876271	0.25545840
0.31800	−56.384379	−0.093834	56.335781	1.60169020	0.28336625	0.45185629	0.61472484
0.31300	−58.560161	1.361702	59.251090	1.93313768	0.29234318	0.44209307	0.78351824
0.30800	−63.058725	2.983663	64.600732	2.66751132	0.30142583	0.41746009	1.17121967
0.30660	−66.438837	3.341741	68.169723	3.25881313	0.30399909	0.39812057	1.48807791
0.30610	−69.199039	3.319785	70.915847	3.77454765	0.30492598	0.38289571	1.76440515
0.30580	−73.302895	3.041520	74.868691	4.61840208	0.30548729	0.36183010	2.21382367

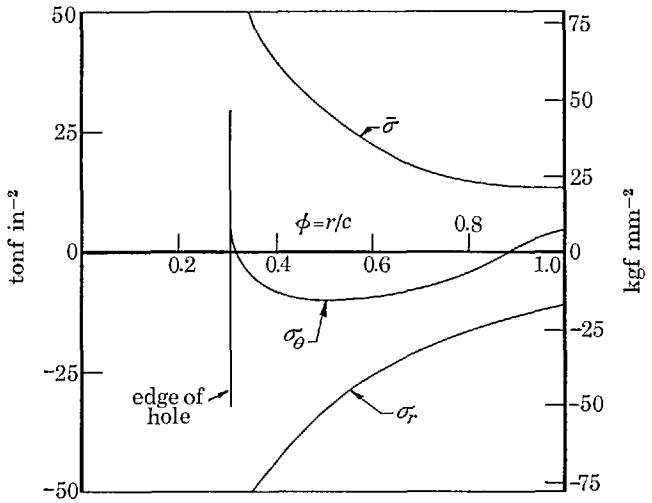


FIGURE 3. Stress distributions

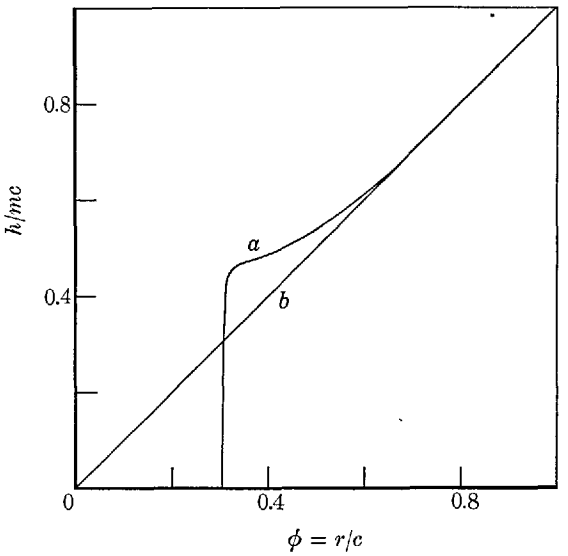


FIGURE 4. Thickness profile; theoretical distribution. *b*, Before deformation; *a*, after deformation.

It was of course necessary to start the actual expansion with a hole of finite radius, and a hole of $\frac{1}{2}$ in (12.7 mm) diameter was made, having a 2° taper to receive a similarly tapered hardened steel mandrel. The expansion of the hole was achieved by forcing the tapered mandrel into the hole whilst slowly rotating the plate in a lathe. Graphite grease lubricant was used to reduce the effect of friction and a continual supply of cold water was run onto the plate to prevent overheating.

The hole in the plate was expanded from 0.5055 in (12.83 mm) diameter to 0.8386 in (21.3 mm), so that the total circumferential strain at the edge of the hole in the experimental plate was $\epsilon_\theta = \ln(0.8386/0.5055) = 0.50619$. It was thus possible to determine from the theoretical solution the fibres in the theoretical plate (expanded from zero radius) which would correspond with the edge of the hole in the experimental plate. In this way the radius to which the theoretical hole would have been expanded to correspond with the experimental solution could be determined. The experimental and theoretical profiles are shown for comparison in figure 5.

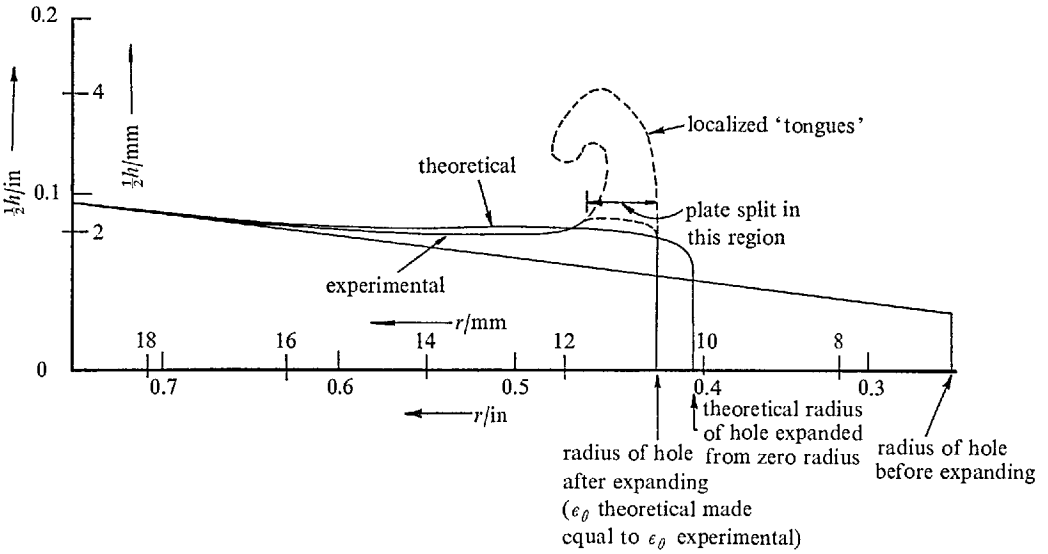


FIGURE 5. Thickness profiles for conical plate.

DISCUSSION

It was found during the experiment that the material at the edge of the hole tended to split and to form into curled segments as indicated in figure 5. However, the portion of the plate which did not split gave a thickness profile which corresponded reasonably well with that predicted. The experimentally determined thickness was slightly less than the theoretical as would be expected in view of the much greater increase of thickness and localized 'tongues' formed in the neighbourhood of the hole where the plate split. The extra volume of material required to give the increased thickness in this region would denude material from the outer zones.

The solution was also modified to apply to the case of expanding a hole in a *flat* plate, on the assumption of geometrical similarity as described previously (Alexander & Ford 1954); Rogers (1967) and an experiment performed on a flat plate of 12 in (305 mm) diameter $\frac{1}{4}$ in (6.35 mm) in thickness. Agreement between the theoretical and experimental thickness profiles was so poor that it was not considered

worth while presenting the results. Clearly the one-dimensional theory developed in this analysis can only be applied with any confidence (as regards deformation in the thickness direction) to the single case of a thin plate having conical profile. An analysis of a flat plate would require proper account to be taken of the boundary conditions, particularly the thickness of the plate in relation to the size of the hole. This would be a problem for which a large deformation finite element technique might provide a solution.

References

Alexander, J. M. & Ford, H. 1954 *Proc. R. Soc. Lond.* A **226**, 543.
Chakrabarty, J. 1971 *Int. J. mech. Sci.* **13**, 439
Chern, J. M. 1969 *Int. J. Mech. Sci.* **11**, 623.
Chern, J. M. & Nemat-Nasser, S. 1969 *J. Mech. Phys. Solids* **17**, 271.
Chern, J. M. & Nemat-Nasser, S. 1970 *Int. J. Solids Struct.* **6**, 829.
Cook, M. & Larke, E. C. 1954 *J. Inst. Met.* **71**, 371.
Hill, R. 1949 *Phil. Mag.* **7**, 971.
Hill, R. 1950 *The mathematical theory of plasticity*, p. 307. Oxford University Press.
Hodge, P. G. & Sankaranarayanan, R. 1958 *Q. appl. Math.* **16**, 73.
Nemat-Nasser, S. 1968 *J. Mech. Phys. Solids* **16**, 195.
Nordgren, R. P. & Naghdi, P. M. 1963 *Int. J. Engng Sci.* **1**, 33.
Nordgren, R. P. & Naghdi, P. M. 1963 *A.S.M.E. J. Appl. Mech.* **30**, 605.
Rogers, T. G. 1967 *Q. Jl Mech. appl. Math.* **20**, (2), 137.
Siddall, J. N. 1971 *Analytical decision making in engineering design.* New York: Prentice Hall.
Taylor, G. I. 1948 *Q. Jl Mech. appl. Math.* **1**, 103.

Appendix B

Curve fitting for stress-strain data

The stress-strain relationships for the workhardening plastic materials are generally non-linear, and there are several forms of expressing these. The relationship used in this analysis, represents most of the material in practice and is given by,

$$\bar{\sigma} = \sigma_o (1 + B\bar{\epsilon}_p)^n \qquad (B.1)$$

where $\bar{\sigma}$, $\bar{\epsilon}_p$ are the equivalent stress and plastic strain and σ_o the initial yield stress.

The unknown coefficients σ_o, B and n are evaluated using a least square analysis of the experimentally obtained stress-strain data. If $\bar{\sigma}_i$ and $\bar{\epsilon}_i$ are the equivalent stress and the strain of the i^{th} experimental value, then we have,

$$e_i = \bar{\sigma}_i - \sigma_o (1 + B\epsilon_i)^n \qquad (B.2)$$

where e_i is the error.

To obtain the values of σ_o, B and n the following function should be minimised,

$$E = \sum_{i=1}^{n} \left\{ \bar{\sigma}_i - \sigma_o (1 + B\bar{\epsilon}_i)^n \right\}^2 \qquad (B.3)$$

The usual method of minimisation by equating the partial derivations of E with respect to σ_o, B and n to zero, leads to extremely tortrous expressions. Several alternative methods, however, could be used. One is a modified Gauss-Newton method (29), in which the equations arising from equation (B.3) are solved using a numerical procedure. The other method employs a direct minimisation procedure known as the Direct Search Simplex Method described by Siddal (69). The two methods give very good results for some stress-strain data

but did not converge for a few cases. Another method which optimises the logarithm of the equivalent stress has been used for such cases and seems to give good results. [This method does not optimise the function given in equation (B.3) so will not give the same optimum given by the other two methods].

Appendix C

General large deformation formulation for the three-dimensional case (Ref. Zienkiewicz (79) p.429)

The most general definition of strain was introduced by Green and St. Venant and is known as Green's strain tensor. Referred to a fixed cartesian system of co-ordinates x, y, z and displacements u, v, w we have,

$$\epsilon_x = \frac{\partial u}{\partial x} + \frac{1}{2}\left(\left(\frac{\partial u}{\partial x}\right)^2 + \left(\frac{\partial v}{\partial x}\right)^2 + \left(\frac{\partial w}{\partial x}\right)^2\right)$$

$$\frac{1}{\sqrt{2}}\epsilon_{xy} = \frac{1}{\sqrt{2}}\left(\frac{\partial u}{\partial y} + \frac{\partial v}{\partial x}\right) + \frac{1}{\sqrt{2}}\left(\frac{\partial u}{\partial x}\cdot\frac{\partial u}{\partial y} + \frac{\partial v}{\partial x}\cdot\frac{\partial v}{\partial y} + \frac{\partial w}{\partial x}\cdot\frac{\partial w}{\partial y}\right)$$

and similarly for the other components.

Derivation of the $\mathbf{B}_L$ matrix

The general Green's strain tensor, can be defined in terms of the small and large displacement components.

i.e. $$\boldsymbol{\epsilon} = \boldsymbol{\epsilon}_o + \boldsymbol{\epsilon}_L \qquad (C.1)$$

where

$$\boldsymbol{\epsilon}_o = \left(\epsilon_x \;\; \epsilon_y \;\; \epsilon_z \;\; \frac{1}{\sqrt{2}}\epsilon_{xy} \;\; \frac{1}{\sqrt{2}}\epsilon_{yz} \;\; \frac{1}{\sqrt{2}}\epsilon_{zx}\right)^t$$

$$= \left\{\frac{\partial u}{\partial x}, \frac{\partial v}{\partial y}, \frac{\partial w}{\partial z}, \frac{1}{\sqrt{2}}\left(\frac{\partial u}{\partial y} + \frac{\partial v}{\partial x}\right),\right.$$

$$\left.\frac{1}{\sqrt{2}}\left(\frac{\partial v}{\partial z} + \frac{\partial w}{\partial y}\right), \frac{1}{\sqrt{2}}\left(\frac{\partial w}{\partial x} + \frac{\partial u}{\partial z}\right)\right\}^t \qquad (1.22)$$

Let $$\boldsymbol{\psi}^t = \left(\boldsymbol{\psi}_x \; \boldsymbol{\psi}_y \; \boldsymbol{\psi}_z\right) \qquad (C.2)$$

where,

$$\boldsymbol{\psi}_x^t = \left(\frac{\partial u}{\partial x} \quad \frac{\partial v}{\partial x} \quad \frac{\partial w}{\partial x}\right)$$

$$\boldsymbol{\psi}_y^t = \left(\frac{\partial u}{\partial y} \quad \frac{\partial v}{\partial y} \quad \frac{\partial w}{\partial y}\right) \qquad (C.3)$$

$$\psi_z^t = \left(\frac{\partial u}{\partial z} \quad \frac{\partial v}{\partial z} \quad \frac{\partial w}{\partial z}\right) \tag{C.3}$$

The nonlinear terms of the Green's strain tensor could be written as,

$$\epsilon_L = \frac{1}{2}\begin{bmatrix} \psi_x^t & 0 & 0 \\ 0 & \psi_y^t & 0 \\ 0 & 0 & \psi_z^t \\ 0 & \frac{1}{2}\psi_z^t & \frac{1}{2}\psi_y^t \\ \frac{1}{2}\psi_z^t & 0 & \frac{1}{2}\psi_x^t \\ \frac{1}{2}\psi_y^t & \frac{1}{2}\psi_x^t & 0 \end{bmatrix} \begin{bmatrix} \psi_x \\ \psi_y \\ \psi_z \end{bmatrix}$$

$$= \frac{1}{2} \mathbf{H}\, \psi \tag{C.4}$$

Therefore,

$$\delta\epsilon_L = \frac{1}{2} \mathbf{H}\, \delta\, \psi + \frac{1}{2}\, \delta\mathbf{H}\, \psi = \mathbf{A}\delta\psi \tag{C.5}$$

Now, ψ can be obtained in terms of the generalised displacements α, so that

$$\psi = \mathbf{S}\, \alpha \tag{C.6}$$

where α is defined in equation (2.15)

and $\mathbf{S}$ is the appropriate 9 x 12 Boolean matrix obtained by differentiating equation (2.13) w. r. t. x, y, z.

Substituting for α from (2.21)

$$\psi = \mathbf{S}\, \mathbf{F}^{-1}\, \rho$$

i.e. $$\psi = \mathbf{G}\, \rho$$

and $$\delta\psi = \mathbf{G}\, \delta\rho \tag{C.7}$$

Therefore,

$$\delta\epsilon_L = \mathbf{H}\, \mathbf{G}\, \delta\, \rho$$

Hence $\mathbf{B}_L = \mathbf{H}\,\mathbf{G}$ (C.8)

Derivation of $\mathbf{k}_\sigma$ matrix

From equation (3.11) we have,

$$\mathbf{k}_\sigma\ \delta\,\boldsymbol{\rho} = \int \delta\ \mathbf{B}_L^t \boldsymbol{\sigma}\ dv$$

Substituting for $\mathbf{B}_L$

$$\mathbf{k}_\sigma\,\delta\boldsymbol{\rho} = \int \mathbf{G}^t\ \delta\mathbf{H}^t\boldsymbol{\sigma}\ dv \qquad (C.9)$$

Expanding $\mathbf{A}$ and $\boldsymbol{\sigma}$, Zienkiewicz (79) has shown that

$$\delta\mathbf{H}^t\boldsymbol{\sigma} = \begin{bmatrix} \sigma_x\mathbf{I}_3 & \sigma_{xy}\mathbf{I}_3 & \sigma_{xz}\mathbf{I}_3 \\ \sigma_{yx}\mathbf{I}_3 & \sigma_y\mathbf{I}_3 & \sigma_{yz}\mathbf{I}_3 \\ \sigma_{zx}\mathbf{I}_3 & \sigma_{yz}\mathbf{I}_3 & \sigma_z\mathbf{I}_3 \end{bmatrix} \begin{bmatrix} \delta\psi_x \\ \delta\psi_y \\ \delta\psi_z \end{bmatrix}$$

$$= \mathbf{M}\,\delta\boldsymbol{\psi}$$

$$= \mathbf{M}\,\mathbf{G}\,\delta\boldsymbol{\rho} \qquad (C.10)$$

Therefore, $\mathbf{k}_\sigma\ \delta\boldsymbol{\rho} = \int \mathbf{G}^t\,\mathbf{M}\,\mathbf{G}\,\delta\boldsymbol{\rho}\ dv$

i.e. $\mathbf{k}_\sigma = \int \mathbf{G}^t\,\mathbf{M}\,\mathbf{G}\ dv$ (C.11)

Here, we have omitted the element subscript g although all of the above matrices would be obtained element by element and assembled in the standard manner.

The above derivation has been obtained following Zienkiewicz (79) and the derivation for the axisymmetric case in Appendix C was obtained on similar lines.

Appendix D

Derivation of the element stiffness matrix for the axisymmetric case

A typical triangular ring element chosen for this case is shown in Fig. 47. The co-ordinate axes are cylindrical with displacements u and v along r and z directions respectively. The strains and the stresses are defined as,

$$\epsilon = \left\{ \epsilon_z \quad \epsilon_r \quad \epsilon_\theta \quad \frac{1}{\sqrt{2}} \epsilon_{rz} \right\} \tag{D.1}$$

$$\sigma = \left\{ \sigma_z \quad \sigma_r \quad \sigma_\theta \quad \sqrt{2}\, \sigma_{rz} \right\} \tag{D.2}$$

A linear displacement function is assumed for the element giving rise to a constant state of stress and strain over the element. (Not strictly true, as ϵ_θ varies with r inside the element, but this is assumed to be negligible and the centroidal value is taken as the average value).

As for the three-dimensional case (Chapter 2), the strain-displacement matrix can be written as,

$$\mathbf{B} = \mathbf{A}\, \mathbf{F}^{-1} \tag{D.3}$$

where

$$\mathbf{A} = \begin{bmatrix} 0 & 0 & 0 & 0 & 0 & 1 \\ 0 & 1 & 0 & 0 & 0 & 0 \\ \frac{1}{r} & 1 & \frac{z}{r} & 0 & 0 & 0 \\ 0 & 0 & \frac{1}{\sqrt{2}} & 0 & \frac{1}{\sqrt{2}} & 0 \end{bmatrix} \tag{D.4}$$

and

$$\mathbf{F}^{-1} = \begin{bmatrix} \mathbf{C}^{-1} & \mathbf{0} \\ \mathbf{0} & \mathbf{C}^{-1} \end{bmatrix} \mathbf{J} \tag{D.5}$$

where,

$$\mathbf{C} = \begin{bmatrix} 1 & r_2 & z_1 \\ 1 & r_2 & z_2 \\ 1 & r_3 & z_3 \end{bmatrix} \tag{D.6}$$

and

$$\mathbf{J} = \begin{bmatrix} 1 & 0 & 0 & 0 & 0 & 0 \\ 0 & 0 & 1 & 0 & 0 & 0 \\ 0 & 0 & 0 & 0 & 1 & 0 \\ 0 & 1 & 0 & 0 & 0 & 0 \\ 0 & 0 & 0 & 1 & 0 & 0 \\ 0 & 0 & 0 & 0 & 0 & 1 \end{bmatrix} \tag{D.7}$$

The stress-strain matrix for the elastic-plastic case can be written as,

$$\mathbf{D}_{ep} = \mathbf{D}_e \left[\mathbf{I}_4 - \frac{3G}{E_p + 3G} \frac{\boldsymbol{\sigma}_D \boldsymbol{\sigma}_D^t}{\boldsymbol{\sigma}_D^t \boldsymbol{\sigma}_D} \right] \tag{D.8}$$

where

$$\mathbf{D}_e = 2G \left[\mathbf{I}_4 + \frac{\nu}{1-\nu} \mathbf{e}_3 \mathbf{e}_3^t \right] \tag{D.9}$$

is the elasticity matrix,

and $\mathbf{e}_3 = \{ 1 \quad 1 \quad 1 \quad 0 \}$ (D.10)

The Green's strain tensor for the axisymmetric case can be written as,

$$\epsilon_z = \frac{\partial v}{\partial z} + \frac{1}{2} \left[\left(\frac{\partial u}{\partial z}\right)^2 + \left(\frac{\partial v}{\partial z}\right)^2 \right]$$

$$\epsilon_r = \frac{\partial u}{\partial r} + \frac{1}{2} \left[\left(\frac{\partial u}{\partial r}\right)^2 + \left(\frac{\partial v}{\partial r}\right)^2 \right] \tag{D.11}$$

$$\epsilon_\theta = \frac{u}{r} + \frac{1}{2} \left(\frac{u}{r}\right)^2$$

$$\frac{1}{\sqrt{2}} \epsilon_{rz} = \frac{1}{\sqrt{2}} \left(\frac{\partial u}{\partial z} + \frac{\partial v}{\partial r} \right) + \frac{1}{\sqrt{2}} \left(\frac{\partial u}{\partial r} \cdot \frac{\partial u}{\partial z} + \frac{\partial v}{\partial r} \cdot \frac{\partial v}{\partial z} \right)$$

Following Appendix C, the initial displacement matrix can be expressed as,

$$\mathbf{B}_L = \mathbf{H}\,\mathbf{G} \tag{C.8}$$

where

$$\mathbf{H} = \begin{bmatrix} \psi_z^t & 0 & 0 \\ 0 & \psi_r^t & 0 \\ 0 & 0 & \psi_\theta^t \\ \frac{1}{2}\psi_r^t & \frac{1}{2}\psi_z^t & 0 \end{bmatrix} \tag{D.12}$$

and

$$\psi_z^t = \left(\frac{\partial v}{\partial z} \quad \frac{\partial u}{\partial z}\right)$$

$$\psi_r^t = \left(\frac{\partial v}{\partial r} \quad \frac{\partial u}{\partial r}\right) \tag{D.13}$$

$$\psi_\theta^t = \left(\frac{u}{r}\right)$$

and $$\mathbf{G} = \mathbf{S}\,\mathbf{F}^{-1} \tag{D.14}$$

where

$$\mathbf{S} = \begin{bmatrix} 0 & 0 & 0 & 0 & 0 & 1 \\ 0 & 0 & 1 & 0 & 0 & 0 \\ 0 & 0 & 0 & 0 & 1 & 0 \\ 0 & 1 & 0 & 0 & 0 & 0 \\ \frac{1}{r} & 1 & \frac{z}{r} & 0 & 0 & 0 \end{bmatrix} \tag{D.15}$$

The initial stress matrix can be expressed as

$$\mathbf{K}_\sigma = \int_v \mathbf{G}^t\,\mathbf{M}\,\mathbf{G}\,dv \tag{C.11}$$

where

$$\mathbf{M} = \begin{bmatrix} \sigma_z\mathbf{I} & \sigma_{rz}\mathbf{I} & 0 \\ \sigma_{rz}\mathbf{I} & \sigma_r\mathbf{I} & 0 \\ 0 & 0 & \sigma_\theta \end{bmatrix}_{5 \times 5} \tag{D.16}$$

Appendix E

Derivation of the element stiffness matrix for the plane-strain case (using natural modes)

The use of the alternative natural mode technique to devise the stiffness matrix is demonstrated here for the plane-strain case. The element is chosen to be a plane triangular element of infinite thickness (Fig. 48). The derivation is carried out on similar lines to the three-dimensional case (Chapter 4).

The natural displacement vector for this case is defined as,

$$\rho_N = (\rho_{12}\ \rho_{23}\ \rho_{31}) \tag{E.1}$$

and the natural load vector as,

$$P_N = (P_{12}\ P_{23}\ P_{31}) \tag{E.2}$$

The cartesian strains and stresses could be expressed as,

$$\epsilon = \left\{ \epsilon_x\ \ \epsilon_y\ \frac{1}{\sqrt{2}}\epsilon_{xy} \right\} \tag{E.3}$$

$$\sigma = \left\{ \sigma_x\ \ \sigma_y\ \sqrt{2}\sigma_{xy}\ \ \sigma_z \right\} \tag{E.4}$$

The element stiffness matrix for the elastic, small displacement case can be written as,

$$k = T\, k_N\, T \tag{E.5}$$

where k and k_N are the cartesian and the natural stiffness matrices of the element,

and

$$T = \begin{bmatrix} -l_\alpha & -m_\alpha & l_\alpha & m_\alpha & 0 & 0 \\ 0 & 0 & -l_\beta & -m_\beta & l_\beta & m_\beta \\ l_\gamma & m_\gamma & 0 & 0 & -l_\gamma & -m_\gamma \end{bmatrix} \tag{E.6}$$

l's and m's are the direction cosines of the edges of the triangular element.

The natural stiffness matrix k_N can be given by,

$$k_N = \int \ell^{-1} \phi_N^{-1} \ell^{-1} \, dv \qquad (E.7)$$

where $\ell = [\ell_{12} \quad \ell_{23} \quad \ell_{31}]$ is a diagonal matrix,

and $$\phi_N = \frac{1}{2G} \left[A - \frac{\nu}{1+\nu} e_4 \, e_4^t \right] \qquad (E.8)$$

where $$e_4^t = (1 \quad 1 \quad 1 \quad 1) \qquad (E.9)$$

and

$$A = \begin{bmatrix} 1 & \cos^2\gamma & \cos^2\beta & 0 \\ \cos^2\gamma & 1 & \cos^2\alpha & 0 \\ \cos^2\beta & \cos^2\alpha & 1 & 0 \\ 0 & 0 & 0 & 1 \end{bmatrix} \qquad (E.10)$$

The plasticity flexibility matrix for the plane-strain case can be given as,

$$\phi_{NP} = \frac{9}{4 E_p \bar{\sigma}^2} \sigma_{ND} \, \sigma_{ND}^t \qquad (E.11)$$

where

$$\sigma_{ND} = (A - e_4 \, e_4^t) \, \sigma_N \qquad (E.12)$$

and $$\bar{\sigma}^2 = \frac{3}{2} \sigma_N^t \sigma_{ND} \qquad (E.13)$$

The elastic-plastic flexibility matrix is obtained in the usual manner as,

$$\phi_{Nep} = \phi_N + \phi_{Np} \qquad (E.14)$$

The geometric matrix for the triangular plane-strain element is given by,

$$k_\sigma = \sum M_{ij} \, k_{\sigma ij} \, M_{ij} \qquad (E.15)$$

where

$$k_{\sigma ij} = \frac{P_{ij}}{ij} \left[I_3 - c_{eij}^t \, c_{eij} \right] \qquad (E.16)$$

is the geometric matrix for the pin jointed bar ij.

$$\mathbf{C}_{eij} = [\, -\mathbf{c}_{ij}\ \mathbf{c}_{ij}] \tag{E.17}$$

where

$$\mathbf{C}_{ij} = [\, \cos(ij, x)\ \cos(ij, y)] \tag{E.18}$$

and

$$\mathbf{M}_{ij} = \underset{6 \times 9}{\begin{bmatrix} \mathbf{I}_3 & \mathbf{0}_3 & \mathbf{0}_3 \\ \mathbf{0}_3 & \mathbf{I}_3 & \mathbf{0}_3 \end{bmatrix}} \quad \text{for } ij = 12 \tag{E.19}$$

and similarly for ij = 12, 23, 31.

Appendix F

F.1 Description and use of the computer programs

The following computer programs have been developed during the course of this project.

(i) Plane stress - constant strain triangular element.
Elastic and Elastic-plastic cases.

(ii) Plane strain - constant strain triangular element.
Elastic, elastic-plastic and large deformation cases.

(iii) Axisymmetric - constant strain tirangular ring element.
Elastic, elastic - plastic and large deformation cases.

(iv) Three-dimensional tetrahedral elements.
Elastic and elastic-plastic cases.

All the programs developed are very similar to each other in most respects (e.g. solution, assembly etc.) except for the evaluation of the element matrices and the stresses and strains, which differ depending on the particular element used. These changes can be effected by simply replacing the appropriate sub-routines. The basic flow chart for a typical program can be given as follows:-

(1) Input data (Geometry, material properties, boundary conditions, etc.).

(2) Initialization of various storage locations.

(3) Formation of the element stiffness matrix by evaluating
(a) The strain-displacement matrix
(b) The elastic or elastic-plastic matrix
(c) The initial stress or geometric matrix.

(4) Assembly of the element stiffnesses to form the overall stiffness matrix.

(5) Specification of the boundary conditions.

(6) Solution of the overall stiffness matrix to obtain the displacements.

(7) Evaluation of the stresses and strains.

(8) Iteration of the stresses.

(9) Scaling to allow for the variable load increment.

(10) Checking elements for yielding and unloading.

(11) Print-out of all displacements, forces, stresses and strains.

F.2 Notations used in the computer program

A - Strain displacement matrix

AREA - Area of element

B - Elastic-plastic stiffness matrix

BE - Elastic stiffness matrix

BX - Constant B of the stress-strain curve

CORD - Nodal point co-ordinates

DS - Incremental displacement

EPS - Incremental strain

FORC - Incremental force

G - Modulus of rigidity

IJK - 3 nodal point numbers of an element

INC - Load increment number

INCRE - Number of load increments

INP - Interval of the print out

IST - = 0, 1 for 1st and subsequent increments

ITR - Iteration number

LY	- = 0, 1, 2 for elastic, plastic, unloading
NA, NB	- Nodal points with prescribed displacements
NAP	- Number of nodal points
NAT	- = 0, 1 for 1st, subsequent runs
NBC	- Boundary point number
NCYCM	- Cycle limit
NITR	- Number of iterations of stresses
NP	- Identity matrix
NPNUM	- Nodal point number
NUMBC	- Number of boundary points
NUME	- Element number
NUMEL	- Number of elements
NUMNP	- Number of nodal points
NYL	- Number of elements yielding during an increment
PR	- Poisson's ratio
PSIG	- Temporary location of stresses
S	- Element stiffness matrix
SCL	- Scale factor
SFORC	- Temporary location of forces
SIG	- Incremental stress
SIGINT	- Initial yield stress
SK	- Geometric matrix
SR	- Temporary location of stiffness
STF	- Overall stiffness matrix
TDS	- Total displacement
TEPS	- Strain
TFORC	- Total force

TOLA - Tolerance for iteration of stresses

TOLER - Tolerance for iteration of displacements

TSIG - Stresses

XFAC - Over-relaxation factor

XN - Constant n of the stress-strain curve

YLSIG - New yield stress of an element which is unloading

YM - Young's modulus

F.3 Description of the programs

F.3.1 Main Program

A listing of a typical program used in this thesis is shown in Appendix G. A short description of the main program, with the call statements for the various subroutines is given below.

Call READIN

This subroutine is called to read data from cards or by calling the subroutine MESHGN.

Initialization I and II

It is important to initialize all or most of the variables used in the program to zero, or to any prefixed initial value. This is effected in two stages: I which is effected only once during a run and II which is repeated once every load increment.

Call READA and PRINTA

These subroutines are used to read data from a previous run and print this data.

Call CHECKA

This subroutine checks for positive area of elements.

Call STIFF

This subroutine is called to form the overall stiffness matrix of the structure or body.

Count of adjacent nodal points

The number of adjacent nodal points to one nodal point is counted and stored in NAP(M); NP(M, MX) stores the nodal point numbers of the adjacent nodal point MX, to the nodal point M. These are later used in the solution of the simultaneous equations.

Call LOADIN

This subroutine takes into account the nodal points with prescribed displacements.

Call INVERT

This subroutine inverts the diagonal terms of the stiffness matrix to be used later during the solution.

Call BOUND

This subroutine is called to take into account the slope boundary conditions.

Call ITERAT

The solution of the simultaneous equations is effected by calling this subroutine.

Call STRSAN

Evaluation of the stresses and the strains after obtaining the nodal displacements.

Iteration on stresses

This is effected by evaluating the sum of the absolute difference between the present and the previous stresses and checking if this is below a required tolerance. If the tolerance

is not achieved iteration using the most recent value of stress is repeated until the required degree of tolerance is obtained.

Scaling of all values for a few elements to yield

This is achieved by using the theory given in section 5.5, and calling the subroutine YIELD to determine the correct incremental loading step.

Call FORCES

Computation of the forces at the nodal points with prescribed displacements.

Updating of all quantities by adding the increments

The cumulative values of the displacements etc. are evaluated by adding the incremental quantities at every loading step.

Call EQUIVAL

This subroutine evaluates the equivalent stress and the equivalent strain of an element.

Call CHECK

This subroutine checks the elements for yielding and unloading.

Print of displacements, forces, stresses and strains

This is done at regular intervals of the load increment to save space in printing and is effected by calling the subroutine PRINTA.

Initialization for the next load increment

All the incremental quantities should be initialized to zero before the next load increment is applied.

Call LOAD

This subroutine evaluates the load increment for the next step.

Call PUNCHA

Before the program stops, after executing the prescribed number of load increments, all current values are punched onto cards to be used in subsequent runs. This is effected by calling the subroutine PUNCHA.

Subroutines

F.3.2 READIN

The data forms a major part of a finite element program. This bulk of data should be checked and rechecked carefully in order to avoid any errors. Although there are provisions in this program to check certain types of errors in the data, there is unfortunately no method available for checking all possible errors present in the data. The tedious job of data preparation could sometimes be avoided, if the finite element mesh idealization is regular or is following a certain pattern. This is easily done for regular geometrics and symmetrical shapes consisting of rectangles and circles. The data after being read or generated is printed immediately so that it can be checked during initial runs.

F.3.3 READA

This is an optional subroutine used if the problem is long and cannot be solved in a single run. The subroutine reads all the current data from a previous run.

F.3.4 PUNCHA

This is used in conjunction with READA and punches all the data onto cards, to be used in a subsequent run.

F.3.5 PRINTA

This subroutine prints all the results after a few load

increments and is sometimes used together with a stress and strain averaging subroutine which gives improved results.

F.3.6 CHECKA

This subroutine evaluates the area (or volume) of the element. A check is made of the order of numbering of the nodal points of the element, in the finite element mesh idealization. If the numbering is not carried out in the proper order (noted by the negative area), further computation is stopped and an error message is printed out giving the number of the particular element.

F.3.7 STIFF

This subroutine forms the element stiffness matrices of all the elements and assembles them to form the overall stiffness matrix for the whole body. The subroutines called from this program are GEOM, STRMAT and GEOMAT. The subroutine has to be slightly changed for the cases of plane stress, plane strain and axisymmetric cases and modified considerably for the three-dimensional case. The stiffness matrix is stored in the bonded form and not more than eight adjacent nodal points to a nodal point can be accommodated. If there are more, NTEST is made equal to 1 and computation is stopped and an error message is printed.

F.3.8 GEOM

This subroutine evaluates the strain-displacement matrix for an element. The matrix is the same for the plane stress and strain cases but is different for the axisymmetric case and the three-dimensional cases. Depending on the case the proper subroutine is substituted in the program.

F.3.9 STRMAT

The formation of the stress-strain matrix is effected by this subroutine. The stiffness matrices are not similar for any two cases. The subroutine consists of two parts. In the first the elastic stiffness is evaluated and if the element is plastic computation is continued to evaluate the complete elastic-plastic stiffness; otherwise return is made to the called program.

F.3.10 GEOMAT

This subroutine forms the initial stress or the geometric matrix for each element. The matrices are all different for the few cases considered in this analysis and therefore the subroutine has to be changed for other cases. The subroutine is only called when large deformations are experienced and hence is optional for small displacement problems.

F.3.11 LOADIN

For all the nodal points with prescribed displacements the force matrix and the overall stiffness matrix should be modified. In this subroutine this is effected by multiplying the diagonal term of the stiffness matrix by a large number and modifying the force term accordingly.

F.3.12 INVERT

This subroutine inverts the diagonal 2 x 2 submatrices of the overall stiffness matrix. The inverted submatrices are later used in the solution of the simultaneous equations.

F.3.13 BOUND

The subroutine modifies the flexibilities of the nodal points with the following boundary conditions.

NFIX = 0 nodal point fixed in x and y directions.

NFIX = 1 nodal point fixed in x direction.

NFIX = 2 nodal point fixed in a direction making an angle with the x-axis.

F.3.14 ITERAT

This subroutine solves the simultaneous equations arising from the overall stiffness matrix, using the Gauss-Siedel iterative technique. This technique is described in more detail in section 5.4.4. The iteration is carried out using a suitable over-relaxation factor until a required degree of tolerance is obtained.

F.3.15 STRSAN

This subroutine evaluates the strains and hence the stresses from the known nodal displacements. The two subroutines GEOM and STRMAT are called to effect this.

F.3.16 EQUVAL

The subroutine evaluates the values of the equivalent stress and the equivalent strain from the stress and the strain of every element.

F.3.17 EQUAD

The subroutine evaluates the value of $\bar{\sigma}\, d\bar{\sigma}$, the product of the equivalent stress and its increment. This is later used to determine the correct load increment for the next step.

F.3.18 MESHGN

This is an optional subroutine which generates the finite element mesh idealization for fairly regular geometries. This eliminates the preparation and punching of large numbers of data cards and is used for the majority of the problems.

F.3.19 CHECK

This subroutine checks the elements for yielding and unloading.

LY = 0 for elastic elements

LY = 1 for elastic-plastic elements

LY = 2 for unloading elements.

After every load increment, the elements are checked to see if they have changed their state, and are assigned the values 0, 1 or 2 depending on their position in the stress-strain curve.

F.3.20 FORCES

The subroutine computes the correct nodal forces at the nodal points with prescribed displacements. The subroutine is very similar to subroutine LOADIN.

F.3.21 LOAD

This subroutine in general provides the incremental loads (forces or displacements) for the next load increment. The magnitude of the incremental load does not matter when the increments are automatically controlled by the number of elements yielding.

Use of the computer programs

To specify a problem for finite element analysis four types of information are generally required:

(i) Geometrical

(ii) Topological

(iii) Rheological

(iv) Boundary conditions.

The geometry of a structure or a body is specified by giving the

co-ordinates of the nodal points. The topology is specified by connecting the nodal points into suitable elements and defining the deformation mode. The rheology of the material forming the body is specified by the stress strain relationship of the material. The boundary conditions are specified as constraints on the forces and displacements at the boundary nodal points.

In the present analysis constant strain triangular elements with three nodal points are used for the two-dimensional cases and constant strain tetrahedra with four nodal points are used for the three-dimensional case. The shape of the triangles should be kept very close to an equilateral triangle and long narrow elements should be avoided. The size and number of elements used depends much on the accuracy required and the storage available. Smaller triangles should be used near the regions of stress concentrations or where the stress gradient appears to be very high.

Having obtained a suitable mesh idealization either in the form of punched cards or in a mesh generation routine, the next problem is to check the accuracy of the data. This can be achieved in two ways. The first is to obtain a plot of the finite element mesh idealization (using the program MESH developed by the author). This would in general eliminate most of the errors. The second method is to apply a hydrostatic stress all around the body and check the value of the stresses obtained.

Preparation of the data

If the geometry of the body is not regular and a mesh generation technique cannot be used, the geometry and the topology has to be punched onto cards. The general information required is

first punched onto cards as follows: NUMEL, NUMNP, INCRE, MITR, TOL, TOLA, XFAC.

Geometry and Topology

Two sets of cards are punched for this. The first set contains the number of the element and the three nodal point numbers associated with it. The second set of cards contains the number of the nodal point, the two co-ordinates, the two displacements and the two forces (if known).

Material properties

The material properties required are the Young's modulus, the Poisson's ratio and the constants of the stress-strain relationship $\bar{\sigma} = \sigma_o (1 + B \bar{\epsilon}_p)^n$ for various temperatures. In addition of course, the temperature distribution of the body should be given.

Boundary conditions

The boundary conditions have been specified in two alternative ways. The first was to specify only those nodal points with the following boundary points and deal with them in two ways as follows:

x and y displacements zero

x displacement zero

Nodal point on a slope.

x displacement prescribed

y displacement prescribed.

In the second method all the nodal points were specified according to the following code:

NBC = 0 Nodal point free

= 1 x-displacement prescribed

= 2 x and y displacements prescribed

= 3 y displacement prescribed.

The second method was used more frequently and the value of NBC was read from the cards containing the number of nodal points and the two co-ordinates.

Appendix G

G.1 Finite element program for the axisymmetric case using TRIAX3 elements.

(i) Elastic

(ii) Elastic-plastic

(iii) Large deformations.

This program uses the 'cartesian stiffness' method.

```
      PROGRAM FLAT(INPUT,OUTPUT,TAPE5=INPUT,TAPE6=OUTPUT,PUNCH)
C
C     FLAT PLATE (STEEL) MESH AXY7
C
C     FINITE ELEMENT DISPLACEMENT METHOD FOR ELASTIC PLASTIC CONTINUA
C     AXISYMMETRIC TRIANGULAR ELEMENTS WITH LINEAR DISPLACEMENT FUNCTIO
C     STRAIN HARDENING LAW ASSUMED TO BE S=SO*(1.+BX*EP)**XN
C     CONSTANTS SO, BX, XN OBTAINED FROM EXPERIMENTS
C
C     MODIFIED TANGENTIAL STIFFNESS METHOD INCLUDING THE EFFECT OF
C     NON-LINEARITY DUE TO LARGE DISPLACEMENTS
C     LOADING ASSUMED TO BE QUASI-STATIC AND INCREMETAL
C     MASTER STIFFENESS MATRIX SOLVED USING THE GAUSS-SIEDEL ITERATIVE
C     TECHNIQUE WITH SUITABLE OVER-RLAXATION
C     ACCURATE SOLUTION WITHIN AN INCREMENT OBTAINED USING ITERATION
C
C     NO SLOPE BOUNDARY CONDITIONS
C     NBC( )=1 X-PRESCRIBED, =2 X Y PRESCRIBED, =3 Y PRESCRIBED
C     N ELEMENTS YIELD AT A TIME
C     EDGE OF THE PLATE IS NOT FIXED
C
      COMMON/AAA/TDS(120,2),TFORC(120,2),DS(120,2),FORC(120,2)
      COMMON/BBB/SIG(140,6),EPS(140,6),LY(140),IJK(140,3),CORD(120,2)
      COMMON/CCC/TSIG(140,6),TEPS(140,6),YLSIG(140),PA(140),TNG(140)
      COMMON/DDD/NP(120,10),STF(120,9,4),NAP(120),SFORC(120,2),SR(120,4)
      COMMON/EEE/NBC(120)
      COMMON/FFF/NPNUM(120),NUME(140)
      COMMON/GGG/AREA(140)
      COMMON/LLL/Z(5,6),AM(5,5)
      COMMON/MMM/SIGINT,BX,XN
      COMMON/OOO/NCYCM,INCRE,NITR,TOLER,TOLA,XFAC,YM,PR,S32
      DIMENSION SIGD(6,2),DSIG(6),DEPS(6),PSIG(140,4),A(6,6),BE(6,6)
     1,R(140)
C
C     READ AND PRINT OF DATA
C
      CALL READIN(NUMEL,NUMNP,NUMBC)
C
C     INITIALISATION 1
C
      NAT=0
      NYL=4
      INP=2
      NLO=0
      IST=0
      SCLSIG=.95  *SIGINT
      NGO=0
      DO 50 I=1,5
      DO 51 J=1,5
      AM(I,J)=0.0
   51 Z(I,J)=0.0
   50 Z(I,6)=0.0
      INC=0
      DO 178 N=1,NUMEL
      DO 176 I=1,4
  176 PSIG(N,I)=0.0
      LY(N)=0
      YLSIG(N)=0.0
      DO 178 I=1,6
```

```
      TSIG(N,I)=0.0
      SIG(N,I)=0.0
      EPS(N,I)=0.0
  178 TEPS(N,I)=0.0
      DO 179 M=1,NUMNP
      DO 179 I=1,2
      TDS(M,I)=0.0
  179 TFORC(M,I)=0.0
C
      DO 177 I=1,4
      DO 177 J=1,6
  177 A(I,J)=0.0
      G=YM    /(1.+PR)
      DO 10 I=1,4
      DO 20 J=1,4
   20 BE(I,J)=0.0
   10 BE(I,I)=G
      PR1=G*PR    /(1.-2.*PR)
      DO 11 I=1,3
      DO 11 J=1,3
   11 BE(I,J)=BE(I,J)+PR1
C
C     INITIALISATION 2
C
      IF(NAT.NE.1) GOTO 503
      CALL READA(NUMNP,NUMEL,INC)
      INO=INC-1
      CALL PRINTA(NUMNP,NUMEL,INO)
      NAT=0
  503 ITR=0
      UND=0.5
      SUMP=10.
      NGO=0
C
C     CHECKING FOR POSITIVE AREA OF ELEMENT
C
      CALL CHECKA(NUMEL)
  501 DO 175 L=1,NUMNP
      DO 170 M=1,9
      DO 171 J=1,4
  171 STF(L,M,J)=0.0
  170 NP(L,M )=0
      NP(L,10)=0
  175 NP(L,1)=L
C
C     FORMATION OF STIFFNESS MATRIX
C
      CALL STIFF(NUMEL,NTEST,A,BE,YM,PR,INC)
      IF(NTEST.EQ.1) GOTO 530
C
C     COUNT OF ADJACENT NODAL POINTS
C
      IF(IST.GT.0) GOTO 264
      DO 206 M=1,NUMNP
      MX=1
  205 MX=MX+1
      IF(NP(M,MX))206,206,205
  206 NAP(M)=MX-1
C
```

```
C      LOAD INITIALISATION
C
  264 CALL LOADIN(NUMNP,KA,KB,IST,ITR)
C
C      N.P. STIFFNESS INVERSION AND BOUNDARY FLEXIBILITY MODIFICATION
C
  265 CALL INVERT(NUMNP)
C
C      ITERATION ON NODAL POINT DISPLACEMENTS
C
      CALL ITERAT(NUMNP,XFAC,SUM,TOLER,NCYCM)
      IF(SUM.GT.TOLER) GOTO 530
C
C      COMPUTATION OF APPROXIMATE STRESSES AND STRAINS
C
      CALL STRSAN(NUMEL,Y1,PR,A,BE)
C
C      ITERATION ON STRESSES
C
      IF(INC.EQ.0) GOTO 400
      IF(ITR.EQ.0) GOTO 260
      SUMS=0.0
      SUMD=0.0
      DO 262 N=1,NUMEL
      DO 262 I=1,4
      DELT=SIG(N,I)-PSIG(N,I)
      SUMS=SUMS+ABS(SIG(N,I))
      SUMD=SUMD+ABS(DELT)
      SIG(N,I)=PSIG(N,I)+DELT*UND
  262 CONTINUE
      SUMD=SUMD/SUMS
      IF(SUMP.GT.SUMD) GOTO 57
      IF(UND-0.21) 58,58,59
   59 UND=0.2
      GOTO 57
   58 UND=0.1
   57 SUMP=SUMD
      WRITE(6,120) ITR,SUMD
      IF(SUMD.GT.TOLA) GOTO 405
      NGO=1
      GOTO 400
  405 IF(ITR.GT.NITR) GOTO 266
  260 DO 263 N=1,NUMEL
      DO 263 I=1,4
  263 PSIG(N,I)=SIG(N,I)
      ITR=ITR+1
C
C      SCALING OF ALL VALUES FOR ONE ELEMENT TO YIELD
C
  400 IF(ITR.GT.1) GOTO 401
      DO 140 N=1,NUMEL
      DO 210 I=1,4
      DSIG(I)=SIG(N,I)
      SIGD(I,1)=TSIG(N,I)
  210 SIGD(I,2)=SIG(N,I)
      CALL EQUVAL(DSIG)
      TSIG(N,6)=DSIG(6)*S32
      IF(LY(N)-1) 141,149,145
  141 SIGONT=SIGINT
```

```
      GOTO 146
  145 SIGONT=YLSIG(N)
  146 CALL EQUAD(SIGD)
      QA=TSIG(N,6)**2
      QB=SIGD(6,1)*1.5
      TEMP=TSIG(N,5)**2-SIGONT**2
      TEMP=SQRT(QB*QB-QA*TEMP)
      R(N)=(TEMP-QB)/QA
      GOTO 140
  149 R(N)=1.E20
  140 CONTINUE
      CALL YIELD(R,RMIN,NUMEL,NYL)
C
      SCL=RMIN
      DO 142 M=1,NUMNP
      DO 142 I=1,2
      DS(M,I)=DS(M,I)*SCL
  142 FORC(M,I)=FORC(M,I)*SCL
      DO 143 N=1,NUMEL
      DO 143 I=1,4
      SIG(N,I)=SIG(N,I)*SCL
      PSIG(N,I)=PSIG(N,I)*SCL
  143 EPS(N,I)=EPS(N,I)*SCL
      CALL CORT(INC)
  401 IST=IST+1
      IF(INC.EQ.0.OR.NGO.EQ.1) GOTO 144
      GOTO 501
C
C     COMPUTATION OF FORCES AT N.P. WITH PRESCRIBED DISPLACEMENTS
C
  144 CALL FORCES(KA,KB)
C
C     UPDATING ALL QUANTITIES BY ADDING THE INCREMENTS
C
  402 DO 506 M=1,NUMNP
      DO 506 I=1,2
      TDS(M,I)=TDS(M,I)+DS(M,I)
  506 TFORC(M,I)=TFORC(M,I)+FORC(M,I)
      DO 507 N=1,NUMEL
      DO 507 I=1,4
      TSIG(N,I)=TSIG(N,I)+SIG(N,I)
  507 TEPS(N,I)=TEPS(N,I)+EPS(N,I)
      DO 511 N=1,NUMEL
      DO 215 I=1,4
      DSIG(I)=TSIG(N,I)
  215 DEPS(I)= EPS(N,I)
      CALL EQUVAL(DSIG)
      CALL EQUVAL(DEPS)
      TSIG(N,6)=DSIG(6)*S32
  511 TEPS(N,6)=DEPS(6)/S32+TEPS(N,6)
C
C     CHECKING THE ELEMENTS FOR YIELDING AND UNLOADING
C
  354 CALL CHECK(NUMEL,SCLSIG)
C
      DO 56 M=1,NUMNP
      DO 56 I=1,2
   56 CORD(M,I)=CORD(M,I)+DS(M,I)
C
```

```
      IF(INC.EQ.0.OR.INC.EQ.INCRE) GOTO 52
      IN=INC/INP
      IN=IN*INP
      IF(IN.NE.INC) GOTO 55
C
C     PRINT OF DISPLACEMENTS, FORCES, STRESSES AND STRAINS
C
   52 CALL PRINTA(NUMNP,NUMEL,INC)
   55 INC=INC+1
      IF(INC.GT.INCRE) GOTO 531
C
C     INITIALISATION FOR THE NEXT LOAD INCREMENT
C
      DO 564 M=1,NUMNP
      DO 564 I=1,2
      DS(M,I)=0.0
  564 FORC(M,I)=0.0
      DO 565 N=1,NUMEL
      DO 565 I=1,6
      SIG(N,I)=0.0
  565 EPS(N,I)=0.0
      CALL LOAD(INC)
      GOTO 503
  266 WRITE(6,269)
C
C     PUNCH ALL RESULTS FOR THE NEXT RUN
C
  531 CALL PUNCHA(INC,NUMEL,NUMNP)
   99 FORMAT(1H1)
  269 FORMAT(27H NO CONVERGENCE OF STRESSES )
  120 FORMAT(I12,E20.6)
  530 STOP
      END
```

```
      SUBROUTINE READIN(NUMEL,NUMNP,NUMBC)
      COMMON/AAA/TDS(120,2),TFORC(120,2),DS(120,2),FORC(120,2)
      COMMON/BBB/SIG(140,6),EPS(140,6),LY(140),IJK(140,3),CORD(120,2)
      COMMON/EEE/NBC(120)
      COMMON/FFF/NPNUM(120),NUME(140)
      COMMON/MMM/SIGINT,BX,XN
      COMMON/OOO/NCYCM,INCRE,NITR,TOLER,TOLA,XFAC,YM,PR,S32
C
C     READING AND PRINTING OF DATA
C
      READ (5,1)NUMEL,NUMNP,NUMBC,NCYCM,NCASE,INCRE,SIGINT,TOLER,XFAC
      WRITE(6,101)NUMEL
      WRITE(6,102)NUMNP
      WRITE(6,106)NCYCM
      WRITE(6,109)INCRE
      WRITE(6,107)TOLER
      WRITE(6,108)XFAC
      WRITE(6,110)SIGINT
      YM=12000.
      PR=0.3
      BX=132.763
      XN=0.269237
      TOLA=0.01
      NITR=50
      S32=SQRT(1.5)
      CALL MESHGN
      WRITE(6,2)(NUME(N),(IJK(N,J),J=1,3),N=1,NUMEL)
      WRITE(6,3)(NPNUM(M),CORD(M,1) ,CORD(M,2),FORC(M,1),FORC(M,2)   ,
     1DS(M,1),DS(M,2) ,NBC(M),M=1,NUMNP)
C
   99 FORMAT(1H1)
  101 FORMAT(29H NUMBER OF ELEMENTS           =,I4/)
  102 FORMAT(29H NUMBER OF NODAL POINTS       =,I4/)
  103 FORMAT(29H NUMBER OF BOUNDARY POINTS    =,I4/)
  106 FORMAT(29H CYCLE LIMIT                  =,I4/)
  107 FORMAT(29H TOERANCE LIMIT               =,E12.4/)
  108 FORMAT(29H OVERRELAXATION FACTOR        =,F8.4/)
  109 FORMAT(29H NUMBER OF LOAD INCREMENTS    =,I4/)
  110 FORMAT(29H INITIAL YIELD STRESS         =,F10.2/)
    1 FORMAT(6I4,F10.3,2F10.8)
    2 FORMAT(4I4)
    3 FORMAT(I4,2F10.5,2F10.2,2F10.8,I4)
    4 FORMAT(2I4,F10.5)
      RETURN
      END
```

```
      SUBROUTINE PRINTA(NUMNP,NUMEL,INC)
      COMMON/AAA/TDS(120,2),TFORC(120,2),DS(120,2),FORC(120,2)
      COMMON/BBB/SIG(140,6),EPS(140,6),LY(140),IJK(140,3),CORD(120,2)
      COMMON/CCC/TSIG(140,6),TEPS(140,6),YLSIG(140),PA(140),TNG(140)
      COMMON/FFF/NPNUM(120),NUME(140)
C
C     PRINT OF DISPLACEMENTS, FORCES, STRESSES AND STRAINS
C
   52 WRITE(6,99)
      WRITE(6,113)INC
      WRITE(6,124)
      WRITE(6,122)(NPNUM(M),TDS(M,1),TDS(M,2),TFORC(M,1),TFORC(M,2),
     1CORD(M,1),CORD(M,2),M=1,NUMNP)
C     WRITE(6,99)
C     WRITE(6,114)
C     WRITE(6,562)(NUME(N),(TSIG(N,I),I=1,4),TSIG(N,6),LY(N),N=1,NUMEL)
      CALL STRITE(NUMEL)
   99 FORMAT(1H1)
  113 FORMAT(6X,*LOAD INCREMENT*,I4/)
  122 FORMAT(I10,2F15.8,2F15.6,2F15.8)
  114 FORMAT(*      ELEMENT      Z-STRESS        R-STRESS        T-STRESS
     1    RZ-STRESS       EQ-STRESS          LY*/)
  124 FORMAT(*       N.P.         R-DISPL.         Z-DISPL.          R-FORCE
     1      Z-FORCE        R-COORD.        Z-COORD. */)
  562 FORMAT(I10,5F15.6,I10)
      RETURN
      END
```

```
      SUBROUTINE PUNCHA(INC,NUMEL,NUMNP)
      COMMON/AAA/TDS(120,2),TFORC(120,2),DS(120,2),FORC(120,2)
      COMMON/BBB/SIG(140,6),EPS(140,6),LY(140),IJK(140,3),CORD(120,2)
      COMMON/CCC/TSIG(140,6),TEPS(140,6),YLSIG(140),PA(140),TNG(140)
      COMMON/NNN/LA,YFORC(20)
C
C     PUNCH ALL RESULTS FOR THE NEXT RUN
C
      PUNCH 1,INC
      PUNCH 2,(M,TDS(M,1),TDS(M,2),TFORC(M,1),TFORC(M,2),CORD(M,1),
     1CORD(M,2),M=1,NUMNP)
      PUNCH 3,(N,(TSIG(N,I),I=1,6),LY(N),N=1,NUMEL)
      PUNCH 2,(N,(TEPS(N,I),I=1,6),N=1,NUMEL)
      PUNCH 5,LA,(YFORC(I),I=1,LA)
    1 FORMAT(I10)
    2 FORMAT(I4,6E12.5)
    3 FORMAT(I4,6E12.5,I2)
    5 FORMAT(I10,3E12.5)
      RETURN
      END
```

```
      SUBROUTINE READA(NUMNP,NUMEL,INC)
      COMMON/AAA/TDS(120,2),TFORC(120,2),DS(120,2),FORC(120,2)
      COMMON/BBB/SIG(140,6),EPS(140,6),LY(140),IJK(140,3),CORD(120,2)
      COMMON/CCC/TSIG(140,6),TEPS(140,6),YLSIG(140),PA(140),TNG(140)
      COMMON/NNN/LA,YFORC(20)
C
C     READS DATA FROM LAST RUN
C
      READ(5,1) INC
      READ(5,2)(M,TDS(M,1),TDS(M,2),TFORC(M,1),TFORC(M,2),CORD(M,1),
     1CORD(M,2),M=1,NUMNP)
      READ(5,3)(N,(TSIG(N,I),I=1,6),LY(N),N=1,NUMEL)
      READ(5,2)(N,(TEPS(N,I),I=1,6),N=1,NUMEL)
      READ(5,5)LA,(YFORC(I),I=1,LA)
    1 FORMAT(I10)
    2 FORMAT(I4,6E12.5)
    3 FORMAT(I4,6E12.5,I2)
    5 FORMAT(I10,3E12.5)
      RETURN
      END
```

```
      SUBROUTINE STIFF(NUMEL,NTEST,A,BE,YM,PR,INC)
      COMMON/BBB/SIG(140,6),EPS(140,6),LY(140),IJK(140,3),CORD(120,2)
      COMMON/CCC/TSIG(140,6),TEPS(140,6),YLSIG(140),PA(140),TNG(140)
      COMMON/DDD/NP(120,10),STF(120,9,4),NAP(120),SFORC(120,2),SR(120,4)
      COMMON/GGG/AREA(140)
      DIMENSION S(6,6),LM(3),A(6,6),B(6,6),BE(6,6),SK(6,6)
C
C     FORMATION OF THE STIFFNESS MATRIX
C
      NTEST=0
      DO 200 N=1,NUMEL
      CALL GEOM(N,A,RB)
      CALL STRMAT(N,B,BF,YM,PR)
   10 FORMAT(6E15.6)
   11 FORMAT(4E15.6)
      DO 182 J=1,6
      DO 182 I=1,4
      S(I,J)=0.0
      DO 182 K=1,4
  182 S(I,J)=S(I,J)+B(I,K)*A(K,J)
      DO 183 J=1,6
      DO 183 I=1,4
  183 B(J,I)=S(I,J)*RB*1.5708          /AREA(N)
      DO 184 J=1,6
      DO 184 I=1,6
      S(I,J)=0.0
      DO 184 K=1,4
  184 S(I,J)=S(I,J)+B(I,K)*A(K,J)
      IF(INC.EQ.0) GOTO 21
      CALL GEOMAT(N,SK)
   30 DO 20 J=1,6
      DO 20 I=1,6
   20 S(I,J)=S(I,J)+SK(I,J)
   21 LM(1)=IJK(N,1)
      LM(2)=IJK(N,2)
      LM(3)=IJK(N,3)
      DO 200 L=1,3
      L2=2*L
      L1=L2-1
      DO 200 M=1,3
      M2=2*M
      M1=M2-1
      LX=LM(L)
      MX=0
  185 MX=MX+1
      IF(NP(LX,MX)-LM(M)) 190,195,190
  190 IF(NP(LX,MX))185,195,185
  195 NP(LX,MX)=LM(M)
      IF(MX-10)196,702,702
  196 STF(LX,MX,1)=STF(LX,MX,1)+S(L1,M1)
      STF(LX,MX,2)=STF(LX,MX,2)+S(L1,M2)
      STF(LX,MX,3)=STF(LX,MX,3)+S(L2,M1)
  200 STF(LX,MX,4)=STF(LX,MX,4)+S(L2,M2)
      GOTO 530
  702 WRITE(6,712)LX
      NTEST=1
  712 FORMAT(34H OVER 8 N.P. ADAJACENT TO N.P. NO. ,I4)
  530 RETURN
      END
```

```
      SUBROUTINE INVERT(NUMNP)
      COMMON/DDD/NP(120,10),STF(120,9,4),NAP(120),SFORC(120,2),SR(120,4)
C
C     INVERSION OF THE N.P. STIFFNESS
C
      DO 210 M=1,NUMNP
      COMM=STF(M,1,1)*STF(M,1,4)-STF(M,1,2)*STF(M,1,3)
      TEMP=STF(M,1,4)/COMM
      STF(M,1,4)=STF(M,1,1)/COMM
      STF(M,1,1)=TEMP
      STF(M,1,2)=-STF(M,1,2)/COMM
  210 STF(M,1,3)=-STF(M,1,3)/COMM
      RETURN
      END
```

```
      SUBROUTINE CHECKA(NUMEL)
      COMMON/BBB/SIG(140,6),EPS(140,6),LY(140),IJK(140,3),CORD(120,2)
      COMMON/GGG/AREA(140)
C
C     CHECKING THE POSITIVE AREA OF ELEMENT
C
      DO 180 N=1,NUMEL
      I=IJK(N,1)
      J=IJK(N,2)
      K=IJK(N,3)
      A1=CORD(J,1)-CORD(I,1)
      A2=CORD(K,1)-CORD(I,1)
      A3=CORD(J,2)-CORD(I,2)
      A4=CORD(K,2)-CORD(I,2)
      AREA(N)=(A1*A4-A2*A3)*.5
      IF(AREA(N))701,701,180
  180 CONTINUE
      GOTO 530
  701 WRITE(6,711)N
  711 FORMAT(32H ZERO OR NEGATIVE AREA, EL.NO.= ,I4)
  530 RETURN
      END
```

```
      SUBROUTINE ITERAT(NUMNP,XFAC,SUM,TOLER,NCYCM)
      COMMON/AAA/TDS(120,2),TFORC(120,2),DS(120,2),FORC(120,2)
      COMMON/DDD/NP(120,10),STF(120,9,4),NAP(120),SFORC(120,2),SR(120,4)
C
C     SOLUTION OF THE SIMULTANEOUS EQUATIONS
C
      WRITE(6,303)
      NCYCLE=0
  244 SUM=0.0
      SUMT=0.0
      DO 290 M=1,NUMNP
      NUM=NAP(M)
  275 FRX=FORC(M,1)
      FRY=FORC(M,2)
      DO 280 L=2,NUM
      N=NP(M,L)
      FRX=FRX-STF(M,L,1)*DS(N,1)-STF(M,L,2)*DS(N,2)
  280 FRY=FRY-STF(M,L,3)*DS(N,1)-STF(M,L,4)*DS(N,2)
      DX=STF(M,1,1)*FRX+STF(M,1,2)*FRY-DS(M,1)
      DY=STF(M,1,3)*FRX+STF(M,1,4)*FRY-DS(M,2)
C     DX=FRX/STF(M,1,1) -DS(M,1)
C     DY=FRY/STF(M,1,4) -DS(M,2)
  286 DS(M,1)=DS(M,1)+XFAC*DX
      DS(M,2)=DS(M,2)+XFAC*DY
      SUM=SUM+ABS(DX)+ABS(DY)
      SUMT=SUMT+ABS(DS(M,1))+ABS(DS(M,2))
  290 CONTINUE
C
      NC=FLOAT(NCYCLE)/50.+1.E-20
      NC=50*NC
      SUM=SUM/SUMT
      IF(NC.NE.NCYCLE) GOTO 302
       WRITE(6,120)NCYCLE,SUM
  302 IF(SUM.LT.TOLER) GOTO 401
      NCYCLE=NCYCLE+1
  310 IF(NCYCM-NCYCLE) 400,400,244
  303 FORMAT(17H ITERATION BEGINS/)
  120 FORMAT(I12,E20.6)
  401 WRITE(6,120)NCYCLE,SUM
  400 RETURN
      END
```

```
      SUBROUTINE CHECK(NUMEL,SCLSIG)
      COMMON/BBB/SIG(140,6),EPS(140,6),LY(140),IJK(140,3),CORD(120,2)
      COMMON/CCC/TSIG(140,6),TEPS(140,6),YLSIG(140),PA(140),TNG(140)
C
C     CHECKING THE ELEMENTS FOR YIELDING AND UNLOADING
C
      DO 145 N=1,NUMEL
      IF(LY(N)-1) 147,146,148
  147 IF(TSIG(N,6).GE.SCLSIG) LY(N)=1
      GOTO 145
  146 IF(TEPS(N,6).GE.TEPS(N,5).OR.TSIG(N,6).GE.TSIG(N,5)) GOTO 145
      LY(N)=2
      YLSIG(N)=TSIG(N,5)
      GOTO 145
  148 IF(TEPS(N,6).LE.TEPS(N,5).OR.TSIG(N,6).LE.YLSIG(N)) GOTO 145
      LY(N)=1
      YLSIG(N)=0.0
  145 CONTINUE
C
      DO 560 N=1,NUMEL
      TSIG(N,5)=TSIG(N,6)
  560 TEPS(N,5)=TEPS(N,6)
      RETURN
      END
```

```
      SUBROUTINE LOAD(INC)
      COMMON/AAA/TDS(120,2),TFORC(120,2),DS(120,2),FORC(120,2)
      COMMON/NNN/LA,YFORC(20)
C
C     LOADS FOR THE NEXT INCREMENT
C
      L=3
      LL=1
      J=1
      KK=0
      DEL=1.
      IF(INC.GT.1) GOTO 20
      DO 11 M=1,L,LL
      MM=21*M-20
   11 YFORC(M)=  TDS(MM,J)
   20 DO 12 M=1,L,LL
      MM=21*M-20
   12   DS(MM,J)=DEL*YFORC(M)
      RETURN
      END
```

```
      SUBROUTINE EQUVAL(S)
      DIMENSION S(6)
C
C     COMPUTATION OF THE EQUIVALENT STRESS AND STRAIN
C
      HS=(S(1)+S(2)+S(3))/3.
      S(1)=S(1)-HS
      S(2)=S(2)-HS
      S(3)=S(3)-HS
      S(6)=0.0
      DO 11 I=1,4
   11 S(6)=S(6)+S(I)**2
      S(6)=SQRT(S(6))
      RETURN
      END
```

```
      SUBROUTINE EQUAD(S)
      DIMENSION S(6,2)
C
C     COMPUTATION OF EQ. STRESS*INCREMENT OF EQ. STRESS
C
      HS=(S(1,1)+S(2,1)+S(3,1))/3.
      S(1,1)=S(1,1)-HS
      S(2,1)=S(2,1)-HS
      S(3,1)=S(3,1)-HS
      S(6,1)=0.0
      DO 11 I=1,4
   11 S(6,1)=S(6,1)+S(I,1)*S(I,2)
      RETURN
      END
```

```
      SUBROUTINE GEOM(N,A,RB)
      COMMON/BBB/SIG(140,6),EPS(140,6),LY(140),IJK(140,3),CORD(120,2)
      DIMENSION D(3,2),A(6,6)
C
C     STRAIN-DISPLACEMENT MATRIX
C
      SQ2=SQRT(.5)
      DO 10 I=1,3
      J=IJK(N,I)
      D(I,1)=CORD(J,1)
   10 D(I,2)=CORD(J,2)
      RB=(D(1,1)+D(2,1)+D(3,1))/3.0
      ZB=(D(1,2)+D(2,2)+D(3,2))/(3.*RB)
      DO 11 I=1,3
      I2=2*I
      I1=I2-1
      K1=I+1
      K2=I+2
      IF(K1.GT.3) K1=K1-3
      IF(K2.GT.3) K2=K2-3
      A(1,I2)=D(K1,1)-D(K2,1)
      A(2,I1)=D(K2,2)-D(K1,2)
      A(3,I1)=(D(K1,2)*D(K2,1)-D(K2,2)*D(K1,1))/RB+A(1,I2)*ZB+A(2,I1)
      A(4,I1)=A(1,I2)*SQ2
   11 A(4,I2)=A(2,I1)*SQ2
      RETURN
      END
```

```
      SUBROUTINE STRMAT(N,B,BE,YM,PR)
      COMMON/BBB/SIG(140,6),EPS(140,6),LY(140),IJK(140,3),CORD(120,2)
      COMMON/CCC/TSIG(140,6),TEPS(140,6),YLSIG(140),PA(140),TNG(140)
      COMMON/MMM/SIGINT,BX,XN
      DIMENSION B(6,6),TS(4),BE(6,6)
C
C     STRESS-STRAIN MATRIX
C
      IF(LY(N).EQ.1) GOTO 50
      DO 60 I=1,4
      DO 60 J=1,4
   60 B(I,J)=BE(I,J)
      GOTO 70
   50 G=YM   /(1.+PR)
      DO 90 I=1,4
   90 TS(I)=TSIG(N,I)+.5*SIG(N,I)
      HSIG=(TS(1)+TS(2)+TS(3))/3.
      TS(1)=TS(1)-HSIG
      TS(2)=TS(2)-HSIG
      TS(3)=TS(3)-HSIG
      EQST=0.0
      DO 28 I=1,4
   28 EQST=EQST+TS(I)**2
      SB=SQRT(1.5*EQST)
      EP=SIGINT*BX*XN*(SB/SIGINT)**(1.-(1./XN))
      T=EP/(1.5*G)
      RA=G/(1.+T)
      DO 29 I=1,4
      DO 29 J=1,4
   29 B(I,J)=BE(I,J)-(TS(I)*TS(J)*RA/EQST)
   70 RETURN
      END
```

```
      SUBROUTINE STRSAN(NUMEL,YM,PR,A,BE)
      COMMON/AAA/TDS(120,2),TFORC(120,2),DS(120,2),FORC(120,2)
      COMMON/BBB/SIG(140,6),EPS(140,6),LY(140),IJK(140,3),CORD(120,2)
      COMMON/GGG/AREA(140)
      DIMENSION A(6,6),B(6,6),D(6),BE(6,6)
C
C     COMPUTATION OF THE STRESSES AND STRAINS
C
      DO 420 N=1,NUMEL
      CALL GEOM(N,A,RB)
      DO 10 I=1,3
      II=2*I-2
      K=IJK(N,I)
      DO 10 J=1,2
      JJ=II+J
   10 D(JJ)=DS(K,J)
      DO 11 I=1,4
      EPS(N,I)=0.0
      DO 11 J=1,6
   11 EPS(N,I)=EPS(N,I)+A(I,J)*D(J)*.5/AREA(N)
      CALL STRMAT(N,B,BE,YM,PR)
      DO 12 I=1,4
      SIG(N,I)=0.0
      DO 12 J=1,4
   12 SIG(N,I)=SIG(N,I)+B(I,J)*EPS(N,J)
  420 CONTINUE
      RETURN
      END
```

```
      SUBROUTINE LOADIN(NUMNP,KA,KB,INC,ITR)
      COMMON/AAA/TDS(120,2),TFORC(120,2),DS(120,2),FORC(120,2)
      COMMON/DDD/NP(120,10),STF(120,9,4),NAP(120),SFORC(120,2),SR(120,4)
      COMMON/EEE/NBC(120)
      COMMON/JJJ/NA(60),NB(60)
C
C     NODAL POINTS WITH PRESCRIBED DISPLACEMENTS
C
      IF(INC.GT.0) GOTO 10
      KA=0
      KB=0
      DO 209 M=1,NUMNP
      IF(NBC(M).EQ.0) GOTO 209
      IF(NBC(M)-2) 101,101,80
  101 KA=KA+1
      IF(KA.GT.60) GOTO 75
      NA(KA)=M
      STF(M,1,1)=STF(M,1,1)*1.E20
      FORC(M,1)=DS(M,1)*STF(M,1,1)
   80 IF(NBC(M).EQ.1) GOTO 209
      KB=KB+1
      IF(KB.GT.60) GOTO 75
      NB(KB)=M
      STF(M,1,4)=STF(M,1,4)*1.E20
      FORC(M,2)=DS(M,2)*STF(M,1,4)
  209 CONTINUE
      GOTO 204
   10 IF(KA.EQ.0) GOTO 20
      DO 11 LA=1,KA
      M=NA(LA)
      STF(M,1,1)=STF(M,1,1)*1.E20
   11 FORC(M,1)=DS(M,1)*STF(M,1,1)
   20 IF(KB.EQ.0) GOTO 204
      DO 12 LB=1,KB
      M=NB(LB)
      STF(M,1,4)=STF(M,1,4)*1.E20
   12 FORC(M,2)=DS(M,2)*STF(M,1,4)
  204 DO 219 M=1,NUMNP
      DO 219 J=1,4
  219 SR(M,J)=STF(M,1,J)
      GOTO 530
   75 WRITE(6,76)
   76 FORMAT(50H MORE THAN 20 PRESCRIBED DISPLACEMENT NODAL POINTS   )
  530 RETURN
      END
```

```
      SUBROUTINE FORCES(KA,KB)
      COMMON/AAA/TDS(120,2),TFORC(120,2),DS(120,2),FORC(120,2)
      COMMON/DDD/NP(120,10),STF(120,9,4),NAP(120),SFORC(120,2),SR(120,4)
      COMMON/EEE/NBC(120)
      COMMON/JJJ/NA(60),NB(60)
C
C     COMPUTATION OF FORCES AT N.P. WITH PRESCRIBED DISPLACEMENTS
C
      IF(KA.EQ.0) GOTO 79
      DO 71 LA=1,KA
      M=NA(LA)
      NUM=NAP(M)
      FORC(M,1)=FORC(M,1)*1.E-20+SR(M,2)*DS(M,2)
      DO 73 L=2,NUM
      N=NP(M,L)
   73 FORC(M,1)=FORC(M,1)+STF(M,L,1)*DS(N,1)+STF(M,L,2)*DS(N,2)
   71 CONTINUE
   79 IF(KB.EQ.0) GOTO 400
      DO 72 LB=1,KB
      M=NB(LB)
      NUM=NAP(M)
      FORC(M,2)=FORC(M,2)*1.E-20+SR(M,3)*DS(M,1)
      DO 74 L=2,NUM
      N=NP(M,L)
   74 FORC(M,2)=FORC(M,2)+STF(M,L,3)*DS(N,1)+STF(M,L,4)*DS(N,2)
   72 CONTINUE
  400 RETURN

      END
```

```
      SUBROUTINE YIELD(R,RMIN,NUMEL,NE)
      DIMENSION R(140)
C
C     COMPUTATION OF THE LOWEST VALUE OF R
C
      DO 20 I=1,NE
      L=1
      RMIN=R(1)
      DO 10 N=2,NUMEL
      IF(RMIN.LE.R(N)) GOTO 10
      RMIN=R(N)
      L=N
   10 CONTINUE
      R(L)=1.E20
   20 CONTINUE
   30 FORMAT(I10,1E20.5)
      RETURN
      END
```

```
      SUBROUTINE GEOMAT(N,SK)
      COMMON/BBB/SIG(140,6),EPS(140,6),LY(140),IJK(140,3),CORD(120,2)
      COMMON/CCC/TSIG(140,6),TEPS(140,6),YLSIG(140),PA(140),TNG(140)
      COMMON/GGG/AREA(140)
      COMMON/LLL/G(5,6),AM(5,5)
      DIMENSION SK(6,6),TK(5,6)
C
C     THE INITIAL STRESS MATRIX OR THE GEOMETRIC MATRIX
C
      I=IJK(N,1)
      J=IJK(N,2)
      K=IJK(N,3)
      RB=(CORD(I,1)+CORD(J,1)+CORD(K,1))/3.
      ZB=(CORD(I,2)+CORD(J,2)+CORD(K,2))/3.
      G(1,2)=CORD(K,1)-CORD(J,1)
      G(1,4)=CORD(I,1)-CORD(K,1)
      G(1,6)=CORD(J,1)-CORD(I,1)
      G(3,2)=CORD(J,2)-CORD(K,2)
      G(3,4)=CORD(K,2)-CORD(I,2)
      G(3,6)=CORD(I,2)-CORD(J,2)
      DO 11 L=1,5,2
      G(2,L)=G(1,(L+1))
   11 G(4,L)=G(3,(L+1))
      G(5,1)=(CORD(J,1)*CORD(K,2)-CORD(K,1)*CORD(J,2))/RB+G(3,2)
     1+G(1,2)*ZB/RB
      G(5,3)=(CORD(K,1)*CORD(I,2)-CORD(I,1)*CORD(K,2))/RB+G(3,4)
     1+G(1,4)*ZB/RB
      G(5,5)=(CORD(I,1)*CORD(J,2)-CORD(J,1)*CORD(I,2))/RB+G(3,6)
     1+G(1,6)*ZB/RB
      TEM=1.5078    *RB/AREA(N)
      AM(1,1)=TSIG(N,1)*TEM
      AM(1,3)=TSIG(N,4)*SQRT(.5)*TEM
      AM(2,2)=AM(1,1)
      AM(2,4)=AM(1,3)
      AM(3,1)=AM(1,3)
      AM(3,3)=TSIG(N,2)*TEM
      AM(4,2)=AM(1,3)
      AM(4,4)=AM(3,3)
      AM(5,5)=TSIG(N,3)*TEM
      DO 12 I=1,5
      DO 12 J=1,6
      TK(I,J)=0.0
      DO 12 K=1,5
   12 TK(I,J)=TK(I,J)+AM(I,K)*G(K,J)
      DO 13 I=1,6
      DO 13 J=1,6
      SK(I,J)=0.0
      DO 13 K=1,5
   13 SK(I,J)=SK(I,J)+G(K,I)*TK(K,J)
      RETURN
      END
```

```
      SUBROUTINE MESHGN
      COMMON/AAA/TDS(120,2),TFORC(120,2),DS(120,2),FORC(120,2)
      COMMON/BBB/SIG(140,6),EPS(140,6),LY(140),IJK(140,3),CORD(120,2)
      COMMON/DDD/NP(120,10),STF(120,9,4),NAP(120),SFORC(120,2),SR(120,4)
      COMMON/EEE/NBC(120)
      COMMON/FFF/NPNUM(120),NUME(140)
C
C     MESH GENERATION FOR THE FLAT PLATE
C     DIMENSIONS OF PLATE FROM EXPERIMENT
C
      READ (5,20)((IJK(N,I),I=1,3),N=81,83)
   20 FORMAT(9I4)
      NUMEL=133
      NUMNP=115
      DO 10 N=1,133
   10 NUME(N)=N
      DO 11 M=1,115
   11 NPNUM(M)=M
      DO 12 J=1,3
      DO 12 I=1,21
      M=21*J+I-21
      CORD(M,1)=FLOAT(I)*0.075+0.175
   12 CORD(M,2)=FLOAT(J-1)*0.0625
      DO 13 J=1,2
      DO 13 I=1,26
      M=26*J+I+37
      CORD(M,1)=FLOAT(I)*0.167+1.658
   13 CORD(M,2)=FLOAT(J-1)*0.125
      DO 14 I=1,2
      DO 14 J=1,20
      N=40*I+2*J-41
      M=N+1
      IJK(N,1)=J+21*I-21
      IJK(N,2)=IJK(N,1)+1
      IJK(N,3)=IJK(N,1)+21
      IJK(M,1)=IJK(N,2)
      IJK(M,2)=IJK(N,1)+22
   14 IJK(M,3)=IJK(N,3)
      DO 15 I=1,25
      N=2*I+82
      M=N+1
      IJK(N,1)=I+63
      IJK(N,2)=I+64
      IJK(N,3)=I+89
      IJK(M,1)=IJK(N,2)
      IJK(M,2)=I+90
   15 IJK(M,3)=IJK(N,3)
      DO 31 I=1,NUMNP
   31 NBC(I)=0
      DO 32 I=2,21
   32 NBC(I)=3
      DO 33 I=64,88
   33 NBC(I)=3
C     NBC(1)=3
      NBC(1)=2
      NBC(22)=1
      NBC(43)=1
      NBC(89)=2
      NBC(115)=1
```

```
C       NBC(89)=3
        DO 16 M=1,115
        DO 16 I=1,2
        FORC(M,I)=0.0
   16   DS(M,I)=0.0
        DS( 1,1)=.005
        DS(22,1)=.005
        DS(43,1)=.005
        RETURN
        END
```

```
      SUBROUTINE STRITE(NUMEL)
      COMMON/BBB/SIG(140,6),EPS(140,6),LY(140),IJK(140,3),CORD(120,2)
      COMMON/CCC/TSIG(140,6),TEPS(140,6),YLSIG(140),PA(140),TNG(140)
      DIMENSION TS(46,6),TE(46,6),L(46)
C
C     AVERAGING SUBROUTINE
C
      DO 1 I=1,46
    1 L(I)=0
      DO 10 I=1,20
      N1=2*I-1
      N2=N1+1
      N3=N1+40
      N4=N1+41
      LI=LY(N1)+LY(N2)+LY(N3)+LY(N4)
      IF(LI.EQ.4) L(I)=1
      DO 11 J=1,6
      TS(I,J)=.25*(TSIG(N1,J)+TSIG(N2,J)+TSIG(N3,J)+TSIG(N4,J))
   11 TE(I,J)=.25*(TEPS(N1,J)+TEPS(N2,J)+TEPS(N3,J)+TEPS(N4,J))
   10 CONTINUE
      DO 12 J=1,6
      TS(21,J)=(TSIG(81,J)+TSIG(82,J)+TSIG(83,J))/3.
   12 TE(21,J)=(TEPS(81,J)+TEPS(82,J)+TEPS(83,J))/3.
      LI=LY(81)+LY(82)+LY(83)
      IF(LI.EQ.3) L(21)=1
      DO 13 I=1,25
      N1=2*I+82
      N2=N1+1
      N=I+21
      LI=LY(N1)+LY(N2)
      IF(LI.EQ.2) L(N)=1
      DO 14 J=1,6
      TS(N,J)=.5*(TSIG(N1,J)+TSIG(N2,J))
   14 TE(N,J)=.5*(TEPS(N1,J)+TEPS(N2,J))
   13 CONTINUE
      WRITE(6,99)
      WRITE(6,114)
      WRITE(6,562)(N,(TS(N,I),I=1,4),TS(N,6),L(N),N=1,46)
      WRITE(6,99)
      WRITE(6,115)
      WRITE(6,563)(N,(TE(N,I),I=1,4),TE(N,6),N=1,46)
      WRITE(6,99)
   99 FORMAT(1H1)
  562 FORMAT(I10,5F15.6,I10)
  563 FORMAT(I10,5F15.8)
  114 FORMAT(*      ELEMENT      Z-STRESS        R-STRESS        T-STRESS
     1    RZ-STRESS       EQ-STRESS          LY*/)
  115 FORMAT(*      ELEMENT      Z-STRAIN        R-STRAIN        T-STRAIN
     1    RZ-STRAIN       EQ-STRAIN    */)
      RETURN
      END
```

```
      SUBROUTINE CORT(INC)
      COMMON/AAA/TDS(120,2),TFORC(120,2),DS(120,2),FORC(120,2)
      COMMON/BBB/SIG(140,6),EPS(140,6),LY(140),IJK(140,3),CORD(120,2)
      COMMON/CCC/TSIG(140,6),TEPS(140,6),YLSIG(140),PA(140),TNG(140)
C
C     MODIFICATION FOR THE STRESS FREE BOUNDARY
C
      FA=0.5
      TST=(TSIG(41,1)+TSIG(42,1))*.5
      TST=TST+FA
      IF(TST.LE.0.) GOTO 100
      X=CORD(44,1)+CORD(43,1)
      Y=CORD(44,1)-CORD(43,1)
      FORC(43,2)=TST*3.14*X*Y *1.1
  100 RETURN
      END
```

G.2 Finite element program for the three-dimensional case using TET4 elements.

(i) Elastic

(ii) Elastic-plastic

(iii) Large deformations.

This program uses the 'natural mode' technique.

```
      PROGRAM EPLAL3(INPUT,OUTPUT,TAPE5=INPUT,TAPE6=OUTPUT)
C     FINITE ELEMENT DISPLACEMENT METHOD (ELASTIC)
C     ADDED PLASTIC AND LARGE DEFORMATIONS
C     THREE DIMENSIONAL
C     ELEMENT SHAPE - TET4
C
C     DIMENSION AND COMMON STATEMENTS
C
      COMMON/BBB/IJK( 85,4),CORD( 50,3),VOL( 85)
      COMMON/CCC/STF(150,57),NP( 50,20),NAP( 50)
      COMMON/DDD/DS( 50,3),FORC( 50,3),SIG( 85,6),EPS( 85,6)
      COMMON/EEE/YM( 85),PR( 85),YLSIG( 85)
      COMMON/FFF/NPB( 50),NDIR( 50),NPNUM( 50),NUME( 85)
      COMMON/GGG/TSIG( 85,8),TEPS( 85,8),TDS( 50,3),TFORC( 50,3),LY( 85)
      COMMON/HHH/PN( 85,6),TPN( 85,6)
      COMMON/III/AL(6),TC(6,3),NS(6,2)
      COMMON/JJJ/          P(6,6),A(6,6),AC( 85,15)
      DIMENSION SIGD(6,2),PSIG( 85,6),D(18,18),TN(18,18)
C
C     READ AND PRINT OF DATA
C
      CALL READPR(NUMEL,NUMNP,NCYCM,TOLER,XFAC,INCPR,SIGINT,SCLSIG,
     1S32,TOLA,NITR,OV)
      CALL DIFFER(D)
C
C     INITIALISATION 1
C
      INC=0
      DO 178 N=1,NUMEL
      LY(N)=0
      YLSIG(N)=0.0
      DO 30 J=1,6
      PSIG(N,J)=0.0
   30 TPN(N,J)=0.0
      DO 178 I=1,8
      TSIG(N,I)=0.0
  178 TEPS(N,I)=0.0
      DO 179 M=1,NUMNP
      DO 179 I=1,3
      TDS(M,I)=0.0
  179 TFORC(M,I)=0.0
      DO 10 I=1,6
      DO 10 J=1,18
   10 TN(I,J)=0.0
C
C     CHECKING FOR POSITIVE VOLUME OF ELEMENT
C
  501 ITR=0
  503 DO 180 N=1,NUMEL
      CALL VOLUME(N,VO)
      IF(VO  )701,701,180
  180 VOL(N)=VO
C
C     INITIALIZATION
C
      DO 175 L=1,NUMNP
      LT=3*L
      DO 170 M=1,19
      MT=3*M
```

```
      DO 171 I=1,3
      MM=MT+I-3
      DO 171 K=1,3
      LL=LT+K-3
  171 STF(LL,MM)=0.0
  170 NP(L,M)=0
      NP(L,20)=0
  175 NP(L,1)=L
C
C     FORMATION OF STIFFNESS ARRAY
C
      NGO=0
      CALL STIFF(NUMEL,NUMNP,INC,ITR,NTEST,TN,D)
      CALL LOADIN(NUMNP)
C
C     ITERATION ON NODAL POINT DISPLACEMENTS
C
      CALL ITERAT(NUMNP,XFAC,SUM,TOLER,NCYCM)
C
C     EVALUATION OF STRESSES AND STRAINS
C
      CALL STRSAN(NUMEL,TN,D)
      IF(INC.EQ.0) GOTO 261
      IF(ITR.EQ.0) GOTO 260
      SUMS=0.0
      SUMD=0.0
      DO 262 N=1,NUMEL
      IF(LY(N).NE.1) GOTO 262
      DO 264 I=1,6
      DELT=SIG(N,I)-PSIG(N,I)
      SUMS=SUMS+ABS(SIG(N,I))
      SUMD=SUMD+ABS(DELT)
      SIG(N,I)=PSIG(N,I)+OV*DELT
  264 CONTINUE
  262 CONTINUE
      SUMD=SUMD/SUMS
      WRITE(6,120) ITR,SUMD
      IF(SUMD.GT.TOLA) GOTO 405
      NGO=1
      GOTO 261
  405 IF(ITR.GT.NITR) GOTO 266
  260 DO 263 N=1,NUMEL
      DO 263 I=1,6
  263 PSIG(N,I)=SIG(N,I)
      ITR=ITR+1
C
C     COMPUTATION OF EQUIVALENT STRESS AND STRAIN
C
  261 RMIN=1.E20
      DO 140 N=1,NUMEL
      DO 210 I=1,6
      SIGD(I,1)=TSIG(N,I)
  210 SIGD(I,2)=SIG(N,I)
      IF(LY(N)-1) 141,140,145
  141 SIGONT=SIGINT
      GOTO 146
  145 SIGONT=YLSIG(N)
  146 CALL EQUAD(SIGD,N,QA,QB,QC)
      QC=QC-(2./3.)*SIGONT**2
```

```
      TEMP=OB*OB-4.*QA*QC
      R=.5*(SQRT(TEMP)-OB)/QA
C
      IF(RMIN.LE.R) GO TO 140
      RMIN=R
  140 CONTINUE
      SCL=RMIN
      DO 142 M=1,NUMNP
      DO 142 I=1,3
      DS(M,I)=DS(M,I)*SCL
  142 FORC(M,I)=FORC(M,I)*SCL
      DO 143 N=1,NUMEL
      DO 143 I=1,6
      PN(N,I)=PN(N,I)*SCL
      SIG(N,I)=SIG(N,I)*SCL
  143 EPS(N,I)=EPS(N,I)*SCL
      IF(INC.EQ.0.OR.NGO.EQ.1) GOTO 402
      GOTO 503
C
C     EVALUATION OF FORCES AT N.P. WITH PRESCRIBED DISPLACEMENTS
C
  402 CALL FORCES(NUMNP)
      CALL TOTALS(NUMNP,NUMEL)
      CALL CHECK(NUMEL,SCLSIG)
      CALL PRINTS(NUMNP,NUMEL,INC)
      INC=INC+1
      IF(INC.GT.INCRE) GOTO 440
C
C     INITIALISATION 3 FOR YHE NEXT LOAD INCREMENT
C
      DO 564 M=1,NUMNP
      DO 564 I=1,3
      DS(M,I)=0.0
  564 FORC(M,I)=0.0
      DO 565 N=1,NUMEL
      DO 31 J=1,6
   31 TPN(N,J)=TPN(N,J)+PN(N,J)
      DO 565 I=1,6
      SIG(N,I)=0.0
  565 EPS(N,I)=0.0
      CALL LOAD(INC)
      GOTO 501
C
C     PRINT OF ERRORS IN INPUT DATA
C
  701 WRITE(6,711)N
      GOTO440
  266 WRITE(6,269)
C
C     FORMAT STATEMENTS
C
  120 FORMAT(1I12,1E20.6)
  711 FORMAT(34H ZERO OR NEGATIVE VOLUME, EL. NO.=I14)
  269 FORMAT(27H NO CONVERGRNCE OF STRESSES )
  440 STOP
      END
```

```
      SUBROUTINE READPR(NUMEL,NUMNP,NCYCM,TOLER,XFAC,INCRE,SIGINT,
     1SCLSIG,S32,TOLA,NITR,OV)
      COMMON/BBB/IJK( 85,4),CORD( 50,3),VOL( 85)
      COMMON/DDD/DS( 50,3),FORC( 50,3),SIG( 85,6),EPS( 85,6)
      COMMON/EEE/YM( 85),PR( 85),YLSIG( 85)
      COMMON/FFF/NPB( 50),NDIR( 50),NPNUM( 50),NUME( 85)
C
C     READ AND PRINT OF DATA
C
      WRITE(6,99)
      READ(5,1)NUMEL,NUMNP,NCYCM,INCRE,TOLER,XFAC,SIGINT
      WRITE(6,101)NUMEL
      WRITE(6,102)NUMNP
      WRITE(6,106)NCYCM
      WRITE(6,107)TOLER
      WRITE(6,108)XFAC
      WRITE(6,109)INCRE
  109 FORMAT(29H NO. OF LOAD INCREMENTS      =,I6/)
  110 FORMAT(29H INITIAL YIELD STRESS        =,F12.2)
      WRITE(6,110)SIGINT
      WRITE(6,99)
C
      DO 391 N=1,NUMEL
      YM(N)=3.E7
  391 PR(N)=0.3
      SCLSIG=.999 *SIGINT
      S32=SQRT(1.5)
      TOLA=.0005
      NITR=10
      OV=1.0
      DO 13 M=1,NUMNP
       DO 13 I=1,3
      DS(M,I)=0.0
   13 FORC(M,I)=0.0
      CALL MEGN31
      WRITE(6,5)(NUME(N),(IJK(N,J),J=1,4),N=1,NUMEL)
      WRITE(6,3)(NPNUM(M),CORD(M,1),CORD(M,2),CORD(M,3),FORC(M,1),
     1FORC(M,2),FORC(M,3),DS(M,1),DS(M,2),DS(M,3), NDIR(M),M=1,NUMNP)
   99 FORMAT(1H1)
  101 FORMAT(29H NUMBER OF ELEMENTS          =,I4/)
  102 FORMAT(29H NUMBER OF NODAL POINTS      =,I4/)
  106 FORMAT(29H CYCLE LIMIT                 =,I4/)
  107 FORMAT(29H TOLERANCE LIMIT             =,E12.4/)
  108 FORMAT(29H OVERRELAXATION FACTOR       =,F6.3/)
    1 FORMAT(4I4,3F15.9)
    3 FORMAT(I4,3F8.5,3E12.5,3F12.8,I8)
    5  FORMAT(5I4)
      RETURN
      END
```

```
      SUBROUTINE PRINTS(NUMNP,NUMEL,INC)
      COMMON/DDD/DS( 50,3),FORC( 50,3),SIG( 85,6),EPS( 85,6)
      COMMON/FFF/NPB( 50),NDIR( 50),NPNUM( 50),NUME( 85)
      COMMON/GGG/TSIG( 85,8),TEPS( 85,8),TDS( 50,3),TFORC( 50,3),LY( 85)
C
C     POINT OF RESULTS
C
      WRITE(6,99)
      WRITE(6,113) INC
      WRITE(6,121)
      WRITE(6,122)(NPNUM(M),DS(M,1),DS(M,2),DS(M,3),FORC(M,1),FORC(M,2),
     1FORC(M,3),M=1,NUMNP)
      WRITE(6,99)
      WRITE(6,123)
      WRITE(6,566)(NUME(N),TSIG(N,8),TEPS(N,8),LY(N),N=1,NUMEL)
C     WRITE(6,124)(NUME(N),(SIG(N,I),I=1,6),N=1,NUMEL)
C     WRITE(6,99)
C     WRITE(6,130)
C     WRITE(6,131)(NUME(N),(EPS(N,I),I=1,6),N=1,NUMEL)
   99 FORMAT(1H1)
  122 FORMAT(I7,4X,3F15.6,4X,3E15.6)
  121 FORMAT(105H    N.P.          X-DISPL.          Y-DISPL.          Z-DISPL.
     1             X-FORCE          Y-FORCE          Z-FORCE       /)
  123 FORMAT(52H      ELEMENT         EQ-STRESS         EQ-STRAIN        LY /)
  566 FORMAT(I10,2X,F16.4,F16.8,I8)
  130 FORMAT(69H   ELEMENT              X-STRAIN              Y-STRAIN
     1     XY-STRAIN)
  131 FORMAT(1I10,6F18.8)
  113 FORMAT(15H LOAD INCREMENT ,I4/ )
      RETURN
      END
```

```
      SUBROUTINE VOLUME(N,V0)
      COMMON/BBB/IJK( 85,4),CORD( 50,3),VOL( 85)
      DIMENSION C(3,3),CC(3)
C
C     CHECKING FOR POSITIVE VOLUME OF ELEMENT
C
      I=IJK(N,1)
      J=IJK(N,2)
      K=IJK(N,3)
      L=IJK(N,4)
      DO 10 M=1,3
      C(1,M)=CORD(J,M)-CORD(I,M)
      C(2,M)=CORD(K,M)-CORD(I,M)
   10 C(3,M)=CORD(L,M)-CORD(I,M)
      CC(1)=C(2,2)*C(3,3)-C(2,3)*C(3,2)
      CC(2)=C(2,3)*C(3,1)-C(2,1)*C(3,3)
      CC(3)=C(2,1)*C(3,2)-C(2,2)*C(3,1)
      DET=0.0
      DO 11 I=1,3
   11 DET=DET+C(1,I)*CC(I)
      V0=DET/6.
      RETURN
      END
```

```
      SUBROUTINE STIFF(NUMEL,NUMNP,INC,ITP,NTEST,TN,D)
      COMMON/BBB/IJK( 85,4),CORD( 50,3),VOL( 85)
      COMMON/CCC/STF(150,57),NP( 50,20),NAP( 50)
      COMMON/III/AL(6),TC(6,3),NS(6,2)
      COMMON/JJJ/          P(6,6),A(6,6),AC( 85,15)
      DIMENSION LM(4) ,SG(18,18) ,SN(18,18),F(18,18)
      DIMENSION TN(18,18),D(18,18),TD(18,18),S(18,18)
C
C       EVALUATION OF STIFFNESS MATRIX
C
      NCON=0
      DO 200 N=1,NUMEL
      CALL STRMAT(N,TN,0)
      CALL MATMUL(6,12,18,TN,D,TD,0)
      NCON=NCON+1
      DO 11 I=1,6
      DO 11 J=1,6
   11 SN(I,J)=VOL(N)*P(I,J)*AL(I)*AL(J)
      CALL MATMUL(6,12,6,SN,TD,F,0)
      NCON=NCON+1
      CALL MATMUL(12,12,6,TD,F,S,1)
      NCON=NCON+1
      IF(INC.EQ.0) GOTO 10
      CALL GEOMAT(N,ITP,SG,INC)
      NCON=NCON+1
   10 DO 13 I=1,4
   13 LM(I)=IJK(N,I)
      DO 200 L=1,4
      DO 200 M=1,4
      LX=LM(L)
      MX=0
  185 MX=MX+1
      IF(NP(LX,MX)-LM(M))190,195,190
  190 IF(NP(LX,MX))185,195,185
  195 NP(LX,MX)=LM(M)
      IF(MX-20)196,702,702
  196 L3=3*L-3
      M3=3*M-3
      LX3=3*LX-3
      MX3=3*MX-3
      DO 200 I=1,3
      LP=L3+I
      LQ=LX3+I
      DO 200 J=1,3
      MP=M3+J
      MQ=MX3+J
  200 STF(LQ,MQ)=STF(LQ,MQ)+S(LP,MP)
C
C       COUNT OF ADJACENT NODAL POINTS
C
  401 DO 206 M=1,NUMNP
      MX=1
  205 MX=MX+1
      IF(NP(M,MX))206,206,205
  206 NAP(M)=MX-1
      GOTO440
  702 WRITE(6,712)LX
  712 FORMAT(33H OVER18 N.P. ADJACENT TO N.P. NO.114)
  440 RETURN
```

END

```
      SUBROUTINE ITERAT(NUMNP,XFAC,SUM,TOLER,NCYCM)
      COMMON/CCC/STF(150,57),NP( 50,20),NAP( 50)
      COMMON/DDD/DS( 50,3),FORC( 50,3),SIG( 85,6),EPS( 85,6)
      DIMENSION F(3)
C
C     ITERATION OF N.P. DISPLACEMENTS
C
      WRITE(6,303)
      NCYCLE=0
  244 SUM=0.0
      SUMT=0.0
      DO 290 M=1,NUMNP
      MM=3*M
      NUM=NAP(M)
      DO 10 I=1,3
   10 F(I)=FORC(M,I)
      DO 280 L=1,NUM
      N=NP(M,L)
      DO 280 I=1,3
      NW=3*L+I-3
      DO 280 J=1,3
      MJ=MM+J-3
  280 F(J)=F(J)-STF(MJ,NW)*DS(N,I)
      DO 11 J=1,3
      MJ=MM+J-3
      DEL=F(J)/STF(MJ,J)
      DS(M,J)=DS(M,J)+DEL*XFAC
      SUM=SUM+ABS(DEL)
   11 SUMT=SUMT+ABS(DS(M,J))
  290 CONTINUE
C
C     CYCLE COUNT AND PRINT CHECK
C
      SUM=SUM/SUMT
      NC=FLOAT(NCYCLE)/20.+1.E-20
      NC=20*NC
      IF(NC.NE.NCYCLE) GO TO 302
      WRITE(6,120)NCYCLE,SUM
  302 IF(SUM.LT.TOLER) GO TO 400
      NCYCLE=NCYCLE+1
  310 IF(NCYCM-NCYCLE)400,400,244
  120 FORMAT(1I12,1E20.6)
  303 FORMAT(17H ITERATION BEGINS/)
  400 RETURN
      END
```

```
      SUBROUTINE LOADIN(NUMNP)
      COMMON/CCC/STF(150,57),NP( 50,20),NAP( 50)
      COMMON/DDD/DS( 50,3),FORC( 50,3),SIG( 85,6),EPS( 85,6)
      COMMON/FFF/NPB( 50),NDIR( 50),NPNUM( 50),NUME( 85)
C
C     LOAD INITIALIZATION
C
      DO 209 M=1,NUMNP
      IF(NDIR(M).EQ.1000) GOTO 209
      MM=3*M
      MA=NDIR(M)/10
      MA=10*MA
      IF(MA.EQ.NDIR(M)) GOTO 10
      STF(MM,3)=STF(MM,3)*1.E22
      FORC(M,3)=STF(MM,3)*DS(M,3)
   10 MB=MA/100
      MB=MB*100
      IF(MA.EQ.MB) GOTO 11
      STF(MM-1,2)=STF(MM-1,2)*1.E22
      FORC(M,2)=STF(MM-1,2)*DS(M,2)
   11 MC=MB/1000
      MC=MC*1000
      IF(MC.EQ.MB) GOTO 209
      STF(MM-2,1)=STF(MM-2,1)*1.E22
      FORC(M,1)=STF(MM-2,1)*DS(M,1)
  209 CONTINUE
      RETURN
      END
```

```
      SUBROUTINE FORCES(NUMNP)
      COMMON/CCC/STF(150,57),NP( 50,20),NAP( 50)
      COMMON/DDD/DS( 50,3),FORC( 50,3),SIG( 85,6),EPS( 85,6)
      COMMON/FFF/NPB( 50),NDIR( 50),NPNUM( 50),NUME( 85)
C
C     EVALUATION OF FORCES AT N.P. WITH PRESCRIBED DISPLACEMENTS
C
      DO 208 M=1,NUMNP
      IF(NDIR(M).EQ.1000) GOTO 208
      MM=3*M
      M3=MM-3
      MA=NDIR(M)/10
      MA=10*MA
      IF(MA.EQ.NDIR(M)) GOTO 40
      STF(MM,3)=STF(MM,3)*1.E-22
   40 MB=MA/100
      MB=MB*100
      IF(MA.EQ.MB) GOTO 41
      STF(MM-1,2)=STF(MM-1,2)*1.E-22
   41 MC=MB/1000
      MC=MC*1000
      IF(MC.EQ.MB) GOTO 42
      STF(MM-2,1)=STF(MM-2,1)*1.E-22
   42 NUM=NAP(M)
      DO 43 J=1,3
      FORC(M,J)=0.0
      DO 43 I=1,NUM
      N=NP(M,I)
      II=3*I-3
      DO 43 L=1,3
   43 FORC(M,J)=FORC(M,J)+STF(M3+J,II+L)*DS(N,L)
  208 CONTINUE
      RETURN
      END
```

```
      SUBROUTINE MEGN31
      COMMON/BBB/IJK( 85,4),CORD( 50,3),VOL( 85)
      COMMON/DDD/DS( 50,3),FORC( 50,3),SIG( 85,6),EPS( 85,6)
      COMMON/FFF/NPB( 50),NDIR( 50),NPNUM( 50),NUME( 85)
C
C     FINITE ELEMENT MESH GENARATION
C
      DO 20 M=1,45
   20 NPNUM(M)=M
      DO 21 N=1,80
   21 NUME(N)=N
      DO 11 NZ=1,5
      R=0.5
      IF(NZ.EQ.1) R=0.49
      JZ=9*NZ-9
      DO 11 NY=1,3
      JY=3*NY-3
      DO 11 NX=1,3
      MX=NX+JY+JZ
      CORD(MX,1)=FLOAT(NX-1)*R
      CORD(MX,2)=FLOAT(NY-1)*R
   11 CORD(MX,3)=FLOAT(NZ-1)*.5
C
      DO 12 I=1,4
      II=4*I-4
      I9=9*I-9
      DO 12 J=1,2
      JJ=2*J-2
      J3=3*J-3
      DO 12 K=1,2
      KK=K+JJ+II
      N=5*KK-4
      L=K+I9+J3
      L0=L/2
      L0=2*L0
      IF(L0.EQ.L) GOTO 13
      IJK(N,1)=L
      IJK(N,2)=L+9
      IJK(N,3)=L+1
      IJK(N,4)=L+3
      N=N+1
      IJK(N,1)=L+1
      IJK(N,2)=L+13
      IJK(N,3)=L+9
      IJK(N,4)=L+10
      N=N+1
      IJK(N,1)=L+4
      IJK(N,2)=L+3
      IJK(N,3)=L+1
      IJK(N,4)=L+13
      N=N+1
      IJK(N,1)=L+3
      IJK(N,2)=L+12
      IJK(N,3)=L+9
      IJK(N,4)=L+13
      N=N+1
      IJK(N,1)=L+1
      IJK(N,2)=L+13
      IJK(N,3)=L+3
```

```
      IJK(N,4)=L+9
      GOTO 12
   13 IJK(N,1)=L
      IJK(N,2)=L+12
      IJK(N,3)=L+9
      IJK(N,4)=L+10
      N=N+1
      IJK(N,1)=L+1
      IJK(N,2)=L+4
      IJK(N,3)=L
      IJK(N,4)=L+10
      N=N+1
      IJK(N,1)=L+4
      IJK(N,2)=L+12
      IJK(N,3)=L+10
      IJK(N,4)=L+13
      N=N+1
      IJK(N,1)=L+3
      IJK(N,2)=L+12
      IJK(N,3)=L
      IJK(N,4)=L+4
      N=N+1
      IJK(N,1)=L
      IJK(N,2)=L+10
      IJK(N,3)=L+4
      IJK(N,4)=L+12
   12 CONTINUE
      DO 15 M=1,45
   15 NDIR(M)=1000
      DO 16 I=1,9
   16 NDIR(I)=NDIR(I)+1
      DO 17 I=1,5
      II=9*I-9
      DO 17 J=1,3
      JJ=J+II
      NDIR(JJ)=NDIR(JJ)+10
      KK=II+3*J-2
   17 NDIR(KK)=NDIR(KK)+100
      DO 18 I=37,45
   18 DS(I,3)=.0001
      DO 40 I=37,45
   40 NDIR(I)=NDIR(I)+1
      RETURN
      END
```

```
      SUBROUTINE GEOMAT(N,ITR,SG,INC)
      COMMON/BBB/IJK( 85,4),CORD( 50,3),VOL( 85)
      COMMON/DDD/DS( 50,3),FORC( 50,3),SIG( 85,6),EPS( 85,6)
      COMMON/HHH/PN( 85,6),TPN( 85,6)
      COMMON/III/AL(6),TC(6,3),NS(6,2)
      DIMENSION GK(3,3),AM(18,18),G(18,18),SH(18,18),SG(18,18)
C
C     GEOMETRIC OR INITIAL STRESS MATRIX
C
      DO 10 I=1,6
   10 TPN(N,I)=TPN(N,I)+.5*PN(N,I)
      DO 15 L=1,6
      DO 16 K=1,3
      DO 17 J=1,3
   17 GK(K,J)=-TC(L,K)*TC(L,J)
   16 GK(K,K)=1.+GK(K,K)
      DO 18 K=1,3
      DO 18 J=1,3
   18 GK(K,J)=      AL(L)*GK(K,J)*TPN(N,L)
      DO 19 I=1,2
      II=3*I-3
      DO 19 M=1,2
      IM=M+I
      IC=1
      MM=3*M-3
      IF(IM.EQ.3) IC=-1
      DO 19 K=1,3
      KK=K+II
      DO 19 J=1,3
      JJ=J+MM
   19 G(KK,JJ)=FLOAT(IC)*GK(K,J)
      NI=3*NS(L,1)-3
      NJ=3*NS(L,2)-3
      DO 20 I=1,6
      DO 20 J=1,12
   20 AM(I,J)=0.0
      DO 21 I=1,2
      II=2*I-2
      DO 21 J=1,3
      JJ=J+II
      KK=J+3*NS(L,I)-3
   21 AM(JJ,KK)=1.
      CALL MATMUL(6,12,6,G,AM,SH,0)
      CALL MATMUL(12,12,6,AM,SH,SG,1)
   15 CONTINUE
      DO 14 I=1,6
   14 TPN(N,I)=TPN(N,I)-.5*PN(N,I)
      RETURN
      END
```

```
      SUBROUTINE STRSAN(NUMEL,TN,D)
      COMMON/DDD/DS( 50,3),FORC( 50,3),SIG( 85,6),EPS( 85,6)
      COMMON/BBB/IJK( 85,4),CORD( 50,3),VOL( 85)
      COMMON/III/AL(6),TC(6,3),NS(6,2)
      COMMON/JJJ/          P(6,6),A(6,6),AC( 85,15)
      COMMON/HHH/PN( 85,6),TPN( 85,6)
      DIMENSION C(12),DT(6,12),TN(18,18),D(18,18),TD(18,18)
C
C     EVALUTATION OF STRESSES AND STRAINS
C
      DO 10 N=1,NUMEL
      NCT=0
      DO 50 I=1,5
      II=I+1
      DO 50 J=II,6
      NCT=NCT+1
      A(J,I)=AC(N,NCT)
   50 A(I,J)=AC(N,NCT)
      DO 60 I=1,6
   60 A(I,I)=1.0
      CALL STRMAT(N,TN,1)
      CALL MATMUL(6,12,18,TN,D,TD,0)
      DO 11 J=1,4
      JJ=3*J-3
      I=IJK(N,J)
      DO 11 K=1,3
      KK=K+JJ
   11 C(KK)=DS(I,K)
      DO 12 L=1,6
      DO 12 M=1,12
   12 DT(L,M)=TD(L,M)*AL(L)
      DO 13 L=1,6
      EPS(N,L)=0.0
      DO 13 M=1,12
   13 EPS(N,L)=EPS(N,L)+DT(L,M)*C(M)
C
C     STRESSES
C
      DO 15 L=1,6
      SIG(N,L)=0.0
      DO 14 M=1,6
   14 SIG(N,L)=SIG(N,L)+P(L,M)*EPS(N,M)
   15 PN(N,L)=VOL(N)*AL(L)*SIG(N,L)
   10 CONTINUE
      RETURN
      END
```

```
      SUBROUTINE DIFFEP(D)
      COMMON/III/AL(6),TC(6,3),NS(6,2)
      DIMENSION D(18,18)
C
C     DIFFERENCE MATRIX
C
      DO 12 I=1,4
      NS(I,1)=I
   12 NS(I,2)=I+1
      NS(4,2)=1
      DO 13 I=5,6
      NS(I,1)=I-4
   13 NS(I,2)=I-2
C
      DO 14 I=1,18
      DO 14 J=1,12
   14 D(I,J)=0.0
      DO 15 I=1,6
      II=3*I-3
      J=3*NS(I,1)-3
      K=3*NS(I,2)-3
      DO 15 L=1,3
      LJ=L+J
      LK=L+K
      MI=L+II
      D(MI,LJ)=-1
   15 D(MI,LK)=1
      RETURN
      END
```

```
      SUBROUTINE MATMUL(L,M,N,A,B,C,NT)
      DIMENSION A(18,18),B(18,18),C(18,18)
C
C     MATRIX MULTIPLICATION
C
      IF(NT-1) 20,21,22
   20 DO 10 I=1,L
      DO 10 J=1,M
      C(I,J)=0.0
      DO 10 K=1,N
   10 C(I,J)=C(I,J)+A(I,K)*B(K,J)
      GOTO 30
   21 DO 11 I=1,L
      DO 11 J=1,M
      C(I,J)=0.0
      DO 11 K=1,N
   11 C(I,J)=C(I,J)+A(K,I)*B(K,J)
      GOTO 30
   22 DO 12 I=1,L
      DO 12 J=1,M
      C(I,J)=0.0
      DO 12 K=1,N
   12 C(I,J)=C(I,J)+A(I,K)*B(J,K)
   30 RETURN
      END
```

```
      SUBROUTINE CURVYA(N,TN,ITEST)
      COMMON/BBB/IJK( 85,4),CORD( 50,3),VOL( 85)
      COMMON/III/AL(6),TC(6,3),NS(6,2)
      COMMON/JJJ/          P(6,6),A(6,6),AC( 85,15)
      DIMENSION Q(6,3),TN(18,18)
C
C     CURVY A MATRIX
C
      DO 10 L=1,6
      II=NS(L,1)
      JJ=NS(L,2)
      I=IJK(N,II)
      J=IJK(N,JJ)
      DO 11 K=1,3
   11 Q(L,K)=CORD(J,K)-CORD(I,K)
      AL(L)=SQRT(Q(L,1)**2+Q(L,2)**2+Q(L,3)**2)
      AL(L)=1./AL(L)
      LL=3*L-3
      DO 12 K=1,3
      LK=LL+K
      TC(L,K)=Q(L,K)*AL(L)
   12 TN(L,LK)=TC(L,K)
   10 CONTINUE
      IF(ITEST.EQ.1) GOTO 530
      DO 14 I=1,6
      DO 14 J=1,6
      A(I,J)=0.0
      DO 15 L=1,3
   15 A(I,J)=A(I,J)+TC(I,L)*TC(J,L)
   14 A(I,J)=A(I,J)**2
      NCT=0
      DO 50 I=1,5
      II=I+1
      DO 50 J=II,6
      NCT=NCT+1
   50 AC(N,NCT)=A(I,J)
  530 RETURN
      END
```

```
      SUBROUTINE STRMAT(N,TN,ITEST)
      COMMON/DDD/DS( 50,3),EOPC( 50,3),SIG( 85,6),EPS( 85,6)
      COMMON/EEE/YM( 85),PR( 85),YLSIG( 85)
      COMMON/GGG/TSIG( 85,8),TEPS( 85,8),TDS( 50,3),TEORC( 50,3),LY( 85)
      COMMON/III/AL(6) ,C(6,3),NS(6,2)
      COMMON/JJJ/          P(6,6),A(6,6),AC( 85,15)
      DIMENSION TS(6),DSIG(6),CA(6,6),DA(6),TN(18,18)
C
C     STRESS-STRAIN MATRIX
C
      TNG=0.0
      CALL CUPVYA(N,TN,ITEST)
      DO 10 I=1,6
      DO 10 J=1,6
   10 P(I,J)=((1.+PR(N))*A(I,J)-PR(N))/YM(N)
      CALL MATINS(P,6)
      IF(LY(N).NE.1) GOTO 13
      DO 21 I=1,6
   21 TS(I)=TSIG(N,I)+.5*SIG(N,I)
      DO 15 I=1,6
      DSIG(I)=0.0
      DO 15 J=1,6
      CA(I,J)= A(I,J)-2./3.
   15 DSIG(I)=DSIG(I)+CA(I,J)*TS(J)
      EQST=0.0
      DO 11 I=1,6
   11 EQST=EQST+DSIG(I)*TS(I)
      EQST=EQST*TNG   /1.5
      DO 16 I=1,6
      DO 16 J=1,6
   16 EQST=EQST+P(I,J)*DSIG(I)*DSIG(J)
      DO 17 I=1,6
      DA(I)=0.0
      DO 17 J=1,6
   17 DA(I)=DA(I)+P(I,J)*DSIG(J)
      DO 12 I=1,6
      DO 12 J=1,6
   12 P(I,J)=P(I,J)-DA(I)*DA(J)/EQST
   13 RETURN
      END
```

```
      SUBROUTINE LOAD(INC)
      COMMON/DDD/DS( 50,3),FORC( 50,3),SIG( 85,6),EPS( 85,6)
      COMMON/GGG/TSIG( 85,8),TEPS( 85,8),TDS( 50,3),TFORC( 50,3),LY( 85)
      DIMENSION YFORC(20)
C
C     INCREMENTS OF LOAD
C
      DEL=0.1
      KK=36
      L=9
      J=3
      IF(INC.GT.1) GO TO 20
      DO 11 M=1,L
      MM=M+KK
   11 YFORC(M)=TDS(MM,J)
   20 DO 12 M=1,L
      MM=M+KK
   12 DS(MM,J)=DEL*YFORC(M)
      RETURN
      END
```

```
      SUBROUTINE MATINS(A,N)
      DIMENSION  A(6,6),U(6,6),Y(6,6)
C
C     MATRIX INVERSION
C
      DO 14 I=1,N
      DO 14 J=1,N
      Y(I,J)=0.0
   14 U(I,J)=0.0
      DO 23 I=1,N
       U(I,I)=A(I,I)
      II=I-1
      IF(II.EQ.0) GOTO 25
      DO 21 K=1,II
   21 U(I,I)=U(I,I)-U(K,I)**2
   25 U(I,I)=SQRT(U(I,I))
      IF(I.EQ.N) GOTO 30
      I1=I+1
      DO 26 J=I1,N
      U(I,J)=A(I,J)
      IF(II.EQ.0) GOTO 22
      DO 20 K=1,II
   20 U(I,J)=U(I,J)-U(K,J)*U(K,I)
   22 U(I,J)= U(I,J)/U(I,I)
   26 CONTINUE
   23 CONTINUE
   30 DO 10 JJ=1,N
      J=N-JJ+1
      Y(J,J)=1./U(J,J)
      DO 10 II=1,J
      I=J-II+1
      I1=I+1
      IF(I1.GT.J.OR.I.EQ.J) GOTO 10
      Y(I,J)=0.0
      DO 11 K=I1,J
   11 Y(I,J)=U(I,K)*Y(K,J)+Y(I,J)
      Y(I,J)=-Y(I,J)/U(I,I)
   10 CONTINUE
      DO 12 I=1,N
      DO 12 J=1,N
      A(I,J)=0.0
      DO 12 L=1,N
   12 A(I,J)=A(I,J)+Y(I,L)*Y(J,L)
      RETURN
      END
```

```
      SUBROUTINE CHECK(NUMEL,SCLSIG)
      COMMON/EEE/YM( 85),PR( 85),YLSIG( 85)
      COMMON/GGG/TSIG( 85,8),TEPS( 85,8),TDS( 50,3),TFORC( 50,3),LY( 85)
C
C     CHECKING THE ELEMENTS FOR YIELDING AND UNLOADING
C
      DO 145 N=1,NUMEL
      IF(LY(N)-1) 147,146,148
  147 IF(TSIG(N,8).GE.SCLSIG) LY(N)=1
      GO TO 145
  146 IF(TEPS(N,8).GE.TEPS(N,7)) GO TO 145
      IF(TSIG(N,8).GE.TSIG(N,7)) GOTO 145
      LY(N)=2
      YLSIG(N)=TSIG(N,7)
      GO TO 145
  148 IF(TEPS(N,8).LE.TEPS(N,7)) GO TO 145
      IF(TSIG(N,8).LE.YLSIG(N)) GO TO 145
      LY(N)=1
      YLSIG(N)=0.0
  145 CONTINUE
C
      DO 560 N=1,NUMEL
      TSIG(N,7)=TSIG(N,8)
  560 TEPS(N,7)=TEPS(N,8)
      RETURN
      END
```

```
      SUBROUTINE TOTALS(     NUMNP,NUMEL)
      COMMON/BBB/IJK( 85,4),CORD( 50,3),VOL( 85)
      COMMON/DDD/DS( 50,3),FORC( 50,3),SIG( 85,6),EPS( 85,6)
      COMMON/GGG/TSIG( 85,8),TEPS( 85,8),TDS( 50,3),TFORC( 50,3),LY( 85)
      DIMENSION DSIG(8),DEPS(8)
C
C     DETERMINATION OF THE TOTAL VALUES BY ADDING THE INCREMENTS
C
      S32=SQRT(1.5)
      DO 506 M=1,NUMNP
      DO 506 I=1,3
      TDS(M,I)=TDS(M,I)+DS(M,I)
  506 TFORC(M,I)=TFORC(M,I)+FORC(M,I)
      DO 507 N=1,NUMEL
      DO 507 I=1,6
      TSIG(N,I)=TSIG(N,I)+SIG(N,I)
  507 TEPS(N,I)=TEPS(N,I)+EPS(N,I)
      DO 511 N=1,NUMEL
      DO 215 I=1,8
      DSIG(I)=TSIG(N,I)
  215 DEPS(I)=TEPS(N,I)
      CALL EQUVAL(DSIG,DEPS,N)
      TSIG(N,8)=DSIG(8) *S32
  511 TEPS(N,8)=DEPS(8)/S32
C
C     MODIFICATION OF THE COORDINATES OF N.P S FOR LARGE DISPLACEMENTS
C
      DO 355 M=1,NUMNP
      DO 355 I=1,3
  355 CORD(M,I)=CORD(M,I)+DS(M,I)
      RETURN
      END
```

```
      SUBROUTINE EQUVAL(S,T,N)
      COMMON/JJJ/          P(6,6),A(6,6),AC( 85,15)
      DIMENSION ST(6),S(8),B(6,6),TT(6),T(8),R(6),TN(18,18)
C
      NCT=0
      DO 50 I=1,5
      II=I+1
      DO 50 J=II,6
      NCT=NCT+1
      A(J,I)=AC(N,NCT)
   50 A(I,J)=AC(N,NCT)
      DO 20 I=1,6
      A(I,I)=1.0
      DO 20 J=1,6
      B(I,J)=A(I,J)
   20 A(I,J)=A(I,J)-1./3.
C     EVALUATION OF EQUIVALENT STRESS AND STRAIN
C
      CALL MATINS(B,6)
      DO 12 I=1,6
      R(I)=0.0
      DO 12 J=1,6
   12 R(I)=R(I)+B(I,J)
      DO 13 I=1,6
      DO 13 J=1,6
   13 B(I,J)=B(I,J)-R(I)*R(J)/3.0
      DO 14 I=1,6
      ST(I)=0.0
      TT(I)=0.0
      DO 14 J=1,6
      TT(I)=TT(I)+B(I,J)*T(J)
   14 ST(I)=ST(I)+A(I,J)*S(J)
      S(8)=0.0
      T(8)=0.0
      DO 11 I=1,6
      T(8)=T(8)+T(I)*TT(I)
   11 S(8)=S(8)+S(I)*ST(I)
      S(8)=SQRT(S(8))
      T(8)=SQRT(T(8))
      RETURN
      END
```

```
      SUBROUTINE FQUAD(S,N,T,Q,R)
      COMMON/JJJ/          P(6,6),A(6,6),AC( 85,15)
      DIMENSION D(6,2),S(6,2),TN(18,18)
C
C     EVALUATION OF THE PRODUCT OF INCREMENT AND EQ. STRESS
C
      NCT=0
      DO 50 I=1,5
      II=I+1
      DO 50 J=II,6
      NCT=NCT+1
      A(J,I)=AC(N,NCT)
   50 A(I,J)=AC(N,NCT)
      DO 20 I=1,6
      A(I,I)=1.0
      DO 20 J=1,6
   20 A(I,J)=A(I,J)-1./3.
      DO 12 J=1,2
      DO 12 I=1,6
      D(I,J)=0.0
      DO 12 L=1,6
   12 D(I,J)=D(I,J)+A(I,L)*S(L,J)
      T=0.0
      Q=0.0
      R=0.0
      DO 13 I=1,6
      R=R+S(I,1)*D(I,1)
      Q=Q+S(I,2)*D(I,1)+S(I,1)*D(I,2)
   13 T=T+S(I,2)*D(I,2)
      RETURN
      END
```